LOCALIZED BUCKLING OF AN ELASTIC STRUT IN A VISCO-ELASTIC MEDIUM

Andrew Ivan Melville Whiting

BE (Sydney)

October 1996

A thesis submitted for the degree of

Doctor of Philosophy of the University of London

and for the

Diploma of Membership of Imperial College

Department of Civil Engineering

Imperial College of Science, Technology and Medicine

London SW7 2BU

Abstract

Certain types of long, axially compressed structures have the potential to buckle locally in one or more regions rather than uniformly along their length. Here, the potential for localized buckle patterns in an elastic layer embedded in a visco-elastic medium is investigated using a strut-on-foundation model. Applications of this model include the growth of geological folds and other time-dependent instability processes.

The model consists of an elastic strut of uniform flexural stiffness supported by a Winkler-type foundation made up of discrete Maxwell elements. Mathematically, this model corresponds to a nonlinear partial differential equation which is fourth-order in space and first-order in time. The nature of the buckling process is characterized by an initial period of elastic deformation followed by an evolutionary phase in which both elasticity and viscosity have a role to play. Two different formulations are studied: the first combines linear strut theory with a nonlinear foundation and is valid for small, but finite, deflections; the other incorporates the exact expression for curvature of the strut resulting in geometrical nonlinearities and is capable of modelling large deflections. The evolution of non-periodic buckle patterns in each system is examined under the constraint of controlled end displacement.

Two independent methods are used to approximate the solution of the governing equations. Modal solutions, based on the method of weighted residuals, complement accurate numerical solutions obtained with a boundary-value solver. In either case, the results suggest that for the perfect system, localized solutions follow naturally from the inclusion of nonlinear elasticity with softening characteristics. Emphasis throughout is on the qualitative features displayed by the phenomenon of localization rather than specific applications. Nevertheless, the ideas and results are a step towards accounting for the rich variety of deformed shapes exhibited by nature.

Acknowledgements

For the past three years I have had the privilege of being able to pursue knowledge for its own sake. It has been a rewarding experience, for which I am indebted to many people and organizations.

I owe a great deal to my supervisor, Professor Giles Hunt, who introduced me to research and allowed me the academic freedom to indulge my curiosity. Despite moving to the University of Bath, he continued to provide support and encouragement. I am also grateful to Professor Roger Hobbs, my co-supervisor, who made helpful suggestions along the way. Special thanks are due to Dr Khurram Wadee of the University of Exeter, for countless invaluable discussions and proof-reading this thesis. My appreciation extends also to Mark Manzocchi for much technical advice, and to Drs (and mothers) Tatjana Micic and Avril Blackmore with whom I shared an office and constantly pestered with questions.

Numerous other people have contributed, either directly or indirectly, to the successful completion of this work. I would like to acknowledge: Dr Gerald Moore of the Department of Mathematics and Dr Alan Champneys of Bristol University, for providing computer programs and advice on their use; Dr Geoff Stephenson of the Mathematics Advice Centre, for assistance with queries of a mathematical nature; staff from the Centre for Computing Services, for answers to computer-oriented queries; Daniel Shields of the Department of Electrical and Electronic Engineering and Dr Ross Wright of the Department of Mathematics, for advice on using LaTeX; Professor Roger Hobbs, and Dr John Cosgrove of the Department of Geology, for providing photographs to illustrate my work; and the library and non-academic staff at the Department of Civil Engineering, for being friendly and helpful.

Imperial College and London are special places because of the range of nationalities they attract. I am indebted to my fellow research students and to the friends I have made outside university for distractions which have added colour to college life. I would like to mention especially the London Goodenough Trust who provide a unique residential environment for international postgraduate students and their families in Bloomsbury.

Financial support was provided generously by many sources. During the first two years of my research I was the recipient of the Sir Robert Menzies Memorial Scholarship in Engineering, sponsored jointly by the Menzies Trust in the United Kingdom and the Menzies Foundation in Australia. My final year was supported by the Eleanor Sophia Wood Travelling Scholarship awarded by the University of Sydney. My thanks are due also to: the Committee of Vice-Chancellors and Principals of the Universities of the United Kingdom (CVCP) for an Overseas Research Students (ORS) Award; the Council of The King's School, Australia, who provided a Stanley Wilson Oxford Scholarship enabling me to survive in London; and the Structures Section of the Department of Civil Engineering who sponsored my attendance at a conference in Paris.

I owe a tremendous amount to my family whose sacrifices over the years have ensured a sound education and up-bringing. Their support has been instrumental in my achievements thus far.

Finally, I thank my wife, Frances, for her constant love and affection.

Contents

List of Figures

List of symbols

The following notation is used in this thesis. Where more than one meaning has been assigned to a symbol, the correct definition will be evident from the context in which it is used. Those not define below are explained in the text.

a_m, F_m	Fourier components
c, k	Foundation stiffness parameters
k^*, s^*	Rigid link stiffness parameters
k_i, l_i	Galerkin coefficients
h	Layer thickness
m	Mass
p_i, q_i	Material constants
r	k/η
r, ϕ	Polar coordinates
s	Perturbation parameter ($=\sqrt{P^c - P}$)
s, k	Spring stiffnesses
t	Time
w	Vertical displacement
$\bar{w}$	Trial solution
w_s, w_d	Spring, dashpot displacements
x	Axial coordinate measured along deformed strut
x_i	Collocation points
A_i	Modal amplitudes (Chapter 5)

$A_i(X)$	Amplitude of cosine mode $\cos i\beta x$ (Chapter 3)
$A_{i,j}(X)$	Coefficient of s^j term in series expansion of $A_i(X)$
$B_i(X)$	Amplitude of sine mode $\sin i\beta x$ (Chapter 3)
$B_{i,j}(X)$	Coefficient of s^j term in series expansion of $B_i(X)$
EI	Bending stiffness
$K(\gamma), E(\gamma)$	Elliptic integrals of the first and second kind
F	Foundation stiffness per unit length
F_s, F_d	Spring, dashpot forces
G, λ	Lamé constants
$G(x)$	Pseudo-forcing function
I_n, I_{cnm}, I_{snm}	Standard integrals
L_d	Dominant wavelength
L	Length
M_i	Collocation coefficients
P	Axial (compressive) load
P_i	Coefficient of s^j term in series expansion of P
P^{c}	Critical axial load ($= 2\sqrt{kEI}$)
R, R_{av}	Residual, average residual
U	Strain energy
V	Potential energy
$V_{ijkl}^{\mathrm{cc}}, V_{ijkl}^{\mathrm{cs}}, V_{ijkl}^{\mathrm{ss}}$	Perturbation coefficients
W_i	Weighting functions
X	Slow space variable ($= sx$)
α, β	Linearized eigenvalues
β^{c}	Critical wavenumber
β_m, ω_m	Fourier wavenumber, frequency
β_d, ω_d	Dominant wavenumber, frequency
γ	Deformation parameter
ϵ, σ	Strain, stress
η	Viscosity
λ	Complex eigenvalue

θ	Tangent angle
θ^*, τ	Shooting parameters
$\mathcal{E}$	End-shortening
ν	Poisson's ratio
χ	Curvature
ϕ	Trial functions
ψ	Residual collocation functions
Δt	Time step
Δx	Spatial interval
Ω	$\beta^c/\sqrt{2P^c}$
$\dot{()}$	Derivative with respect to t
$()'$	Derivative with respect to x

Chapter 1

Introduction

"Nonlinear equations are much richer and more diverse than linear ones, so are more likely to describe real phenomena."

— Philip Drazin (1991)

The last thirty years or so have seen an increased awareness of nonlinear effects throughout the physical sciences. This has resulted from the enormous growth in computing facilities, enabling researchers to investigate nonlinear behaviour previously considered too difficult to solve manually. An associated development has been the application of concepts and methods from one field of endeavour to another. This interdisciplinary activity, not confined by traditional thoughts and boundaries, has resulted in a number of successful breakthroughs and offers at the very least alternative viewpoints.

The growing demand for strength, and the accompanying requirement for efficiency in the use of materials, has led to the increasing possibility of instability failures in engineering structures. Classical methods of analysis, involving linear equations, are unable to account for the differences observed in the buckling of various structural members. This is because buckling, and instability in general, is an inherently nonlinear phenomenon. Likewise, early attempts to simulate the process of geological folding considered only linear behaviour. In so doing, they predicted purely periodic forms and were unable to explain the diverse range of folded structures found in deformed rock.

The following sections introduce three topics which are of central importance to this thesis, namely, localization, visco-elasticity and strut-on-foundation models.

1.1 Localized phenomena

Localization is a term used to describe deformation which is concentrated, or local, in nature. There are two principal forms of localization — structural and material. An example of the first type occurs in steel structures under compressive loading where it is observed that the final buckle pattern is often confined to one or more regions of limited size. This phenomenon is referred to as localized buckling. Material localization, on the other hand, generally involves an instability at the microscopic level. The distinguishing feature between structural and material localization, besides the scale on which they take place, is that the latter represents a yielding or fracturing of the material while the former may involve only elastic deformations and hence can be entirely reversible.

Localization phenomena are of great importance in engineering problems since they govern the load carrying capacities of structures and, in many cases, the strength of materials. They are currently attracting a great deal of interest amongst the scientific and engineering community, as demonstrated by a forthcoming special issue of the *Philosophical Transactions of the Royal Society of London* (Champneys *et al.*, 1996) which is devoted to localization and solitary waves in solid mechanics.

While structural and material localizations manifest themselves spatially, there are other localization phenomena which are temporal in nature. One new and exciting development is wavelet theory which involves a data signal with a localized oscillatory form (Young, 1993). Wavelets have the potential to improve the way that digital data is processed, stored and transmitted, with application in sonar and radar. This is especially significant in today's society with a worldwide digital revolution taking place and the encapsulation of virtually all forms of information into binary format.

A number of instances of localization are described below. These are drawn from the fields of structural engineering and geoscience — a reflection of the intent of this thesis to apply ideas from the former to shed light on aspects of the latter.

1.1.1 Structural localization

Structural members in compression have post-buckling responses which, like all bifurcation phenomena, may be classified as either supercritical or subcritical. For members of the first type, buckling under dead load conditions is a stable process and the resulting pattern is distributed along the entire length of the structure; the longitudinally compressed plate is a good example (Timoshenko & Gere, 1963). The outcome is markedly different for shell structures and struts on softening elastic foundations which buckle subcritically (Potier-Ferry, 1983). Under rigid load conditions, localized buckling prevails with the deformation concentrated in a small part of the structure. This phenomenon has been studied both experimentally (Moxham, 1971) and theoretically (Tvergaard & Needleman, 1980; Tvergaard & Needleman, 1983). An example of a localized buckle profile in railway tracks is shown in Figure 1.1.

Apparent localization may arise simply from a variation of stress within a structure, caused, for example, by the presence of a second (overall) buckling mode. This may be distinguished from the localized buckling which occurs in long elastic structures under uniform stress and which has an equal likelihood of buckling at any location along the length. It is the latter, pure form of localization which is of interest here. Although initially triggered by an imperfection, such behaviour is an intrinsic property of the perfect system (Hunt *et al.*, 1989).

Geological structures may also display localized or quasi-periodic features. Figure 1.2 shows a photograph of folds in a specimen of sedimentary rock. Although the prevailing character is one of near periodicity the thickest (white) layer shows a definite tapering of amplitude towards the right-hand side. The governing equations for folding have traditionally been linearized so that until recently geological structures were analysed in terms of strictly regular or periodic forms evolving under conditions of constant axial load (Biot, 1961; Ramberg, 1964). Recent analyses, incorporating nonlinear terms, have considered the development of folds under the more realistic conditions of controlled end displacement, akin to a tectonic event (Mühlhaus *et al.*, 1994; Hunt *et al.*, 1996a).

Figure 1.1 Localized buckling in a non-operational track caused by subsidence due to underground mining. (Source: British Rail, Derby)

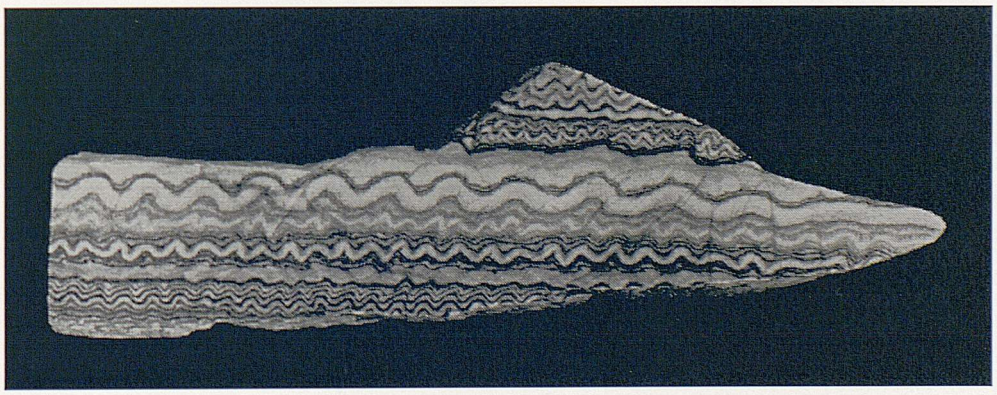

Figure 1.2 Folding in a specimen (maximum dimensions 12 cm x 4 cm) of evaporite from New Mexico. (Source: Dr. J. W. Cosgrove, Imperial College)

1.1.2 Material localization

A rod in tension arrives at the maximum load in a state of uniform strain. At this point, theory states that a bifurcation occurs with two equilibrium paths emerging: one of uniform strain and the other localized (Needleman, 1972). In practice, the strain continues to increase in only a small part of the rod, allowing the remainder to unload while at the same time maintaining uniform tension throughout. This plastic deformation (or "necking") is analogous in many ways to localized buckle patterns (Tvergaard & Needleman, 1980). The fracture mechanism of rock under constant stress also involves material localization (Horii & Okui, 1994). A specimen subjected to a sustained compressive load, less than the uniaxial compressive strength, fails after some time. The failure mechanism involves the growth of microcracks which coalesce leading to localization and, ultimately, fracture of the specimen. A similar localization phenomenon occurs in the formation of shear bands in rock where deformation is concentrated within narrow zones (Mühlhaus *et al.*, 1992).

1.1.3 Solitons

The relationship between large deflections of elastic structures and solitary waves, or "solitons", has been discussed by several authors, for example Konno & Jeffrey (1983), El Naschie (1989; 1990b) and Buffoni *et al.* (1996). A soliton is a solution of a nonlinear partial differential equation which has a permanent localized shape and which may interact with other solitons without losing its original form. Solitons owe their discovery to a Scottish civil engineer by the name of Scott Russell who, in 1834, observed a large solitary wave of water develop in a canal when a moving barge stopped suddenly. He watched the wave travel for a considerable distance and was sufficiently interested in this phenomenon to perform laboratory experiments. His empirical work and the subsequent mathematical studies by Boussinesq, Rayleigh, Korteweg and de Vries, amongst others, gave rise to the subject of solitons (Drazin, 1991).

Today, solitons are a fashionable topic of research for many investigators. They have numerous physical applications ranging from the structure of galaxies, to water waves and the propagation of dislocations (flaws) in a crystal (Drazin & Johnson,

1989). Their universality, and therefore importance, stems from the fact that they are solutions of many fundamental mathematical equations, including the Korteweg-de Vries (KdV) equation of shallow water waves and the nonlinear Schrödinger equation of quantum mechanics. An eminently readable account about the applications of solitons is the *New Scientist* article by Drazin (1991).

1.2 Visco-elasticity

The behaviour of some materials, when subjected to an applied load, is strongly time-dependent and may be described as visco-elastic. For such materials, which include soil, concrete, polymers and metals at high temperatures, the duration and rate of applied load influence their response. Excellent summaries of the subject may be found in the articles by Lee (1962), Flügge (1975), and Bazant & Cedolin (1991).

The mechanical behaviour of a material can be assumed to be governed by a constitutive relation. Customarily, this relation between the internal stress and strain is formulated as a differential equation. This may be accomplished by replacing the material with an idealized model consisting of springs and dashpots. A linear spring is described by the relation $\sigma = E\epsilon$ and a dashpot by the relation $\sigma = \eta\dot{\epsilon}$, where σ is the internal stress, ϵ is the strain and a dot ($\dot{}$) is used to denote a derivative with respect to time. The spring modulus E and dashpot viscosity η are often called the elastic and viscous constants, respectively, although they may depend on temperature and other thermodynamic variables. A linear elastic spring is used to represent a Hookean solid, with the internal stress proportional to the strain of the body. Examples of elastic materials include metals such as steel and aluminium. A linear viscous dashpot is used to represent a Newtonian fluid in which the stress depends on the rate of deformation, typical examples being oil, water and air. The characteristic property of a fluid is that it cannot support a shearing stress indefinitely, so that if a shearing stress is applied and maintained, the fluid will flow and continue to do so as long as the stress remains.

These fundamental mechanical models are purely phenomenological as they have no connection with the actual physical mechanism of visco-elastic deformation. Nevertheless, the elementary units may be combined to form compound models whose behaviour under stress mimics that of real visco-elastic materials (Roscoe, 1950). The simplest compound models are the Maxwell unit, comprising a spring and dashpot in series, and the Kelvin-Voigt unit, comprising a spring and dashpot in parallel. The behaviour of these, and other, visco-elastic models is characterized by their response to constant stress (see Figure 1.3) and constant strain (see Figure 1.4). Under constant stress, a visco-elastic material continues to deform (or creep) indefinitely. If the creep curve is bounded, the material is regarded as a solid. Thus, the elastic spring and Kelvin-Voigt unit are solids. Fluids are those materials for which the creep curve is unbounded, such as the viscous dashpot and Maxwell unit. To emphasize the distinction between these types of visco-elastic behaviour, Ramsay (1967) referred to solids as *visco-elastic* materials and to fluids as *elasto-viscous* materials. In reality, the distinction between solids and fluids in visco-elasticity is blurred, especially for materials which deform very slowly.

Linear visco-elastic theories combine the effects of more than one stress history using the principle of superposition. For example, Boltzmann (1876) proposed a theory in which the stress depends on the history of infinitesimal strain by means of an integral representation. Nonlinear time-dependent behaviour, regarded by some as visco-plastic (Bažant & Cedolin, 1991), is also possible. The nonlinearity may arise in the elastic part, the viscous part, or in a more complicated manner involving both components. In this case, the concept of individual rheological elements may no longer be suitable.

1.3 Struts on elastic and visco-elastic foundations

The problem of a thin elastic layer supported by a continuous foundation has been treated extensively in the engineering and scientific literature for more than a century. Many of the early contributions were concerned primarily with elastic foundations (Zimmerman (1888) and Hetényi (1946), for example). More recent works gen-

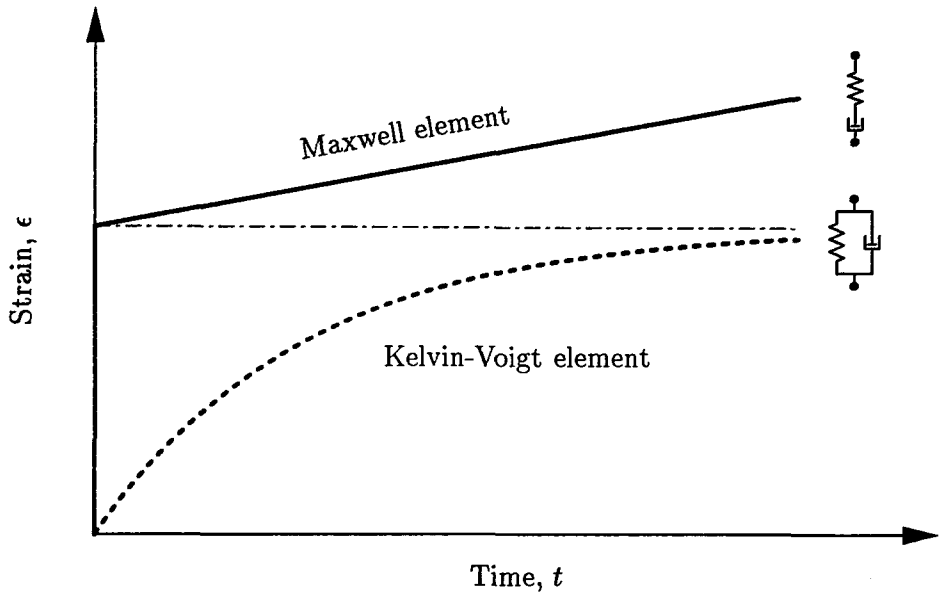

Figure 1.3 Creep response for rheological models under constant stress.

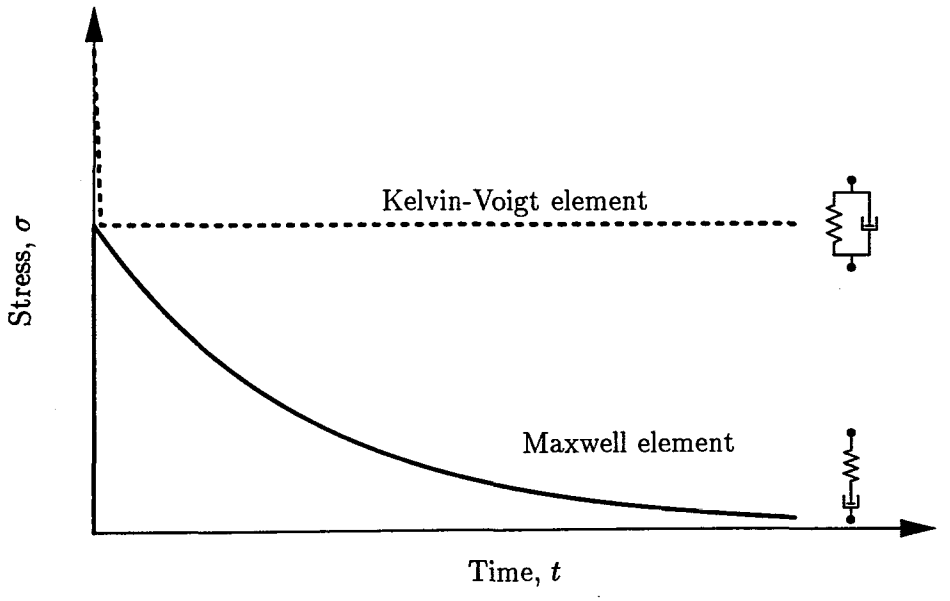

Figure 1.4 Stress relaxation for rheological models under constant strain.

eralized the problem to consider time-dependent foundation properties (Freudenthal & Lorsch (1957), Hoskins & Lee (1959) and Pister & Williams (1960), for example). The majority of these papers relate to the deformation of a horizontal beam[1] under a vertical load and were used to model the surface deflections of railway tracks and pavements under traffic loading. As a result no axial loads were applied and, typical of most bending theories, only the first-order response was considered. Other studies have focused on the problem of stability for a strut supported by either an elastic foundation (Kerr, 1969) or a visco-elastic foundation (Leu & Yang, 1989).

The analysis of a strut (or plate) resting on a deformable foundation is based on assumptions regarding the behaviour of the constituents: the strut, the foundation, and the conditions of continuity at the interface between the strut and foundation. The strut may be described using the classical Euler-Bernoulli assumptions (that plane cross-sections remain plane during deformation), as a Timoshenko beam incorporating shear stiffness, or as an elastic solid. The behaviour of the foundation may be modelled as an idealized set of independent elements, as a continuum, or as a hybrid model incorporating features of both. Finally, the conditions of continuity at the interface may be adhesive (or "welded"), in which case the displacements of the strut and foundation are compatible, or they may be frictionless. A number of different assumptions are possible and the interested reader is directed to the classic work of Hetényi (1946) for further details.

Two different models of an elastic strut on a visco-elastic foundation are depicted in Figure 1.5. The usual approach in formulating problems represented by a strut-on-foundation model is to include the foundation reaction in the differential equation for the strut. Although the medium is often rather complex, of concern is the response of the foundation at the contact area and not the stresses and displacements within the foundation material itself. A discussion of several types of visco-elastic foundation was given by Kerr (1964).

[1]Note the distinction between a *beam*, which in an engineering context refers to a structural element under (lateral) loading which causes bending, and a *strut* (or beam-column), which may be subjected to axial as well as lateral loads, and which is susceptible to both buckling and bending.

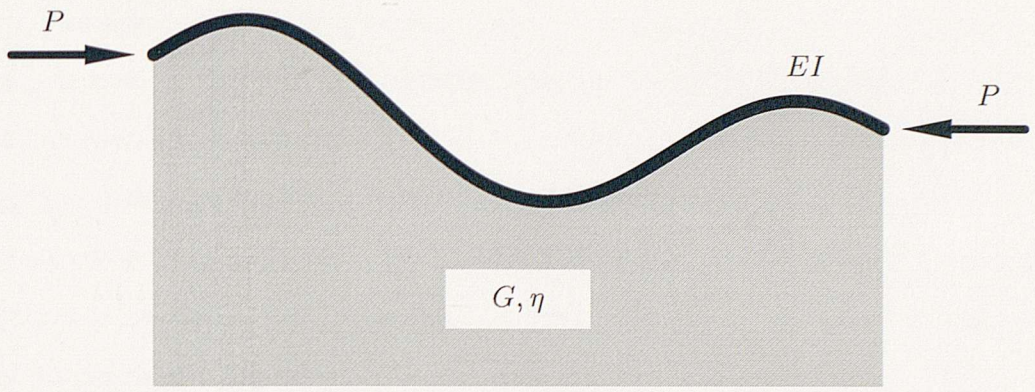

(a)

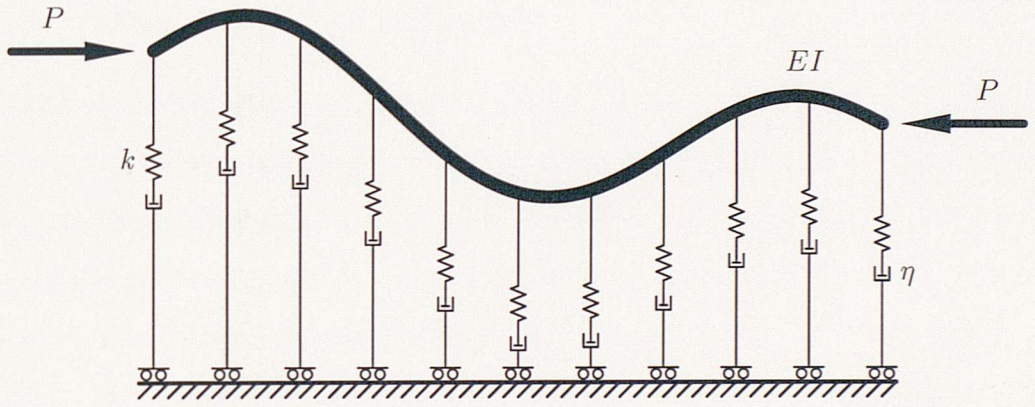

(b)

Figure 1.5 Models of an elastic strut on a visco-elastic foundation: (a) two-dimensional halfspace; (b) Winkler-type foundation.

1.3.1 Winkler foundation

The simplest representation of an elastic foundation was proposed by Winkler (1867) who suggested that the supporting medium consisted of a continuously distributed set of linear springs. This formulation assumes the deflection at any point within the foundation depends only on the *local* pressure at that point, and is independent of pressures in other parts of the system. For some applications, the Winkler assumption is satisfied very well, for example, railway tracks on a frictional bed of gravel, while for other applications where the local reaction depends also upon the deflections at adjacent points, it is not so good. This discrepancy led to the development of several alternative foundation models.

The principal criticism directed at the Winkler model is that the surface deflection is local to the point of load. This argument is valid only when the foundation is considered in isolation rather than as an integral part of a system. In a strut-on-foundation model, the cause of deformation is an instability of the compressed layer which is a continuous body so that any lateral deformation will have more than simply local effects. Kerr (1964) has also suggested that the Winkler model, in spite of its simplicity, may often more accurately represent the actual condition existing in certain foundations than do some of the more complicated analyses in which the foundation is regarded as a continuous isotropic body.

1.3.2 Two-dimensional halfspace

An alternative foundation is the semi-infinite halfspace, or continuum, which represents the case of complete continuity within the supporting medium. It is however, a much more difficult problem to solve, although a number of solutions for specific cases are available in the literature (Biot, 1937; Hetényi, 1946; Timoshenko & Gere, 1963). Biot (1937) analysed the bending of a beam resting on a two-dimensional elastic continuum by removing the beam and studying the effect of a sinusoidal load bearing directly on the foundation. He solved a two-dimensional elasticity problem to obtain the deflection of the surface and concluded that, for the special case of sinusoidal loading, the deflection was inversely proportional to the wavelength. This is in contrast to the *local* Winkler hypothesis.

In order to describe materials with microstructure it is necessary to use generalized continua with either additional kinematic degrees of freedom (Cosserat continua) or higher deformation gradients (higher-grade continua). Details about these continuum models, and their application to granular materials, are presented by Vardoulakis & Sulem (1995).

1.3.3 Hybrid models

Numerous attempts have been made to achieve a compromise between the mathematical simplicity of the Winkler foundation and the close physical representation of the solid continuum. These hybrid models either assume some form of interaction between the independent visco-elastic elements, for those based on a Winkler hypothesis, or introduce simplifying assumptions about the displacements or stresses, for those based on a continuum model. An example of the first type was proposed by Hetényi (1950) who embedded a continuous beam in the discontinuous foundation. Another example is the Pasternak foundation which incorporates shear interaction in the foundation by connecting incompressible shear elements between the springs (Pasternak, 1954). Several workers have proposed foundation models of the second type by assuming the deflection at any point depends on foundation pressures over a certain length in the vicinity of the point of interest, mostly through the use of Fourier integrals (Wieghart, 1922; Biot, 1937; Reissner, 1937).

1.4 Applications of strut model to physical problems

Strut-on-foundation models have a wide range of physical applications. In the examples cited below, a distinction is made between elastic and visco-elastic foundation behaviour.

1.4.1 Elastic foundations

Models of beams on elastic foundations were originally used for determining the vertical surface deflections and stresses in railway tracks beneath passing trains (Winkler, 1867; Hetényi, 1946). Struts on elastic foundations are a natural extension of these earlier models and have application to the buckling of railway tracks and pipelines due to constrained thermal expansion. The strut model has also been used by analogy in other applications, such as the buckling of cylindrical shells and sandwich structures. A number of examples for the application of an elastic strut on an elastic foundation are presented in Figure 1.6.

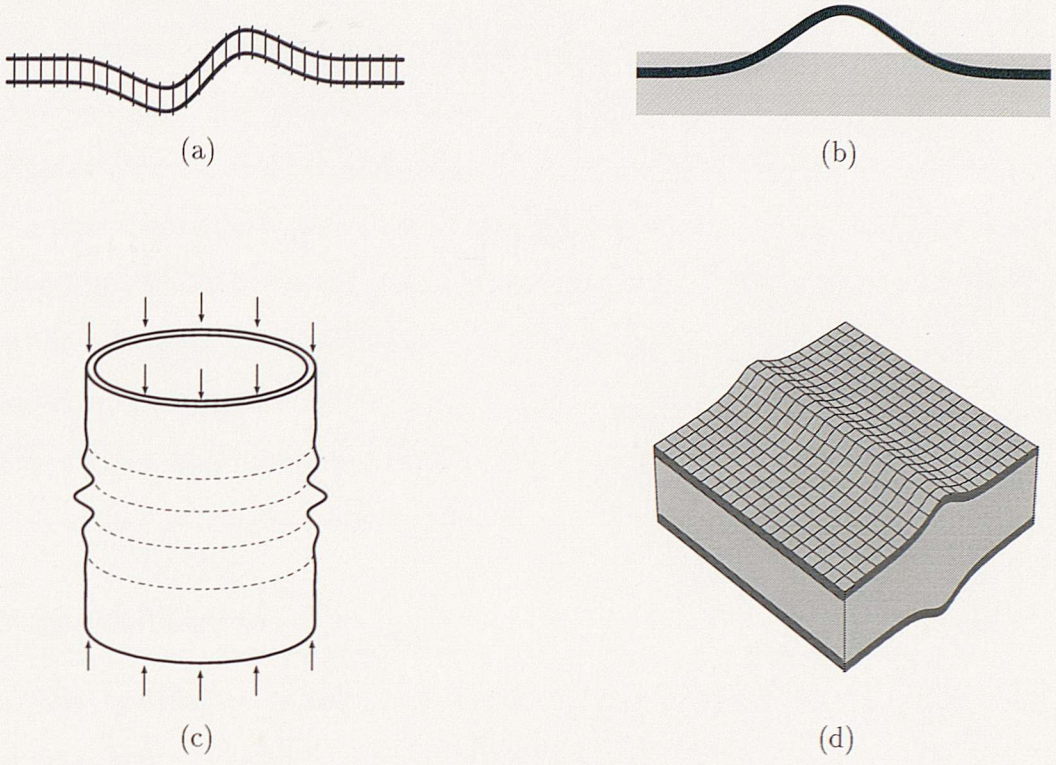

Figure 1.6 Applications for the model of an elastic strut on an elastic foundation: (a) railway tracks; (b) submarine pipelines; and structural analogies: (c) axisymmetric deflection of cylindrical shells; and (d) sandwich structures.

Railway tracks

Railway tracks are often welded together to form continuous tracks, supported at close intervals by ties. In hot weather, the increase in temperature of the track results in a build-up of longitudinal compressive stresses which may cause either lateral or vertical buckling. In the case of the vertical mode, the ties and ballast act as the deformable foundation, and are usually approximated with an equivalent continuous foundation of the Winkler type. For the lateral mode, it is the friction between the track and ballast which resists horizontal deflection (Tvergaard & Needleman, 1981). The vertical mode has attracted a great deal of attention over the years as evidenced by the review paper by Kerr (1974) containing nearly 50 references to the problem. A summary of analyses of thermal buckling in the lateral plane was also presented by Kerr (1975). Actual track buckling may proceed in a more complicated manner involving both modes of deformation.

Pipelines

The development of off-shore oil and gas fields has led to submarine pipelines being used to convey products between sites. The fluid is usually transported at elevated temperature and pressure, conditions which may induce compressive axial stresses if the pipe is restrained. As with track buckling, both vertical ("upheaval") and lateral buckling ("snaking") modes are possible (Blackmore, 1995). The vertical buckling mode is possible in buried pipes, while lateral buckling is more common in pipes which are laid unprotected on the sea bed. In practice, the lateral mode occurs at a lower axial load than the vertical mode and is therefore more prevalent unless the pipe is laid in a trench (Hobbs, 1981).

Structural analogies

In the buckling of cylindrical shells, axisymmetric deflections give rise to hoop stresses which restrain further radial displacement. A longitudinal element of the cylinder can therefore be regarded as a strut on an elastic foundation, the modulus of which is a function of the cross-sectional dimensions and material properties of the tube (Hetényi, 1946; Calladine, 1983). The case of localized buckle patterns in cylinders has been modelled by El Naschie (1974; 1989) using a strut on a nonlinear foundation.

Sandwich structures are used extensively in the aerospace industry because of their high strength-to-weight ratio (Allen, 1969). They are often composed of relatively stiff flanges, carbon-fibre reinforced plastic for example, and a soft core material, such as polystyrene. Each flange acts like a strut while the core plays the role of a supporting foundation. Like other structures which are efficient at carrying load, sandwich panels have a tendency for complex, and sometimes catastrophic, failure modes (Hunt *et al.*, 1988).

1.4.2 Visco-elastic foundations

The strut model also has important physical applications in visco-elastic systems. It has been used, for example, to determine the force exerted by floating ice sheets on stationary objects like oil platforms and bridge piers (Hui, 1986). In this instance,

however, the ice is modelled as a linear visco-elastic strut and the water as an elastic (Winkler) medium. Similarly, Leu & Yang (1989) have investigated the stability of a continuously supported visco-elastic strut.

Models of beams on visco-elastic foundations were devised as extensions of the earlier beam-on-elastic-foundation models with the aim of evaluating the rate effects of surface traffic loads on deformable subgrades (Freudenthal & Lorsch, 1957; Hoskin & Lee, 1959). Applications for an elastic strut on a visco-elastic foundation include the formation of geological folds and the buckling of pavements due to constrained thermal expansion. Most of the examples depicted in Figure 1.6 are equally applicable here provided the foundation is assumed to have time-dependent characteristics.

Geological folds

Folds are a feature of deformed rock which may develop in response to compressive stresses induced by tectonic plate movement. A typical scenario involves a relatively thin layer of stronger rock, such as sandstone, embedded within a thick layer of weaker material, like shale. In the most general case, both layer and surrounding matrix are assumed to be visco-elastic, although in certain circumstances the layer may be considered as elastic. The process of folding has been investigated both theoretically (Biot, 1961) and experimentally (Biot *et al.*, 1961). Folding of multiple layers is also possible as indicated by the photograph in Figure 1.2.

Concrete highways and airfields

"Blowups" of concrete pavements have been a problem for highway and airport engineers for many years (Kerr & Dallis, 1985). They are caused by axial compression induced in the pavement by a rise in temperature and ingress of moisture, and lead to a form of upheaval buckling. Although they usually occur at joints or cracks, due to the infiltration of debris at these points, they have also been observed in continuous reinforced pavements.

1.5 Objectives of thesis

Over the past couple of decades a number of publications have explored the potential for structural localization in elastic systems (Tvergaard & Needleman (1980), Hunt *et al.* (1989), Wadee (1993) and Hunt & Blackmore (1996), for example). These works have gone some way towards explaining how and why localized buckle patterns appear in many engineering structures, such as railway tracks and submarine pipelines. This thesis is an attempt to transfer some of this recently acquired knowledge to the visco-elastic domain in order to account, in part, for some of the diverse range of geological folds observed in nature.

The implementation of these ideas involves three key steps:

- the selection of suitable mathematical models and the derivation of their governing equations;
- the development of solution procedures, both classical and numerical, for the solution of these equations; and
- the application of these procedures to investigate the effect of various nonlinearities within the formulation.

The first step involves choosing a strut-on-foundation model to simulate the process of folding. A simple one-dimensional model suffices as it is known to capture many of the phenomena common to a variety of buckling problems, most importantly that of localization. Classical methods of solution, while only approximate, are useful for revealing the underlying structure of the nonlinear problem. An accurate and robust numerical technique is essential for tracing localized solutions as they evolve in time. In tandem, these methods provide an independent check on one another. The final step is to make use of these procedures to investigate the variety of solutions displayed by the governing equations. The emphasis throughout is on the qualitative features of these solutions rather than trying to model specific material behaviour.

1.6 Outline of thesis

This thesis is divided into seven chapters, a list of references, and four appendices. The early chapters deal with the subjects of geological folding and elastic buckling, although they do contain elements of original work. The major contributions come later with the development and application of a new numerical procedure for isolating localized solutions.

Chapter 2 concentrates on visco-elastic models for the time-dependent process of geological folding. First, the deformation process itself is described and then an account is given of various buckling models presented in the literature. Next, various forms of visco-elastic behaviour are discussed in terms of the fundamental rheological units of an elastic spring and a viscous dashpot. Linear Fourier analyses for the buckling of an elastic strut on elastic, viscous and visco-elastic foundations are then presented. These formulations are suitable for identifying characteristics of the solution when fold amplitudes are infinitesimally small. Finally, a rigid link model is used to introduce the concept of post-buckling in a closely related one-degree-of-freedom system.

Chapter 3 is devoted to the subject of elastic buckling in the strut model. This is important because it is the buckling instability of the purely elastic system that triggers the onset of a fold and which is the driving force behind its subsequent growth and evolution. The chapter begins with a review of methods for the analysis of elastic buckling, highlighting the important role that nonlinear terms have in determining the post-buckling behaviour of structures. The large-deflection equation governing the response of an elastic strut on a Winkler foundation is derived and the linearized form is considered to determine the behaviour of the solution for small deflections. Finally, a perturbation method is used to reveal the underlying structure of the post-buckling response of the system.

Chapter 4 describes the numerical methods which are employed throughout this thesis. It begins with a review of those methods which are suitable for the solution of localized boundary-value problems, distinguishing between initial-value (shooting) methods and boundary-value approaches. The procedure for solving the governing

partial differential equation is outlined, including how the conditions of rigid end displacement are enforced. In the remainder of the chapter, the numerical methods are validated by comparison with an analytical solution and alternative solution procedures.

Chapter 5 explores the potential of classical solution techniques for determining localized buckle patterns in the strut-on-foundation model. The chapter commences with an overview of the method of weighted residuals and variational principles, and a discussion of suitable trial functions for these methods. The benefits and limitations of two methods, one based on collocation and the other a Galerkin procedure, are examined. The latter method, while generating the better results, is restricted to the case of a purely elastic foundation (Whiting, 1996). The collocation method is an improvement of the modal approach presented by Hunt *et al.* (1996a). The results of both methods are compared with independent numerical solutions.

Chapter 6 investigates the effect of different sources of nonlinearity on the behaviour of the strut model. Two different models are studied. One uses linear strut theory together with a nonlinear foundation and is valid for small, but finite, deflections. The other uses nonlinear strut theory with a linear foundation and is capable of modelling arbitrarily large deflections. In either case, the evolution of non-periodic buckle patterns is examined under conditions of controlled end displacement. Some of these results are to be published shortly (Whiting & Hunt, 1996).

In Chapter 7 conclusions are drawn from the preceding research and areas worthy of further investigation are noted. Pointers are given as to how other features may be incorporated in the model to investigate other phenomena.

Chapter 2

Folding of geological strata

This chapter introduces the time-dependent process of geological folding. It begins with a description of the deformation process itself and an account of theoretical buckling models presented in the literature. Different types of visco-elastic behaviour are discussed in terms of combinations of springs and dashpots. A model of an elastic strut on a visco-elastic foundation, which will be used extensively throughout this thesis, is defined. Linear Fourier analyses are presented for the three separate cases of an elastic strut on an elastic, viscous and visco-elastic foundation. These formulations are suitable for identifying characteristics of the folding process when amplitudes are very small. Finally, a rigid link model is used to illustrate aspects of the nonlinear post-buckling response of a closely related system.

2.1 Introduction

Folds are a common feature found in deformed rock and usually develop as a result of a buckling instability arising from a collision between tectonic plates. They occur on all levels, from the microscopic to the regional, and exist in a diverse range of rock compositions and environmental conditions. As a result they display an incredible variety of shapes and sizes. Minerals and hydrocarbons are often associated with folds, in concentrations which are economically viable for extraction. So there are commercial as well as academic interests in understanding how folds develop.

While there is a well established bulk of work pertaining to the appearance, description and classification of folds, the mechanisms of their formation are still poorly understood. Specifically, it appears that results gained from mathematical models do not reflect the complexity of shapes and forms observed in nature (Mühlhaus *et al.*, 1994).

2.1.1 The geological process of folding

In the upper levels of the earth's crust the contrast between rheological properties of adjacent layers of rock tends to be large, providing the necessary ingredients for the development of folds. Although the mechanisms leading to their formation are complex and not well understood, structural geologists recognize four main stages in the progressive development of a mature fold. These are described in Chapter 15 of the text by Price & Cosgrove (1990), entitled "The life and times of a buckle fold."

A typical scenario involves a competent layer of sandstone or limestone, say, embedded in a softer medium such as shale. A collision between tectonic plates, or a similar event, is followed immediately by a period of *homogeneous thickening* of the layer. This is a stable process which becomes unstable with the onset of *fold initiation.* The instability may be triggered by a geometric irregularity, such as local layer thickening, or by local variations in rheological properties of the layer or embedding medium. The transition from homogeneous thickening to folding is unlikely to be abrupt and is probably characterized by a progressive localization of deformation within the layer. The resistance to deformation falls as strain-softening sets in, causing the rate of deformation to increase. Fold initiation is, therefore, followed by a rapid growth in the amplitude of the buckle. This continues until some geometrical or mechanical constraint results in the onset of strain-hardening, causing the process of folding to slow, and eventually cease. This is known as the *finite development* stage. At this point the fold is said to have locked up and further shortening of the layer takes place by *post-buckle flattening.*

2.1.2 Approaches to understanding the development of folds

Geologists use three complementary techniques to help them understand the formation of folds. These are: field work, theoretical analyses and experimental work. *Field work* provides a description and classification of various naturally occurring folds and is often used as a reference with which to compare the results of theoretical and experimental studies. The extent to which geometrical characteristics of folds and internal strain distribution can be used to determine the history of deformation is described by Hudleston & Lan (1993). Many *theoretical analyses*, including a number of buckling theories, have been proposed to account for the phenomenon of folding. However, the range of parameters which control the development of folds is so large that no single theory of buckling can completely account for all types of folding behaviour. *Experimental work*, using real rocks or analogue materials, helps not only in understanding fold initiation and growth, but also provides valuable information about the rheological properties of rocks. An example is the experimental verification presented by Biot *et al.* (1961) of his own folding theories for elastic and viscous media in compression (Biot, 1961).

2.2 Developments in the analysis of folding

The process of geological folding is often idealized as a thin layer of rock under axial compression surrounded by a thick layer of softer material. The ensuing instability models the evolution of a fold in a geological environment, from an initially horizontal state to its final deformed shape. The rheological behaviour of the layer and embedding medium are typically assumed to be either elastic, viscous, plastic or a combination of all three. A number of reviews of theoretical buckling models are available in the literature (Ramsay, 1967; Hobbs *et al.*, 1976; Johnson, 1977; Price & Cosgrove, 1990).

2.2.1 Linear buckling theories

Beam theory was first introduced to geologists by Willis (1894) to account for the formation of fold trains in mountain belts. Another pioneer was Smoluchowski (1909)

who modelled the deformation of the earth's crust on a soft mantle, treating it as an elastic layer floating on a dense fluid. In the 1940s several engineers (Gough *et al.*, 1940; Bijlaard, 1946) investigated the buckling of an elastic layer in a soft elastic medium. These analyses were based on plate theory and restricted the problem to one of static instability. Purely elastic theories, however, are unlikely to explain real geological phenomena as viscosity is required to account for their time-dependent nature.

Biot (1957) considered an elastic layer of thickness h in a viscous matrix and found that, for a constant load P, there is a stable wavelength,

$$L_d = \pi h \sqrt{\frac{E}{(1-\nu^2)P}}, \tag{2.1}$$

where E is Young's modulus and ν is Poisson's ratio. Disturbances of this wavelength exhibit the maximum rate of growth in time and, because of this selective amplification, the shape of the deformed layer is eventually dominated by this wavelength. Biot (1961) called this the *dominant wavelength.* Similarly, for a buckling model involving a viscous layer, of viscosity η, embedded in a viscous matrix of viscosity η_b, Ramberg (1959) and Biot (1965) report a prevailing wavelength

$$L_d = 2\pi h \sqrt[3]{\frac{\eta}{6\eta_b}}. \tag{2.2}$$

Although these analyses were restricted to fold initiation, the principal results concern the relationship between the wavelength/thickness ratios and competence contrast between layer and matrix. The dominant wavelength theories of Biot (1957; 1959; 1961) and Ramberg (1959; 1960) suggest that a layer with many random small imperfections embedded in a weaker viscous matrix will develop into a regular train of folds when subjected to a constant end load. The dominant wavelength in an elastic system depends on the magnitude of the applied load and properties of the layer, yet is independent of the viscosity of the surrounding medium. By contrast, the dominant wavelength of the viscous system depends on the ratio of layer and matrix viscosities and the layer thickness.

Maurice Biot is generally regarded as having contributed more than any other individual to the present understanding of folding. His pioneering studies, though strictly valid only for infinitesimal deflections, have provided direction for all other studies to date. Besides the dominant wavelength expressions for a thin layer in a viscous medium, he also introduced the idea of wavelength selection to folding theory, developed general anisotropic models for layered visco-elastic media, and derived one of the early first-order solutions for the buckling of a deep beam (Biot, 1965).

The main characteristic of these early theoretical studies is their dependence on the critical load obtained by a linear stability analysis. They typically assume conditions of plane strain, small amplitudes, sinusoidal profiles, and linear rheological properties. They tend also to neglect gravitational effects and adherence between layers. The advantage of such linear theories is that second-order terms are extremely small and can be ignored. While this considerably simplifies the mathematics of the problem, it limits their application to the very early stages of deformation. Linear theories cannot be used to predict changes of layer thickness or changes in the shape of folds as they develop. Geologists have traditionally resorted to laboratory and field work to gain insight into the amplification of buckling instabilities into finite structures.

Many of the shortcomings of these early buckling models have been overcome with the advent of computing facilities which have enabled effects arising from non-linear materials and large deflections to be modelled. Some of these studies are described in § 2.2.3.

2.2.2 Correspondence principle

Formal analogies between the rheological equations of visco-elasticity, involving *rates* of stress and strain, and those of elastic media, relating stress to strain, have been known for some time. Alfrey (1944) showed the analogy is applicable to problems involving incompressible and isotropic media. The complete analogy, including compressibility and anisotropy, was derived by Biot (1954) in the context of thermodynamics, and is referred to as the *correspondence principle*. A brief description

of the analogy is presented below for the case of a plate on a foundation. A more general and comprehensive account is provided by Biot (1957) and Flügge (1975).

The flexural deformation of an elastic plate, embedded in a general visco-elastic medium of vertical resistance F, and subjected to a compressive load P, is governed by the differential equation (Biot, 1965)

$$\frac{Eh^3}{12(1-\nu^2)} w'''' + Pw'' + F = 0. \tag{2.3}$$

In order to make use of the correspondence principle, the elastic coefficients E and ν are first expressed in terms of the Lamé constants G and λ, where

$$\frac{E}{(1-\nu^2)} = 4G\frac{G+\lambda}{2G+\lambda}. \tag{2.4}$$

The Lamé constants, G and λ, are in turn replaced by their corresponding visco-elastic operators $R(\partial_t)$ and $S(\partial_t)$, respectively, so that Equation (2.3) becomes

$$\frac{h^3}{12} B_s(w'''') + Pw'' + B_b(w) = 0, \tag{2.5}$$

in which $\partial_t = \frac{\partial}{\partial t}$, and

$$B_s = 4R_s(\partial_t)\frac{R_s(\partial_t)+S_s(\partial_t)}{2R_s(\partial_t)+S_s(\partial_t)}, \quad B_b = 4R_b(\partial_t)\frac{R_b(\partial_t)+S_b(\partial_t)}{2R_b(\partial_t)+S_b(\partial_t)}. \tag{2.6}$$

The operators $B_s(\partial_t)$ and $B_b(\partial_t)$ characterize the visco-elastic properties of the strut and surrounding medium. For an incompressible elastic strut $B_s = 4G_s$, while for an incompressible viscous base $B_b = 4\eta\frac{\partial}{\partial t}$.

The existence of a formal correspondence between linear elastic and visco-elastic problems means that the large volume of work which exists for elastic materials can be applied to problems of visco-elasticity. The ability to transfer solutions from the stability of elastic systems to the visco-elastic domain stems from the preservation of linearity of the stress-strain relations during linear visco-elastic deformation. Consequently, the solution of *nonlinear* visco-elastic problems cannot be derived from related elastic solutions using the correspondence principle.

2.2.3 Nonlinear theories

Buckling models which incorporate nonlinear rheological behaviour and which permit large deflections are valid beyond the initial phase of folding. They are more likely, therefore, to account for the variety of deformed structures observed in nature than are linear equations derived from first-order models. In general, the resulting nonlinear equations do not possess exact solutions and it is usually necessary to resort to approximate or numerical methods for their solution. For this reason, few studies of large-amplitude folding or nonlinear material behaviour were carried out prior to the availability of computers.

One of the first large-amplitude buckling studies in geology was prompted by the close resemblance between the meandering forms of ptygmatic folds and the highly deformed elastica rod (Johnson, 1970). More recently, Mühlhaus (1993) investigated the influence of geometric nonlinearities in the finite-amplitude buckling of a deep, extensible elastic layer in a viscous medium. This analysis was restricted to the case of constant axial stress and the results suggest that nonlinearities have a destabilizing influence which merely amplifies the behaviour of a linear stability analysis. The only significant difference is that a critical time is reached at which the amplitudes of the nonlinear problem become infinite.

In a subsequent paper, Mühlhaus *et al.* (1994) considered the influence of axial constraint on the buckling response of an elastic layer and a viscous layer embedded in a viscous medium. This model, unlike Biot-type models which have free ends, included a variable axial stress which was determined by the constraint of constant end-shortening. In the case of the elastic layer, the end-shortening was held constant after the application of load. During the initial stages of fold evolution the profile of the fold was governed by Biot's (1965) dominant wavelength. The fold then went through various transitional stages until, after infinite time, the appearance of the fold was dominated by the only stable mode — a half-sine wave over the length of the plate.

The papers of Mühlhaus (1993) and Mühlhaus *et al.* (1994) use semi-analytical procedures to approximate the solution of the nonlinear problem. Finite element methods (Triantafyllidis & Leroy, 1994; Barnichon, 1994) and finite difference meth-

ods (Zhang *et al.*, 1996) have also been applied to the problem of geological folding. Zhang *et al.* (1996) used a solid modelling code to examine the influence of initial imperfections in the geometry of the layer on the buckling process and resultant fold shapes. They employed a dynamic relaxation (finite difference) technique to solve the discretized equations for two different systems: a visco-elastic (Maxwell) layer in a medium of the same material, and an elasto-plastic (Mohr-Coulomb) layer also in a medium of the same material. This choice of two different types of rheology reflects the difficulty in prescribing appropriate mechanical flow laws in complex geological conditions. Ord (1991) suggests that elasto-plastic models are applicable to folding of rocks in the upper crust while visco-elastic rheology is more appropriate for rock behaviour at high temperatures or deeper lithospheric levels.

Zhang *et al.* (1996) found that fold growth is very small in the early stages of deformation, wavelength and amplitude being stabilized at the values of the initial perturbations. However, after a certain amount of axial displacement, a period of explosive growth takes place with the onset of wavelength selection. After a period of time, the growth of the fold slows down. This growth feature is consistent with the results of Mühlhaus *et al.* (1994) for velocity boundary conditions. Zhang *et al.* (1996) also show that fold growth is exponential if stress boundary conditions are used. The occurrence of constant stress is an unlikely condition for natural folding and is one of the major shortcomings of early linear theories. The authors suggested that single-layer buckling is essentially a process of selection, amplification and propagation of initial perturbations, subject to the influence of competence contrast (the ratio between material properties of the layer and embedding matrix). They concluded that the indeterminate number of initial imperfections and competence contrasts which exist in natural situations probably accounts for the complexity of natural folds.

Figure 2.1 shows two sets of results obtained by Zhang *et al.* (1996) for a single isolated imperfection in the centre of a layer. The evolution sequence (a) for a visco-elastic system shows that the early stages of folding are dominated by a gradual amplification of the initial imperfection, with the remainder of the layer remaining relatively flat. As the end displacement increases, new perturbations form in the

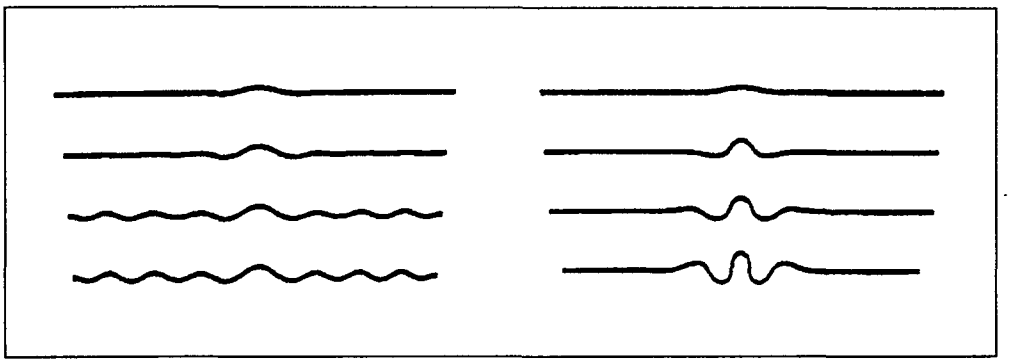

Figure 2.1 Fold development from an initial imperfection in a competent layer: (a) visco-elastic layer and matrix; and (b) elasto-plastic layer and matrix (after Zhang *et al.* (1996)).

layer adjacent to the initial imperfection through a sideways propagation. This development of folds correlates closely with the progressive fold propagation theory of Cobbold (1975). For the elasto-plastic model (b), a yield point develops at the point of maximum amplitude in the initial imperfection. The onset of plastic yielding means that further deformation occurs preferentially in this area, resulting in a localized fold train. The formation of new folds along the layer is less prominent than for the visco-elastic material.

Barnichon (1994) used a finite element code (Geosim-2D) to study the growth of fold structures from initial periodic imperfections in purely elastic systems. The program he used was developed especially for simulating geological deformations, both faults and folds. It uses a Green-Lagrange strain tensor to model large deflections of a layer, unlike many other finite element packages which use an incremental deformation tensor. The report by Barnichon (1994) was a parametric study to identify the effect of length and thickness on the dominant wavelength of an embedded layer. Like the earlier studies, controlled end-shortening was used to deform the layer and surrounding matrix. His numerical studies were confined to the development of purely periodic forms in elastic structures and are, therefore, of limited significance to this study.

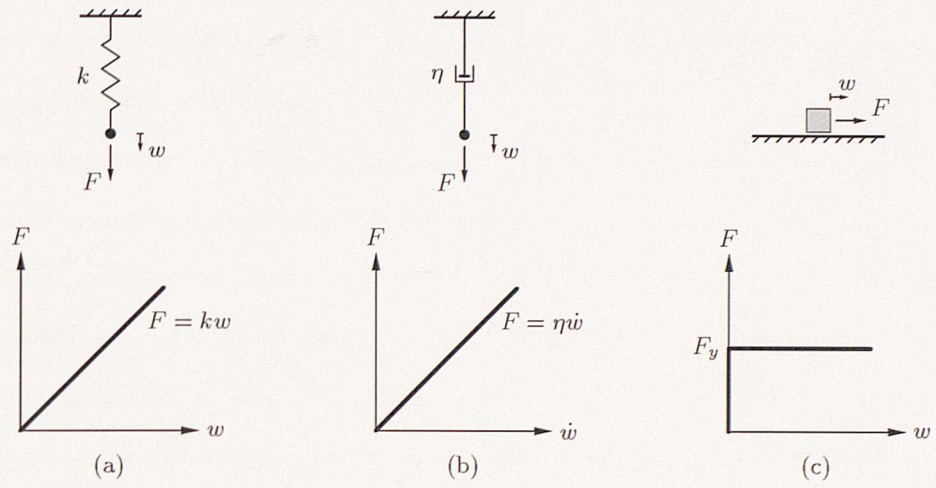

Figure 2.2 Fundamental rheological models: (a) an elastic spring (Hookean model); (b) a viscous dashpot (Newtonian model); and (c) an elasto-plastic block (St. Venant model).

The instability of a layer resting on a halfspace has also been discussed by Vardoulakis & Sulem (1995) and Johnson & Fletcher (1994). The first authors used a theory based on incremental continuum mechanics to investigate folding of elastic and visco-elastic media as a bifurcation problem. Their analysis is particularly suitable for multi-layers and materials with microstructure, neither of which are dealt with in this thesis. The treatment by Johnson & Fletcher (1994) is confined to the folding of viscous layers and gives no consideration to elastic layers.

2.3 Rheological models

The behaviour of rock under stress is often described using the analogous mechanical models shown in Figure 2.2. The fundamental models are a spring, a dashpot and a block, representing elastic, viscous and plastic behaviour, respectively. These models may be combined in various ways to form compound rheological models whose behaviour under stress mimics that of rock materials established by laboratory experiments (Ramsay, 1967). The elements whose combination represents linear visco-elasticity are the linear spring, which obeys Hooke's law, $F = kw$, and represents an ideal elastic solid, and the dashpot, which is filled with a Newtonian fluid obeying the relation $F = \eta\dot{w}$, where $\dot{w} \equiv \frac{\mathrm{d}w}{\mathrm{d}t}$. The spring modulus, k, and dash-

pot viscosity, η, are assumed to remain constant with time, in contrast to the aging behaviour used in models of concrete creep (Bažant & Cedolin, 1991). Plasticity is not considered in this thesis.

The behaviour of deforming rock is a complex process which is affected by temperature, chemical environment and numerous other factors. There are also many mechanisms of internal deformation, for example, grain boundary movement and development of crystal dislocations. As none of the rheological models relates directly to the structure of matter, it is impossible for them to offer more than a qualitative description of rock behaviour under stress. Nevertheless, realistic descriptions of the time-dependent deformation of rock may be obtained by combining the fundamental models together. The main compound rheological models are described next.

2.3.1 Maxwell model

In the late 19th century J. C. Maxwell, from Britain, first described visco-elastic material behaviour using a spring and dashpot connected in series, as depicted in Figure 2.3 (a). The motion of the perforated piston inside the dashpot produces a resisting force in the liquid which is proportional to the velocity of the piston. With the spring and dashpot arranged in series, the unit exhibits an instantaneous elastic response when stressed. The total deformation, w, is the sum of the elastic deformation, w_s, and viscous deformation, w_d. The corresponding differential equation, describing the time-dependent stress-strain (or force-displacement) relationship, is

$$\frac{1}{k}\dot{F} + \frac{1}{\eta}F = \dot{w}. \tag{2.7}$$

When a Maxwell model is subjected to a sudden displacement of one end, the entire stress is taken by the spring, the development of viscous strain requiring finite time. If the boundary displacement then remains constant, the stress in the spring gradually induces viscous deformation of the dashpot and the spring stress diminishes asymptotically to zero. This response is known as *stress relaxation* (see Figure 1.4). Alternatively, if the model is subjected to a constant force, the deformation grows linearly after the instantaneous elastic response. This represents constant rate of strain, or *creep* (see Figure 1.3).

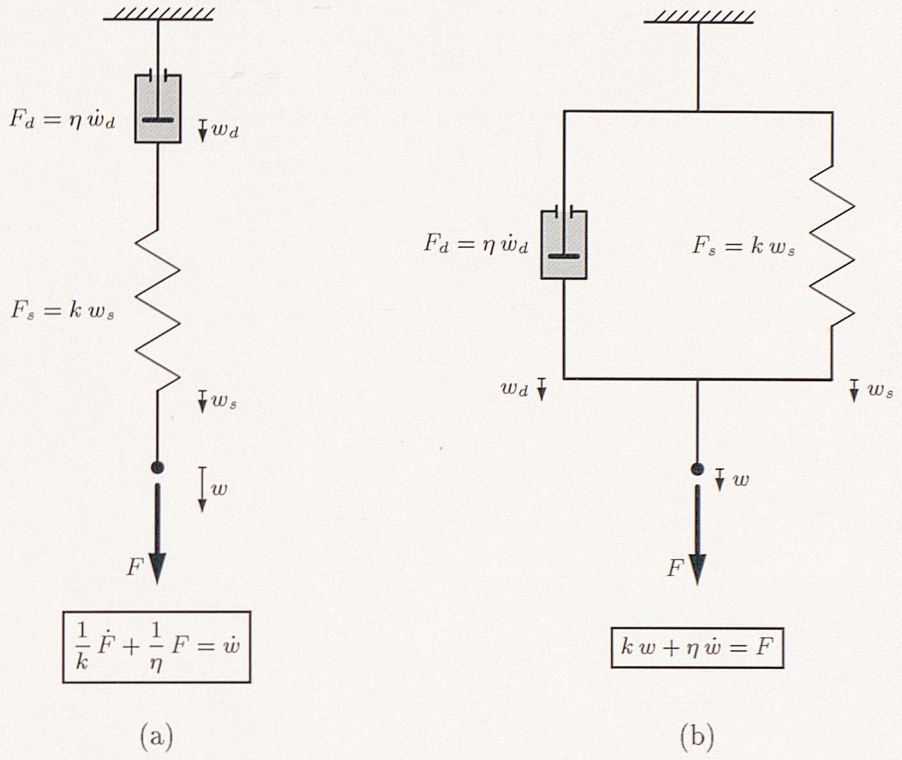

Figure 2.3 Visco-elastic models: (a) Maxwell model; and (b) Kelvin-Voigt model.

2.3.2 Kelvin-Voigt model

Real materials rarely behave like perfect solids and it is often found that some time elapses after the application (or removal) of an applied stress, before the system responds. Lord Kelvin, from Britain, and Voigt, of Germany, used a simple model to describe this damping mechanism by combining a spring and dashpot in parallel, as shown in Figure 2.3 (b). The total stress, F, applied to a Kelvin-Voigt model is the sum of the elastic stress, F_s, and viscous stress, F_d, and the corresponding differential equation is

$$F = k\,w + \eta\,\dot{w}. \tag{2.8}$$

In contrast to the Maxwell model, there is no instantaneous elastic deformation after the application of a load. Instead, viscous movement of the dashpot is required before elastic strains can develop. Under constant stress the deformation increases asymptotically from zero to its final, elastic value, as shown in Figure 1.3.

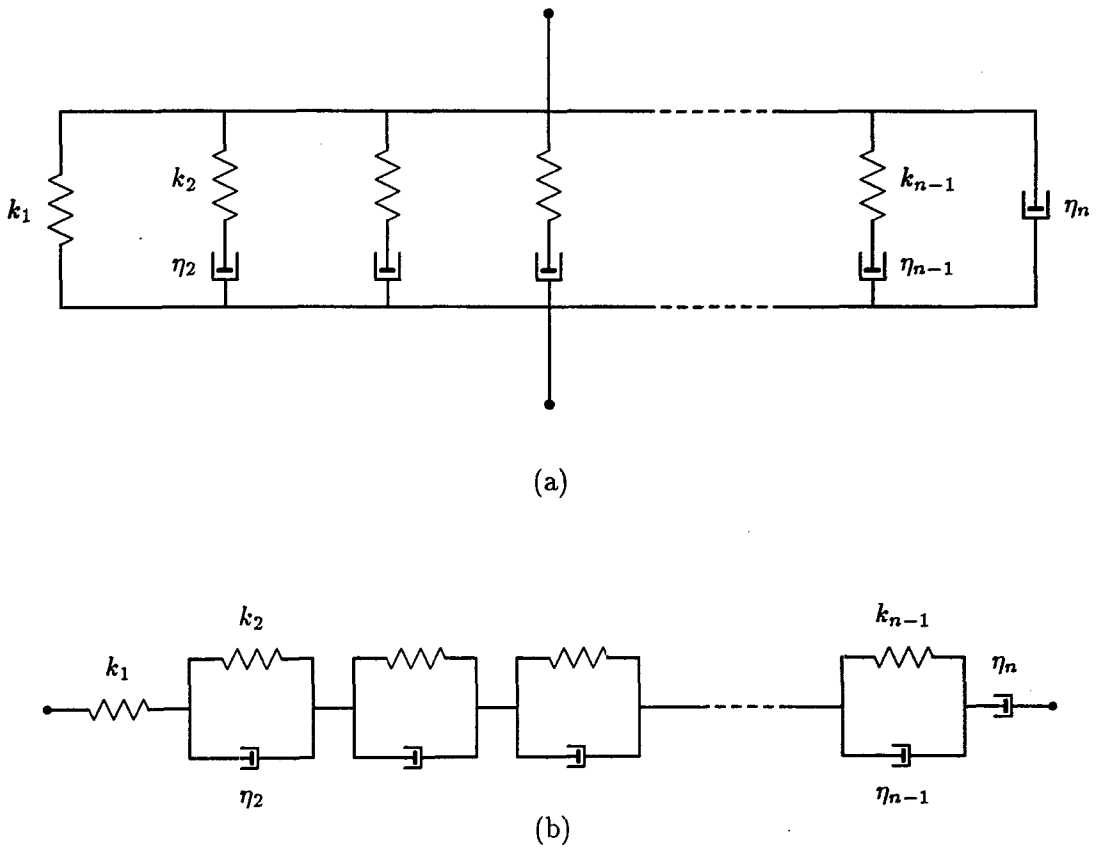

Figure 2.4 Visco-elastic chains: (a) Maxwell chain; and (b) Kelvin chain.

2.3.3 Other visco-elastic models

Roscoe (1950) showed that all types of linear visco-elastic behaviour, which can be represented by combinations of springs and dashpots, may be described using one of two canonical models. His work made use of the analogy between electrical circuits and mechanical systems in which resistors are replaced by springs and dashpots by capacitors; the relation between current and potential difference in an electrical network is then equivalent to that between force and extension in the mechanical model. The two canonical models are: a Maxwell chain, comprising a sequence of Maxwell units coupled in parallel, and a Kelvin chain, consisting of a number of Kelvin-Voigt units in series. These Maxwell and Kelvin chain models, shown in Figure 2.4, are capable of describing all forms of linear visco-elastic behaviour, so there is no need for other arrangements of springs and dashpots to be considered.

The differential equation for both chain models has the general form

$$\mathbf{P}[F(x,t)] = \mathbf{Q}[w(x,t)], \tag{2.9}$$

where the differential operators $\mathbf{P}$ and $\mathbf{Q}$ are defined as

$$\begin{aligned} \mathbf{P} &= p_0 + p_1 \frac{\partial}{\partial t} + p_2 \frac{\partial^2}{\partial t^2} + \cdots, \\ \mathbf{Q} &= q_0 + q_1 \frac{\partial}{\partial t} + q_2 \frac{\partial^2}{\partial t^2} + \cdots, \end{aligned} \tag{2.10}$$

in which p_i and q_i are material constants relating to spring stiffnesses and dashpot viscosities. For a Maxwell model, the constitutive relation (2.7) is retrieved by setting $p_0 = \frac{1}{\eta}$, $p_1 = \frac{1}{k}$, $p_i = 0$ for $i \geq 2$, and $q_1 = 1$, $q_i = 0$ for $i \neq 1$. For linear material behaviour, Laplace transformations can be used to manipulate the differential equation (2.9) into an algebraic relation between stress and strain (Flügge, 1975).

Visco-elastic materials may be classified as fluids or solids. *Fluids* are those materials for which the creep curve at constant stress is unbounded, for example, the viscous element and Maxwell model. When the creep curve is bounded the material is called a *solid*, for example, the elastic element and Kelvin-Voigt model. The Maxwell chain represents a solid if at least one Maxwell unit in the chain is without a dashpot. The Kelvin chain represents a solid provided no Kelvin-Voigt units are without springs. In general, if a path exists through a chain which traverses only spring elements, the model represents a solid. Conversely, if a path exists traversing only dashpot elements, the model represents a fluid, unless there is an alternative path involving only springs. In reality it is often difficult to distinguish between the two, especially for very slow rates of deformation.

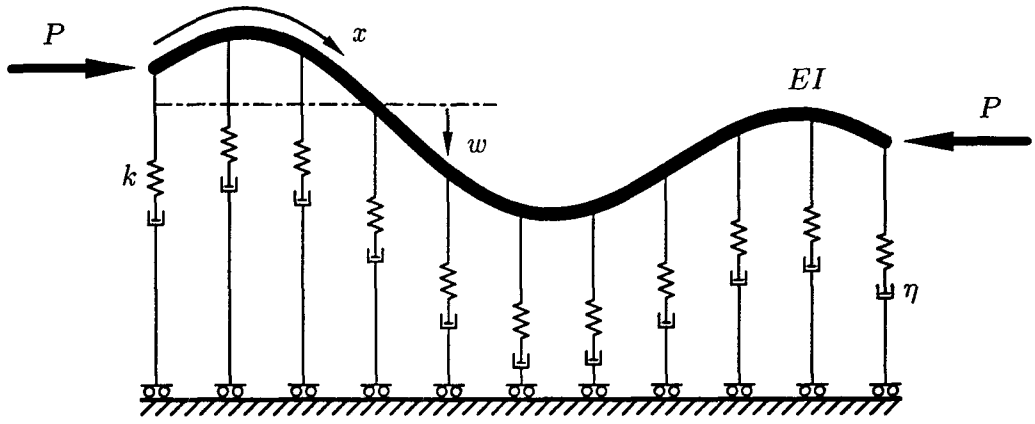

Figure 2.5 Model of an elastic strut on a visco-elastic (Maxwell) foundation.

2.4 Strut-on-foundation model

The process of folding may be modelled using an incompressible elastic strut, of flexural stiffness EI, embedded in a visco-elastic medium of vertical resistance per unit length F, and compressed horizontally by an axial load P. For the strut model shown in Figure 2.5, the governing equation is

$$EI\left[w''''\left(1-w'^2\right)^{-1}+4w'''w''w'\left(1-w'^2\right)^{-2}+w''^3\left(1+3w'^2\right)\left(1-w'^2\right)^{-3}\right] + Pw''\left(1-w'^2\right)^{-3/2}+F=0, \tag{2.11}$$

where F obeys the Maxwell relation (2.7). The derivation of this equation is deferred until the next chapter.

Inertia terms are ignored on the premise that geological folding is an inherently slow process requiring many thousands of years (Price & Cosgrove, 1990). The effect of neglecting axial inertia terms is to assume that the axial wave speed far exceeds the bending wave speed, so the axial force along the length of the strut is identical everywhere to the external load.

2.4.1 Maxwell foundation

A Maxwell foundation of the Winkler-type is chosen for the strut model so that the immediate response of the system mirrors that of pure elasticity, yet in the long-term is governed by the viscous component of the embedding medium. This choice of

foundation is based on the increasing acceptance by geologists of the importance of elasticity in the early stages of fold formation. This situation is succinctly expressed by Price & Cosgrove (1990):

> "...elastic behaviour governs fold initiation in the upper levels in the crust ...Geologists for the last two decades have been misleading themselves by ignoring this situation."

Maxwell constitutive relations have been used extensively in buckling models for folds (Biot, 1959; Chapple, 1968; Zhang *et al.*, 1996). This is because the Maxwell model is well-suited to modelling the response of the earth's crust, which is observed to undergo short-term elastic deformation when subjected to a rapid loading, but which gradually flows if the load is maintained for long periods (Turcotte & Schubert, 1982). This idea is supported by Johnson & Fletcher (1994) who suggest that on short geological time scales (1–10^4 seconds) rocks act as elastic solids, as evidenced by the fact that seismic shear waves propagate through the earth's mantle with relatively little attenuation, and behave as viscous fluids on large geological time scales ($> 10^{11}$ seconds). In particular, a Maxwell model can predict the irrecoverable deformation of rocks at high temperature, slow strain rates and high confining pressures (Zhang *et al.*, 1996).

2.5 Linear Fourier analysis

In this section the linear equation for the strut model is examined to identify features of the folding process when amplitudes are very small. The small displacement response is governed by the equation (Biot, 1965)

$$EI\frac{\partial^4 w}{\partial x^4} + P\frac{\partial^2 w}{\partial x^2} + F = 0, \tag{2.12}$$

where x is measured horizontally. The vertical deflection w is expressed as an infinite set of Fourier components with amplitudes a_m,

$$w = \sum_{m=0}^{\infty} a_m \cos \beta_m x, \tag{2.13}$$

and the bedding force is similarly defined,

$$F = \sum_{m=0}^{\infty} F_m \cos \beta_m x, \tag{2.14}$$

where $\beta_m = 2\pi m/L$. Inserting these periodic forms in the differential equation (2.12) and collecting coefficients results in the amplitude equation

$$EI\beta_m^4 a_m - P\beta_m^2 a_m + F_m = 0. \tag{2.15}$$

Now the response of the system, measured in terms of the amount of each of the harmonic components, can be examined for different types of foundation behaviour.

2.5.1 Elastic foundation

Consider an embedding medium which is purely elastic. The amplitudes of the bedding force are related to the amplitudes of the buckle pattern by the Winkler relation

$$F_m = k a_m, \tag{2.16}$$

where k is the foundation stiffness. After substituting F_m into Equation (2.15) and rearranging, the following expression is found

$$P = EI\beta_m^2 + \frac{k}{\beta_m^2}, \tag{2.17}$$

in which each wavenumber β_m is associated with a different critical load. Differentiating this expression with respect to β_m and equating the result to zero gives the minimum critical load

$$P^{\mathrm{c}}_{\mathrm{min}} = 2\sqrt{k\,EI}, \tag{2.18}$$

and corresponding mode

$$\beta^{\mathrm{c}}_{\mathrm{min}} = \sqrt[4]{\frac{k}{EI}}. \tag{2.19}$$

Thus, for an elastic strut on an elastic foundation, a sinusoidal buckle pattern of wavelength $L = 2\pi/\beta^{\mathrm{c}}_{\mathrm{min}}$, emerges at the minimum critical load $P^{\mathrm{c}}_{\mathrm{min}}$. This wavelength depends on the material properties but is independent of the length.

2.5.2 Viscous foundation

Now suppose the supporting medium is purely viscous, so that the amplitudes of the bedding force F are

$$F_m = \eta \dot{a}_m, \tag{2.20}$$

where η is the bedding viscosity, and $\dot{()} \equiv \frac{\partial}{\partial t}$. Substituting F_m into Equation (2.15) gives

$$EI\beta_m^4 a_m - P\beta_m^2 a_m + \eta \dot{a}_m = 0. \tag{2.21}$$

The variation of amplitude for each mode with time is assumed to have the form of the eigenmode solution $a_m = A_m e^{\omega_m t}$, leading to the *dispersion relation*

$$\omega_m = \frac{1}{\eta}\left(P\beta_m^2 - EI\beta_m^4\right), \tag{2.22}$$

which determines the frequency ω_m for a given wavenumber β_m. Thus, a single buckle profile represented by a sum of modes will change its shape as time evolves by virtue of the different growth rates of the constituent modes, causing the profile to spread out or "disperse".

For conditions of constant load, at time t all wavelengths apart from that for $m = 0$ have a nontrivial form. Plotting ω_m against β_m gives the curves of Figure 2.6. The wavelength of the most rapidly growing amplitude, which occurs when ω_m is a maximum, is found by setting $\mathrm{d}\omega_m/\mathrm{d}\beta_m = 0$. The associated wavenumber is

$$\omega_d = \frac{P}{2\eta}\beta_d, \quad \text{where} \quad \beta_d = \sqrt{\frac{P}{2EI}}. \tag{2.23}$$

This corresponds to the *dominant wavelength* of Biot (1965) for an incompressible elastic plate on a viscous foundation given in Equation (2.1). The most noticeable feature of this expression is that the wavelength depends on the applied load, in contrast to the previous elastic system. A useful relation exists between the dominant viscous wavenumber β_d and the minimum-load elastic wavenumber $\beta^{\mathrm{c}}_{\mathrm{min}}$:

$$\beta_d = \beta^{\mathrm{c}}_{\mathrm{min}} \sqrt{\frac{P}{P^{\mathrm{c}}_{\mathrm{min}}}}. \tag{2.24}$$

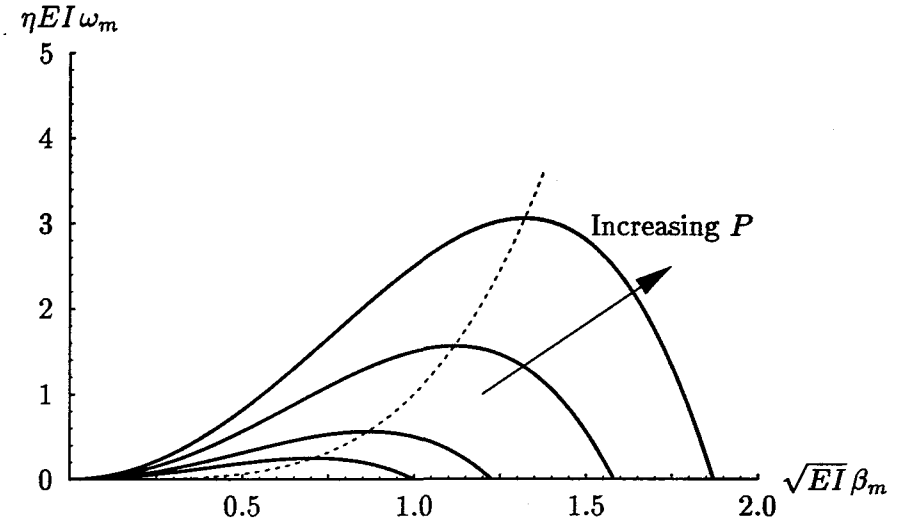

Figure 2.6 Dispersion relations for an elastic strut in a purely viscous medium.

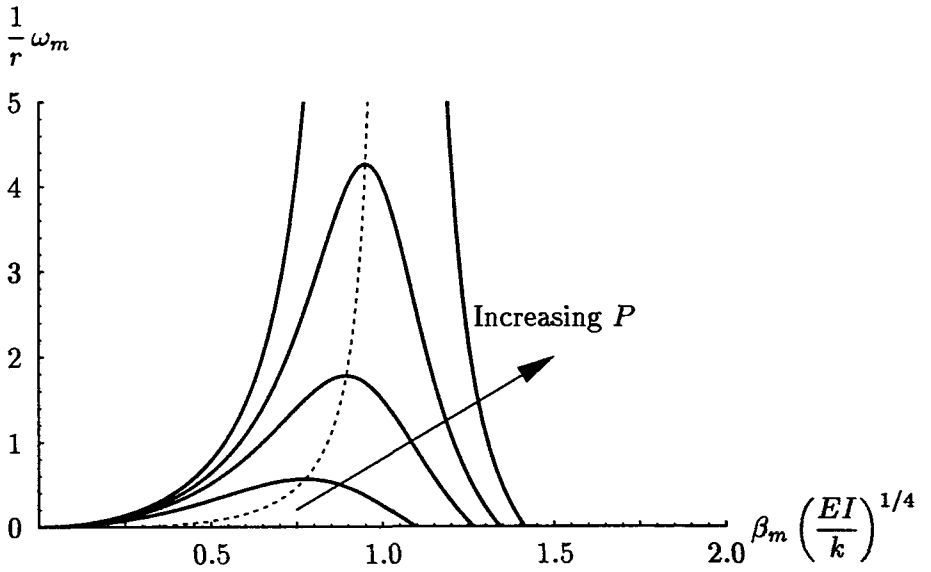

Figure 2.7 Dispersion relations for an elastic strut in a visco-elastic medium.

2.5.3 Visco-elastic foundation

The strain rate equation for a bedding material with a Maxwell constitutive law is

$$\frac{1}{k}\dot{F}_m + \frac{1}{\eta}F_m = \dot{a}_m. \tag{2.25}$$

Under conditions of constant load ($\dot{P} = 0$), and with the same assumption of periodicity in x and eigensolution as before, the visco-elastic dispersion relation is

$$\omega_m = r\,\frac{P{\beta_m}^2 - EI{\beta_m}^4}{EI{\beta_m}^4 - P{\beta_m}^2 + k}, \tag{2.26}$$

where $r = k/\eta$. Plotting ω_m against β_m gives the family of curves shown in Figure 2.7. As P approaches the elastic critical load $P^c_{\min}$, the denominator of Equation (2.26) vanishes and ω_m approaches infinity.

2.6 Rigid link models

Mechanical models, consisting of rigid links and linear springs, have often been used to gain insight into the nonlinear response of more complex systems (Hayman, 1978; Providência e Costa, 1994). In this section such a model is used to introduce a number of important concepts of stability. The model, which has a single degree of freedom, displays many of the features of the continuous problem of a strut on a foundation, yet is amenable to exact nonlinear analysis. It is particularly useful for demonstrating the effect of bending stiffness and foundation stiffness on the post-buckling response of the purely elastic system and for observing the contribution of a time-dependent foundation.

The simple mechanical model, shown in Figure 2.8, consists of two simply-supported rigid bars of negligible mass connected at the centre pin by a rotational spring and a Maxwell unit. The rotational spring represents the bending stiffness of an elastic strut while the vertical spring-dashpot unit corresponds to the resistance provided by a visco-elastic foundation. The springs and dashpot are assumed to respond linearly with spring constants s and k, and dashpot viscosity η. The governing equation for the rigid link model may be obtained by considering the forces

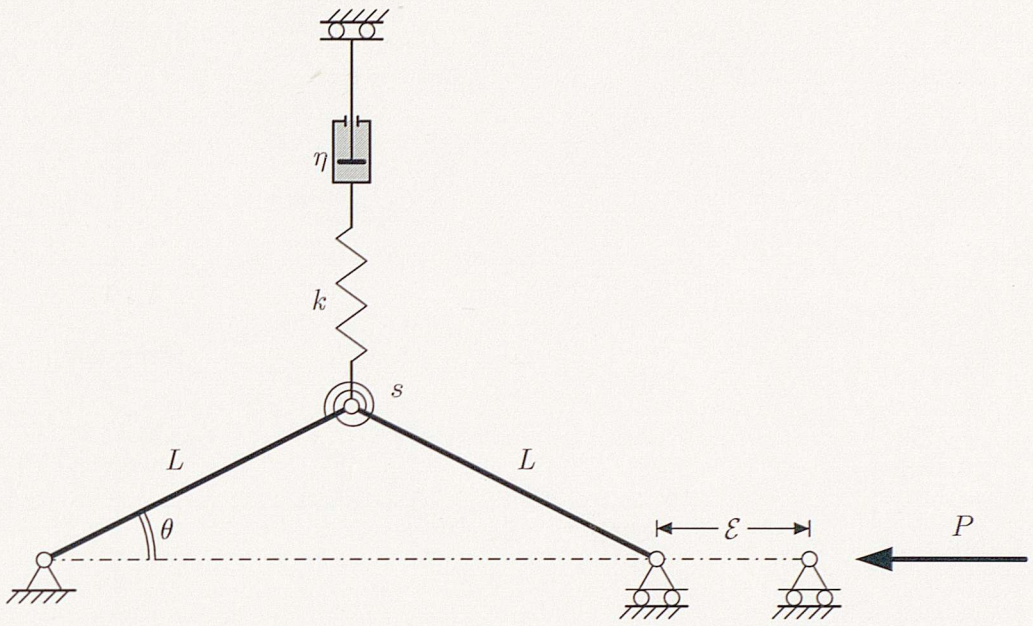

Figure 2.8 One-dimensional rigid link model supported by a Maxwell unit.

acting on half the structure. Taking moments about one end leads to the equilibrium equation

$$\frac{1}{2}FL\cos\theta + 2s\theta - PL\sin\theta = 0, \tag{2.27}$$

where P is the applied load, F is the vertical resistance of the Maxwell unit acting on the central pin, and θ is the angle of inclination of each link from the initially horizontal position. When the model is subjected to a sudden displacement of the end, it adopts the equilibrium position shown in the figure. For a Maxwell foundation, the response is characterized by two phases: an instantaneous phase of elastic deformation followed by a period of visco-elastic flow as the dashpot begins to move.

2.6.1 Elastic foundation

Consider first the initial response where the dashpot does not have time to respond. The foundation reaction is therefore purely elastic and proportional to the vertical displacement of the centre pin, so that $F = kL\sin\theta$. Thus, providing $\theta \neq 0$, the load for the post-buckled state is

$$P = \frac{2s}{L}\frac{\theta}{\sin\theta} + \frac{1}{2}kL\cos\theta. \tag{2.28}$$

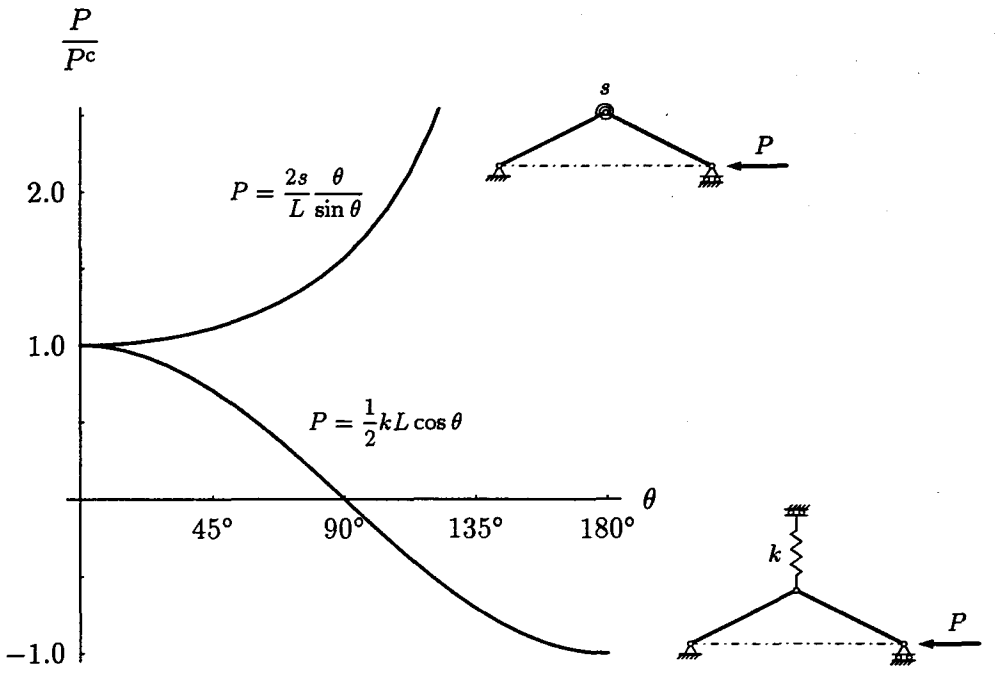

Figure 2.9 Post-buckling behaviour for degenerate rigid link models.

To appreciate fully this post-buckling response, observe the individual contributions for each linear spring shown in Figure 2.9. When the model is constrained by a rotational spring only, corresponding to the case of no foundation response ($k = 0$), the post-buckling response is stable with increasing end load required to induce further deformation. This corresponds very closely with the post-buckling response of an Euler column without a supporting foundation (Allen & Bulson, 1980). In contrast, when the model is constrained by a vertical spring alone, the case of no bending stiffness ($s = 0$), the response is an unstable symmetric bifurcation with the equilibrium path falling from the critical point. The curves in the figure are nondimensionalized with respect to the critical loads for each model. This is possible only when a reduced model is considered, having either a rotational spring or a vertical spring but not both.

Given that rotational and vertical spring models exhibit such contrasting post-buckling characteristics, a natural question to ask is: what happens when both springs are present simultaneously? This is, after all, the model for a strut on an elastic foundation. The answer is that either stable or unstable post-buckling behaviour is possible depending on the relative magnitudes of the spring stiffnesses.

This point is illustrated in Figure 2.10 where the results are plotted in terms of a rotational spring parameter, $s^* = s/L$, and a vertical spring parameter, $k^* = kL$. The top figure shows various post-buckling solutions for a range of k^* values while s^* remains constant. These results are useful when considering the response of a strut of known bending stiffness resting on a foundation of unknown stiffness. The critical buckling load increases with k^* and there is an increasing tendency for unstable post-buckling behaviour to occur. In the lower figure, the values of s^* and k^* are scaled so the critical load is the same for each solution. This is useful when considering behaviour in a system where neither of the material parameters are clearly defined, as for example, in layers of rock.

The figures indicate that for low k^* values, in other words when the stiffness of the strut predominates, the equilibrium branch increases monotonically with increasing θ. For larger values of k^*, the equilibrium branch falls at first and then rises, a behaviour which is initially unstable under load control. It is the *relative* amounts of s^* and k^* (and hence s and k) that dictate whether the post-buckling behaviour of the system is stable or unstable. Identical results have been obtained in connection with the buckling response of floating ice sheets (Kerr, 1980) and axially compressed embedded layers with linear (Kerr, 1986) and nonlinear (Kerr, 1989) foundation reactions. Unlike the results for the degenerate models with only one restraining spring, the results here cannot be made independent of the spring constants. A final point of interest is that, like the Euler strut and unlike the axially compressed cylinder, the post-buckling behaviour of the rigid link model is not severe and is therefore not highly imperfection sensitive.

2.6.2 Visco-elastic foundation

Consider now the time-dependent response of the rigid link model when an initial angle of deformation θ_0 is maintained indefinitely. Recall that some of the initial (elastic) post-buckled states of the model are unstable under dead (constant) load conditions. Rigid load conditions must be used to ensure that all deformed configurations of the system can be attained. The evolution response of the model for $k^* = 2$ and $s^* = 0.5$ is shown in Figure 2.11. The initial response (curve A) corresponds

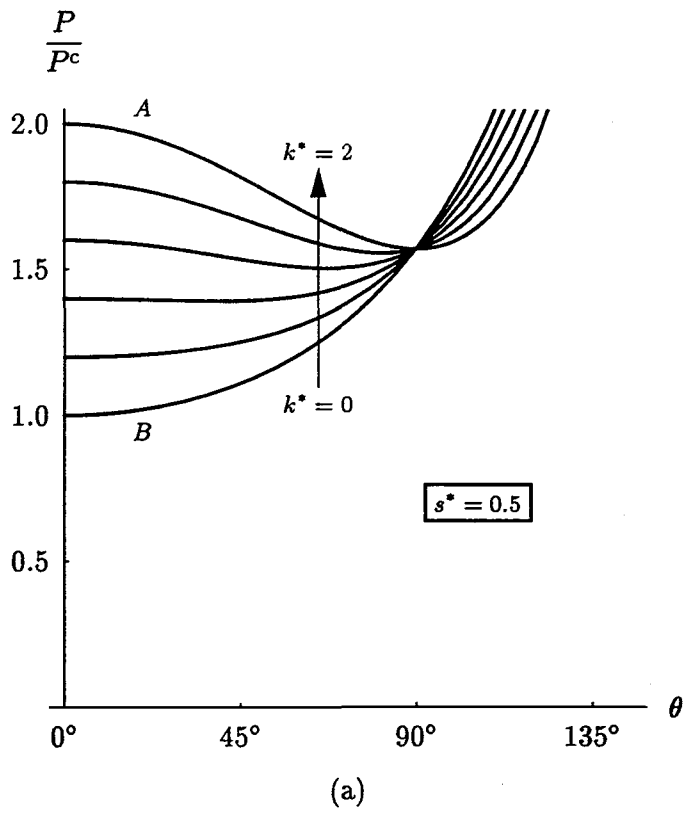

(a)

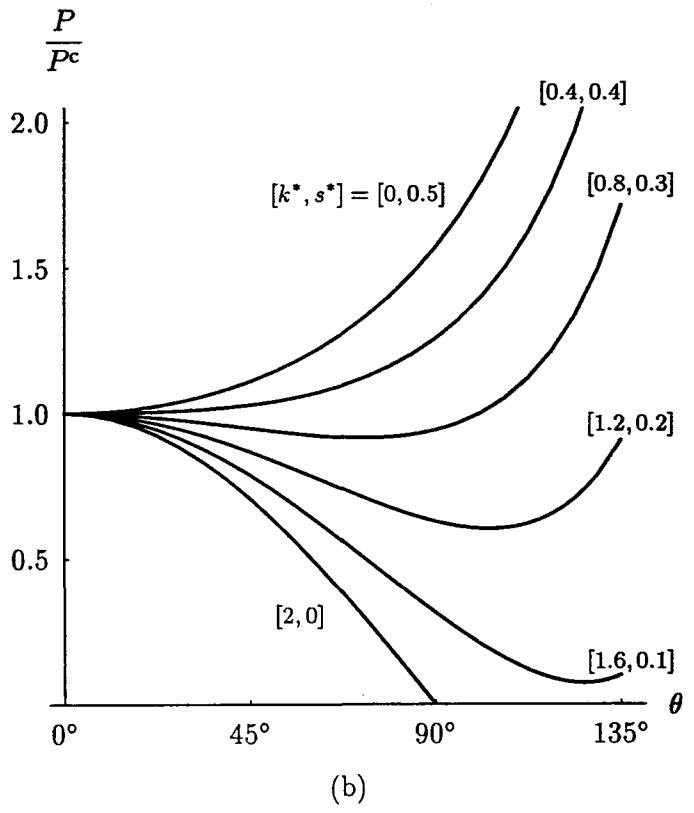

(b)

Figure 2.10 Post-buckling behaviour of rigid link model for different values of spring parameters k^* and s^*.

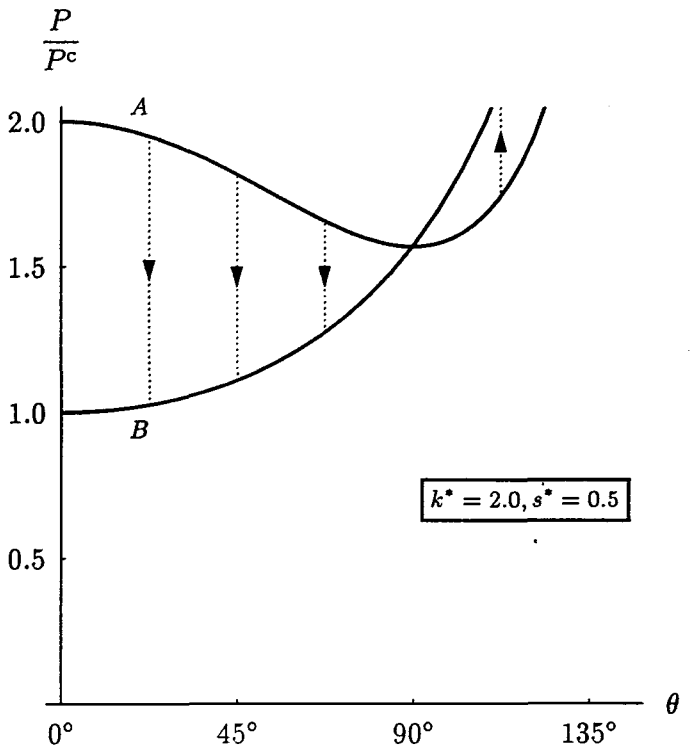

Figure 2.11 Evolution response of rigid link model supported by a Maxwell unit.

to the top curve of Figure 2.10 (a). As time passes, the stress in the vertical spring is alleviated by the viscous flow of the dashpot; ultimately, the bending energy of the strut is the only energy remaining in the system. The response in time is one of exponential decay with the passage of time indicated by arrows. The final state (curve B) corresponds to the lowest curve in Figure 2.10 (a) and coincides with the case of a simply-supported strut.

2.6.3 Chain models

The post-buckling behaviour of the rigid link model of the previous sections was a relatively straightforward bifurcation. The complexity is greatly increased if a number of these models, say n, are connected in series to form a chain. The potential then exists for a multiplicity of solutions as each cell has the capacity to buckle independently of adjacent cells. In the limit, as $n \to \infty$, there are infinitely many possible outcomes. Ikeda *et al.* (1993), Wadee (1996) and Hunt *et al.* (1996b) have used initial-value techniques to investigate the myriad of eventualities for the elastic

system, finding periodic, quasi-periodic, localized and chaotic solutions. Although the system admits a range of solutions, in reality, it is the solution that emerges from the bifurcation point with the least stiff response that is favoured. This is the primary localized solution, although it is not unique as it may develop in any part of the chain.

Recent applications of localized buckling patterns to the physical phenomenon of folding appear in unpublished works by Gattermann & Ulke (1994) and Wadee (1994). These authors considered the long-term behaviour of a discrete system subjected to a compressive load, and supported at the nodes by Kelvin-Voigt elements and Maxwell elements, respectively. They conducted a series of numerical experiments to determine the long-term response of rigid link models to various initially displaced configurations. The latter work, using springs and dashpots in series, is more pertinent to the work here. Wadee (1994) concluded that, under rigid load conditions, an initially localized buckle profile: tended toward periodicity if the end-shortening decreased with time; remained unchanged with time if the end-shortening was fixed; and became more localized if the end-shortening continued to increase with time.

2.7 Concluding remarks

The number of parameters governing the process of folding is so vast that no single theory of buckling can possibly account for all types of behaviour exhibited in the field. This is because theoretical models, in spite of their mathematical sophistication, are much less complex than the real geological situations they represent. The difficulty in modelling this natural process was aptly described by Johnson (1970):

> "It is not easy to understand, with theory or experiment, phenomena which have required millions of years to create."

Chapter 3

Buckling of elastic structures

The subject of this chapter is the buckling exhibited by elastic structures under conservative loading. This treatment is important because the underlying assumption for the model of a strut on a visco-elastic foundation presented in this thesis is that the buckling instability is triggered by the response of the purely elastic system. First, the major developments in methods for the analysis of elastic buckling are reviewed. The equation governing the response of a strut on an elastic foundation is then derived and the linearized form is analysed to reveal the behaviour of the solution when deflections are small. Finally, a perturbation method is used to reveal the underlying structure of the post-buckling response for the strut on an elastic foundation.

3.1 Developments in the analysis of elastic buckling

3.1.1 Historical perspective

The earliest consideration of elastic stability was by Euler (1744) who studied an elastic rod under axial compression. He employed his recently-developed *calculus of variations* to find minimum energy states of the rod and determined that as the load on the structure increased it eventually reached a *critical load*, where the fundamental equilibrium solution was no longer stable. This was the first bifurcation analysis of a structural system. It was, however, only much later that structural engineering

developed to the point where such a degree of mathematical sophistication became necessary (Hunt, 1983).

The theory of elastic stability then remained largely undeveloped until early this century when increasing use was made of plate and shell structures. *Linear eigenvalue analyses* by Timoshenko (1910) and Southwell (1914) could only determine the critical buckling load of these structures. They were unable to account for experimental observations which revealed that plates were capable of supporting compressive loads well above the critical load of the *perfect* structure while cylindrical shells collapsed catastrophically well below the critical load (Donnell, 1934).

It was not until Koiter (1945), in Holland, devised a general theory of elastic stability, accounting for both post-buckling effects and imperfections, that these observations could be adequately explained. He appreciated that elastic buckling was a large deflection phenomenon and that the associated nonlinearity was the key feature which previous works in structural engineering had overlooked. Koiter's theory was based on the concept of total potential energy for continuous structures and was able to explain, for the first time, the fundamental differences in the structural behaviour of struts, plates and shells.

Theories for discrete systems were developed independently in Great Britain by Thompson (1963) and Sewell (1965). These methods used a modal analysis or a finite element approach with localized shape functions to describe the buckle pattern and, like Koiter's theory, used the total potential energy as the basis for determining equilibrium and stability. The potential function was reduced to its simplest form by removing the contaminating effects of higher modes using a procedure known as the *elimination of passive coordinates.* In this way, the number of degrees of freedom of the system was reduced to the minimum necessary for an adequate description of the behaviour. This work resulted in a general bifurcation theory for elastic structures (Croll & Walker, 1972; Thompson & Hunt, 1973).

A great deal of work has been carried out on nonlinear post-buckling of elastic structures since the development of these independent frameworks and a number of general reviews are available (Hutchinson & Koiter (1970), Tvergaard (1976), Budiansky & Hutchinson (1979), and Hunt (1983), for example).

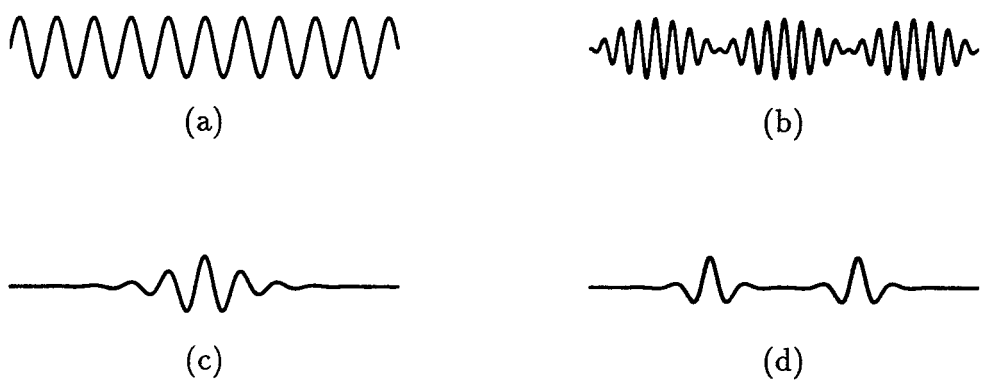

Figure 3.1 Solutions of the differential equation governing the response of an elastic strut on a nonlinear elastic foundation: (a) & (b) periodic; (c) & (d) localized.

3.1.2 Localized buckling

Most of the developments in the field of elastic stability have been confined to analysing periodic configurations. However, for long elastic structures that are unstable in the post-buckling range, periodic deflection patterns are rarely observed in practice because localized buckle patterns require the input of less mechanical energy (Hunt *et al.*, 1989). Localized buckle patterns have been observed in a variety of axially compressed structures, for example in steel plates (Moxham, 1971), railway tracks (Kerr & El-Aini, 1978) and cylinders (Uemura, 1964). Structures which are susceptible to localized deformation tend to buckle at loads much lower than the critical load predicted by classical analyses. A complete understanding of the post-buckling character is, therefore, essential to enable civil engineers to design structures which are safe.

Some of the possible solutions for a buckled strut on a nonlinear elastic foundation are illustrated in Figure 3.1. The top two are periodic with finite amplitude; the first has a single wavelength while the second has two superimposed wavelengths. The bottom two are localized solutions, with (from left to right) one and two peaks respectively. The single-peak solution (or *primary mode*) is characterized by a profile which starts from the flat state ($w = w' = w'' = w''' = 0$) at negative infinity and has

an oscillating nature which grows until it passes through a point of symmetry, before returning to the flat state as $x \to \infty$. Passage through points of anti-symmetry are also possible.

Champneys & Toland (1993) proved that, in addition to the primary mode, the governing equation admits localized solutions with two, three, and any number of peaks. They have also shown that for each multi-peaked solution an infinity of solutions exists, each corresponding to a different distance between adjacent peaks. In the limit, the family of solutions may be regarded as an "infinite set of infinite sets of solutions".

From amongst the multitude of competing solutions the analyst must determine which are physically realizable. Theoretically, for a perfect system of infinite length, the localized configuration requires the least energy to trigger. In reality, other modulated or periodic states may be favoured by the system if it is of finite length or imperfections are present. The significance of a localized form may be appreciated by considering the nature of the end-shortening, that is, the amount the two ends of the strut move towards each other when a load is applied. For an infinitely long and inextensional strut, a periodic buckle pattern of finite amplitude will have an infinite end-shortening and therefore require an input of infinite energy. In contrast, the end-shortening for a localized buckle pattern is finite, so the energy required for this deformation process is also finite.

An essential ingredient for localization is a softening nonlinearity (Potier-Ferry, 1983), that is, one which causes an unstable post-buckling response. The strut-on-elastic-foundation model has two potential sources of nonlinear behaviour: it arises naturally when *geometric* effects of large deflections are included in the formulation (Hunt *et al.*, 1993), or it may be introduced into the small-deflection equation by considering nonlinear *material* behaviour in the form of a destiffening foundation reaction (Hunt & Wadee, 1991). Localized solutions with similar qualitative features have been found in both systems (Wadee, 1993).

A strut on a piecewise linear foundation also exhibits localized buckling patterns. Nielsen *et al.* (1990) report a number of localized failures in pipelines resulting from vertical (upheaval) buckling. As the pipe lifts off the supporting bed, the effective

stiffness of the foundation is suddenly reduced to zero. The tendency for localization in bilinear systems has been studied theoretically by Tvergaard & Needleman (1980) who considered a finite length strut with sinusoidal imperfections and found there was a delay between the maximum load and the point of bifurcation that leads to failure. This mode of failure has also been investigated by Blackmore & Hunt (1996) and Blackmore (1995) using concepts from the theory of dynamical systems.

Tvergaard & Needleman (1983) have investigated the tendency for localized buckling in a strut-on-foundation model subjected to dynamic loading. This is applicable for shock-absorbing devices where the primary concern is the amount of energy absorbed by the structure and the load-deflection relationship during crushing. In this case, progressive collapse under constant rate of end displacement results in the development of localized buckle profiles in preference to an amplification of the pre-existing periodic imperfections.

3.1.3 Dynamical analogy

Concepts and techniques from the field of nonlinear dynamics have been used extensively to describe the phenomenon of localization in structural systems (Mielke & Holmes, 1988; Thompson & Virgin, 1988; Hunt *et al.*, 1989; Blackmore & Hunt, 1996). This approach, termed the *dynamical analogy* (Hunt *et al.*, 1989), replaces the time variable t in a conventional dynamical system by the spatial variable x of the structural problem. This is equivalent to using an initial-value approach to solve a boundary-value problem. An important advantage of the dynamical analogy is that a great deal of knowledge already exists for temporal systems which may be readily adapted to the structural domain.

The relation between certain static and dynamic systems is not a new idea. For example, the correspondence between the swinging pendulum and elastica strut has been known for some time (Kirchhoff, 1859; Timoshenko & Gere, 1963) and is referred to as *Kirchhoff's dynamical analogy*. Figure 3.2 emphasizes that the differential equation for the deflected curve of an elastica strut and the equation for the large oscillations of a pendulum share the same form. The load P on the strut is equivalent to the weight of the pendulum multiplied by the distance of the centre

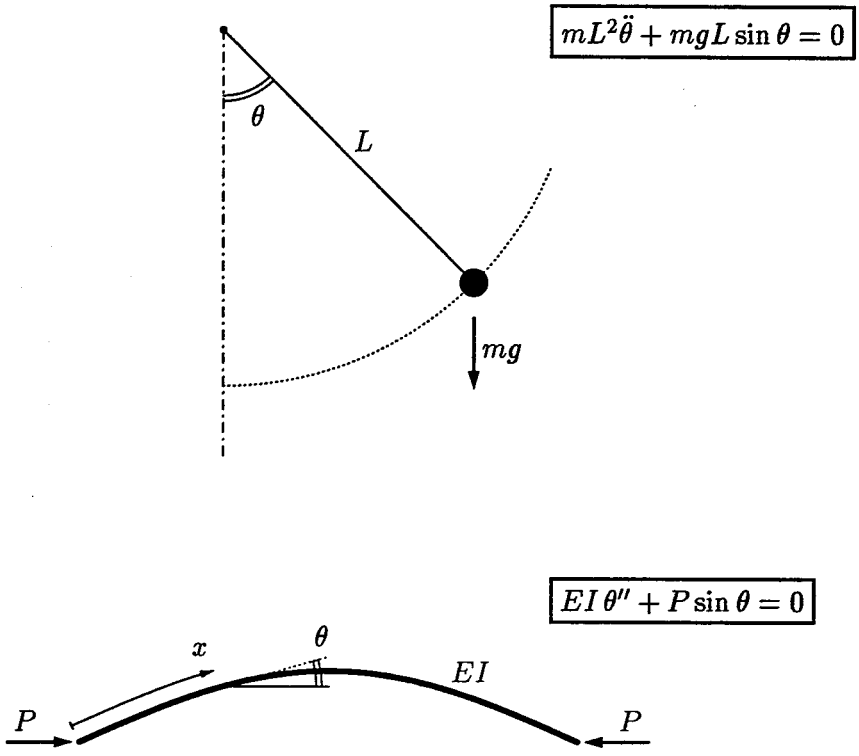

Figure 3.2 The analogy between the dynamical system of the swinging pendulum and the statical elastica strut under axial compression.

of gravity from the axis of rotation and the bending stiffness EI is equivalent to the moment of inertia of the pendulum. In recent years this analogy has been revived, owing perhaps to advances in nonlinear dynamics — or at least their exposure to wider audiences — and better computational facilities.

One of the most important concepts from dynamical systems theory is that of a *homoclinic orbit*, a solution of a system of ordinary differential equations that tends to the same saddle point as $t \to \pm\infty$. An example of a homoclinic solution occurs when the pendulum bob in Figure 3.2 is released from the fully inverted position. An infinitesimal perturbation is sufficient to cause the pendulum to swing around under the influence of gravity, reaching a maximum velocity at the lowest point, and, in the absence of friction, continue around to the starting point; the complete cycle taking infinite time. In the case of static buckling, the analogy is translated to a single loop at the centre of an infinitely long strut.

Thompson & Virgin (1988) used the dynamical analogy to examine the potential for spatial chaos and localization phenomena in the large-deflection (elastica) problem. It is known that oscillations of a rigid pendulum become chaotic when driven by a periodic forcing frequency (Thompson & Stewart, 1986). This suggests that sinusoidal spatial imperfections may lead to randomly spaced loops in a thin rod of elastic material in tension. El Naschie (1990a) has considered the dynamical analogy in three dimensions between a spherical pendulum and an elastica strut which is no longer confined to planar deformations.

3.1.4 Perturbation analyses

The study of post-buckling behaviour is an inherently nonlinear problem, the solution of which can rarely be obtained in closed-form. An important group of techniques for obtaining asymptotic solutions to nonlinear systems is the perturbation method (Jordan & Smith, 1987). The basic idea of these methods is to start from a point where an exact solution is known and then to use a series expansion about that point to describe the behaviour of the solution at adjacent points. As the name implies, perturbation methods are useful only when the equation is close to (or "is a perturbation of") an exact solution. Their main advantage over numerical methods is that the role of different variables and parameters in the solution is more apparent. Conversely, numerical methods have the advantage of being applicable for a greater range of parameter values.

Koiter (1945) and Thompson & Hunt (1973) used constant amplitude perturbation methods to describe periodic buckling. However, for localized post-buckling analysis, a non-periodic method is desirable. Various multiple-scale techniques have been adapted from the field of fluid mechanics to incorporate the modulation of amplitude exhibited by localized systems (Amazigo *et al.*, 1970; Lange & Newell, 1971). In particular, Pomeau (1981) drew an analogy between Bernard's convection and plate buckling. Subsequent works by Potier-Ferry (1983; 1987), although applied to the case of a strut on a hardening foundation, acknowledge that an extension is possible for localized buckling if a softening foundation is used instead. Hunt *et al.* (1989) used the differential equation for the strut on a quadratic foundation as the

basis for developing periodic and localized asymptotic results. They obtained good agreement with numerical solutions close to the critical load. A perturbation approach based on the total potential energy functional was devised by Hunt & Wadee (1991) and Wadee (1993).

3.2 Strut-on-elastic-foundation model

A simply-supported strut subjected to a compressive load will buckle in a single half-sine wave at the *Euler critical load*, $\pi^2 EI/L^2$, as this shape minimizes the bending energy of the strut. Higher buckling modes, with correspondingly higher critical loads and shorter wavelengths, may occur if the strut is constrained in some manner. In a strut-on-foundation model, such a restraint is provided by the foundation. The nature of the buckling problem is then fundamentally changed, for although the elastic foundation increases the bifurcation limit, it can have a destabilizing effect on the post-buckling behaviour (El Naschie, 1974). The critical load and subsequent post-buckling behaviour are governed by the material properties of the strut and foundation: the stiffer the strut, the longer the wavelength and vice versa. The presence of the foundation also ensures that the buckling load is finite and independent of the length, unlike the simply-supported strut for which the buckling load tends to zero as the length tends to infinity. The effect of the foundation on the post-buckling response of a strut was demonstrated in § 2.6 using a rigid link model.

3.2.1 Formulation of governing equation

The differential equation governing the response of a compressed strut on an elastic foundation may be derived either: directly by equilibrating forces on an element of the strut; from the principle of virtual work; or by using an energy formulation. Problems of elastic stability are usually tackled using energy methods because, unlike static analyses, the stability of the perfect system can be determined without reference to imperfections. In keeping with this tradition, the latter approach is used here. The formulation follows closely the method described by Thompson &

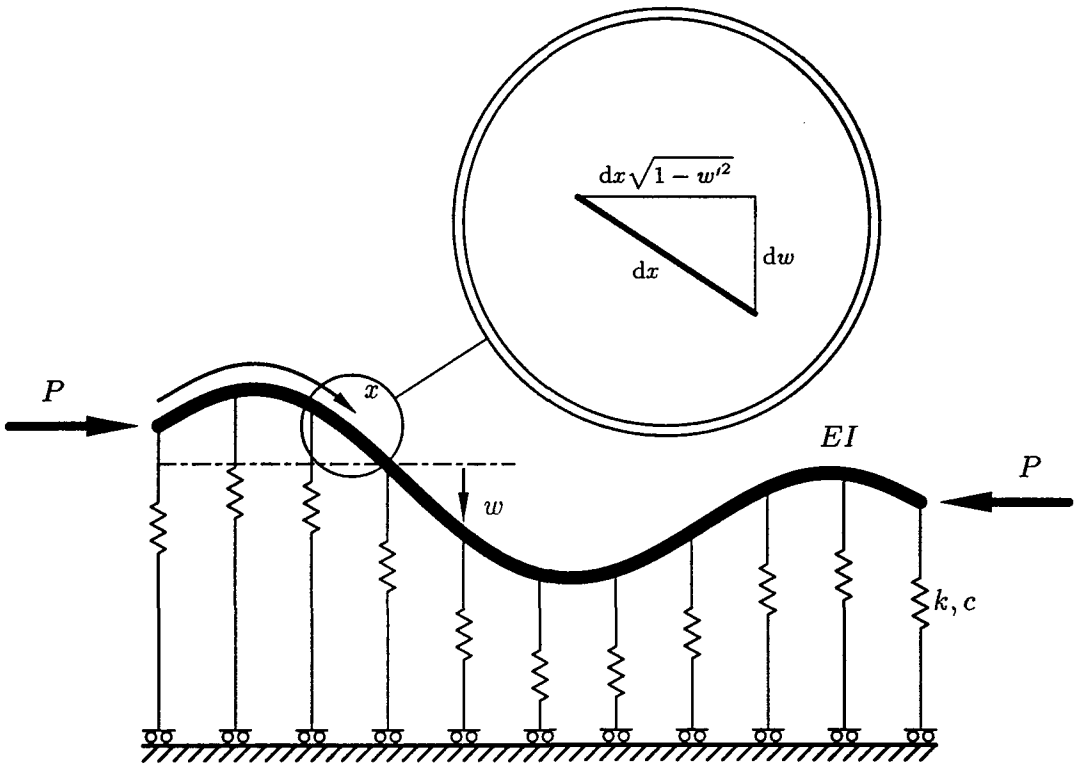

Figure 3.3 An elastic strut supported by a nonlinear elastic (Winkler) foundation.

Hunt (1984) and is completely general, retaining nonlinear terms of both geometric and material origin. The system is subsequently linearized to identify the character of the solution for small displacements. The effect on the behaviour of the system due to individual nonlinear components is discussed in Chapter 6.

Consider an incompressible strut of length L (which may be infinite) and uniform flexural stiffness EI, resting on an elastic foundation of stiffness per unit length F, and subjected to a conservative axial load P. The total potential energy for this system, which is illustrated in Figure 3.3, may be written as

$$V = U - P\mathcal{E}, \tag{3.1}$$

where the first term represents the strain energy of the system, comprising the bending energy of the strut and the foundation energy of the deformed springs, and the second relates to the work done by the load P in moving a distance $\mathcal{E}$ in the direction of P.

In a first-order linear theory, equilibrium equations are formulated on the basis of the initial undeformed shape of the structure. An analysis of stability, however, requires that equilibrium conditions are based on the final, deformed shape of the structure. This is ensured by measuring x along the length of the deflected strut and by using the exact expression for the curvature,

$$\chi = w'' \left(1 - w'^2\right)^{-1/2}, \tag{3.2}$$

where a prime ($'$) is used to denote differentiation with respect to x. The strain energy stored in the deformed strut is

$$\begin{aligned} U_S &= \frac{1}{2} EI \int_0^L \chi^2 \, \mathrm{d}x \\ &= \frac{1}{2} EI \int_0^L w''^2 \left(1 - w'^2\right)^{-1} \, \mathrm{d}x. \end{aligned} \tag{3.3}$$

The resistance of the foundation is assumed to have the general form $F = kw - cw^n$, where k and c are the linear and nonlinear components of foundation stiffness, respectively, and $n \geq 2$ is an integer. The energy stored in the foundation springs, due to the deformed shape of the strut, is

$$U_F = \int_0^L \left(\frac{1}{2} k\, w^2 - \frac{1}{n+1} c\, w^{n+1} \right) \mathrm{d}x. \tag{3.4}$$

The total strain energy of the system is the sum of the bending energy of the strut and the foundation energy, $U = U_S + U_F$. The second part of the total potential energy requires the end-shortening of the strut,

$$\begin{aligned} \mathcal{E} &= L - \int_0^L \left(1 - w'^2\right)^{1/2} \mathrm{d}x \\ &= \int_0^L \left\{ 1 - \left(1 - w'^2\right)^{1/2} \right\} \mathrm{d}x. \end{aligned} \tag{3.5}$$

The total potential energy functional can now be written as

$$V = \int_0^L \mathcal{L}\left(w, w', w''\right) \, \mathrm{d}x, \tag{3.6}$$

where the integrand is

$$\mathcal{L} = \frac{1}{2}EIw''^2\left(1-w'^2\right)^{-1} - P\left[1-\left(1-w'^2\right)^{1/2}\right] + \frac{1}{2}kw^2 - \frac{c}{n+1}w^{n+1}. \quad (3.7)$$

The governing differential equation is obtained by minimizing the total potential energy using the calculus of variations (Stephenson & Radmore, 1990). After some manipulation this leads to the Euler-Lagrange equation,

$$\frac{\partial \mathcal{L}}{\partial w} - \frac{\mathrm{d}}{\mathrm{d}x}\left(\frac{\partial \mathcal{L}}{\partial w'}\right) + \frac{\mathrm{d}^2}{\mathrm{d}x^2}\left(\frac{\partial \mathcal{L}}{\partial w''}\right) = 0. \quad (3.8)$$

Inserting the integrand $\mathcal{L}$ gives the so-called *elastica* equation for a strut on an elastic foundation:

$$EI\left[w''''\left(1-w'^2\right)^{-1} + 4w'''w''w'\left(1-w'^2\right)^{-2} + w''^3\left(1+3w'^2\right)\left(1-w'^2\right)^{-3}\right] + Pw''\left(1-w'^2\right)^{-3/2} + F = 0, \quad (3.9)$$

which is valid for large displacements. The foundation resistance F is arbitrary and was specified previously for the purpose of illustration only.

3.2.2 Analysis of linearized equations

Although a study of post-buckling behaviour requires a nonlinear analysis, an understanding of the linearized equations facilitates this by identifying the behaviour of the system for small deflections, as for example, in the tails of a localized solution where $w \to 0$ as $x \to \pm\infty$. The linear equation is obtained by assuming the slope along the deformed strut is very small, $w' \ll 1$, and by using the approximate form for curvature, $\chi \approx w''$. This reduces the integrand (3.7) to

$$\mathcal{L} = \frac{1}{2}EI\,w''^2 - \frac{1}{2}P\,w'^2 + \frac{1}{2}k\,w^2, \quad (3.10)$$

and leads, via the calculus of variations, to the linear differential equation

$$EI\,w'''' + P\,w'' + kw = 0. \quad (3.11)$$

Alternatively, this expression may be obtained directly from the large-deflection equation (3.9) by replacing the square root terms with a binomial expansion and truncating all nonlinear terms (those involving products of w and/or its derivatives). The characteristic equation corresponding to the linear form is obtained by adopting the general solution $w = Ae^{\lambda x}$, with the result

$$EI\,\lambda^4 + P\,\lambda^2 + k = 0, \tag{3.12}$$

where $\lambda = \alpha + \mathrm{i}\beta$ is a complex variable. Substituting for λ leads to the positive real and imaginary parts of the eigenvalue for the linearized system,

$$\alpha = \sqrt{\frac{1}{2}\sqrt{\frac{k}{EI}} - \frac{P}{4EI}}, \qquad \beta = \sqrt{\frac{1}{2}\sqrt{\frac{k}{EI}} + \frac{P}{4EI}}. \tag{3.13}$$

The real part, α, controls the rate of exponential growth or decay of the solution and is associated with the inset and outset of the nonlinear solution, while the imaginary part, β, governs the periodic component of the solution. The values of α and β depend on the load P as shown in Figure 3.4. A qualitative change occurs in the solution when $\alpha = 0$, corresponding to the critical load

$$P^{\mathrm{c}} = 2\sqrt{kEI}, \tag{3.14}$$

and critical wavelength

$$\beta^{\mathrm{c}} = \sqrt[4]{\frac{k}{EI}}. \tag{3.15}$$

When P is greater than the critical load P^{c} only periodic solutions exist, while for P less than $-P^{\mathrm{c}}$ ($\beta = 0$) purely exponential solutions arise. For $-P^{\mathrm{c}} < P < P^{\mathrm{c}}$, both α and β are non-zero, giving rise to oscillating solutions whose amplitudes grow and decay exponentially. A solution of this type is shown in Figure 3.4 (c).

The linear deflection, given by the general solution of Equation (3.11), is

$$w = e^{\alpha x}\left(A\cos\beta x + B\sin\beta x\right) + e^{-\alpha x}\left(C\cos\beta x + D\sin\beta x\right), \tag{3.16}$$

where A, B, C and D are constants defined by the boundary conditions of the

$$EI\lambda^4 + P\lambda^2 + k = 0$$

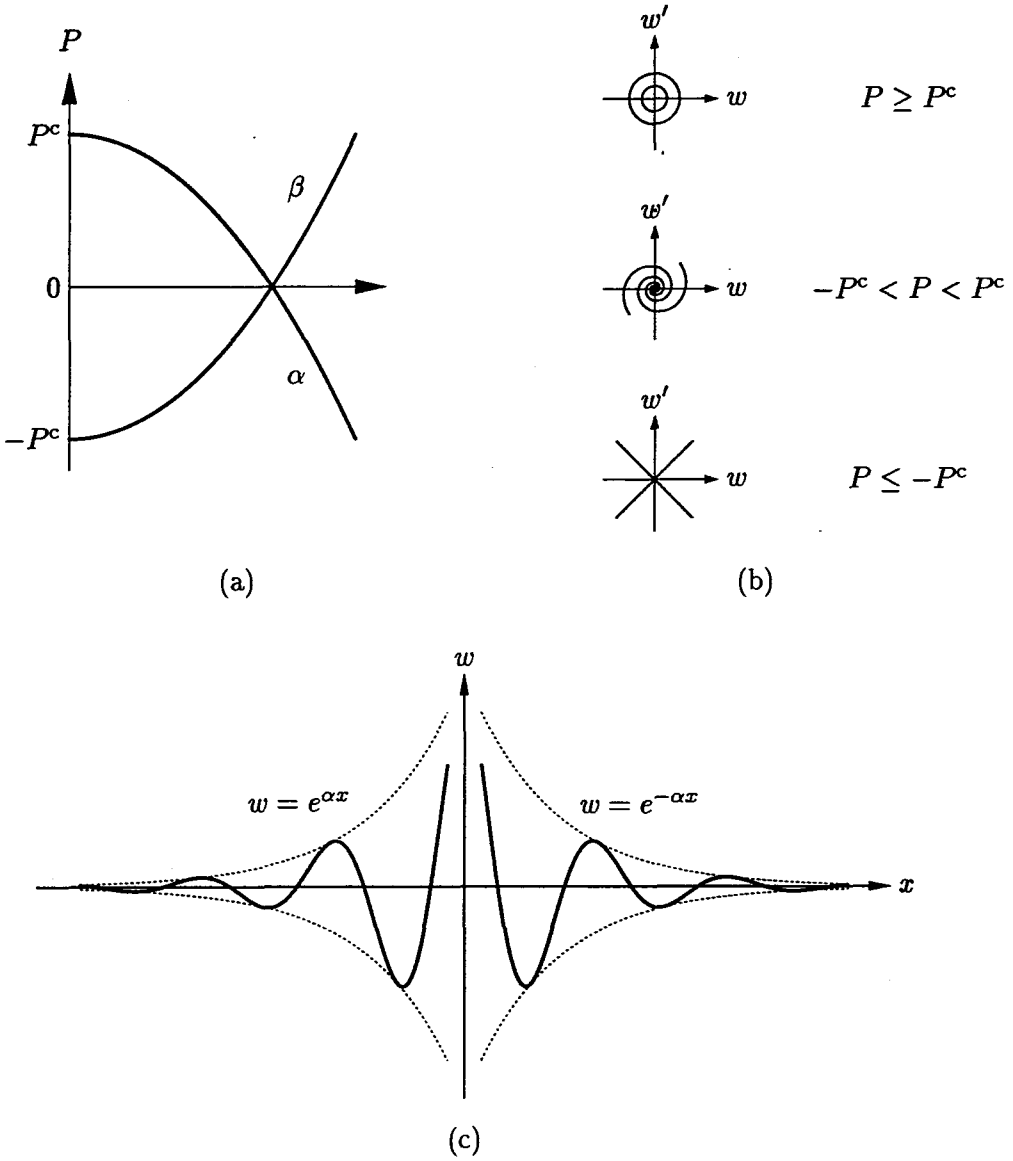

Figure 3.4 The root structure of the fundamental equilibrium state of the equation $EIw''' + Pw'' + kw = 0$: (a) variation of α and β with load; (b) phase-plane trajectories for various loads; and (c) linearized inset and outset for $-P^c < P < P^c$.

problem. If symmetric solutions, about $x = 0$, are sought then the general solution may be simplified by requiring B and D to be zero. The end conditions for the infinite boundary-value problem are determined by repeated differentiation of w with respect to x. The constants are eliminated to give the following linearized outset conditions as $x \to -\infty$:

$$\begin{aligned} w'' - 2\alpha w' + \left(\alpha^2 + \beta^2\right) w &= 0, \\ 2\alpha w''' - \left(3\alpha^2 - \beta^2\right) w'' + \left(\alpha^2 + \beta^2\right)^2 w &= 0. \end{aligned} \tag{3.17}$$

The corresponding linearized inset conditions as $x \to \infty$ are obtained simply by reversing the direction of x (or replacing α by $-\alpha$). These relations are valid only while the amplitude is very small, for as w grows the influence of nonlinear terms becomes increasingly important and, ultimately, the inset and outset may join to form a localized solution.

3.3 Perturbation method

Traditional periodic analyses such as the Rayleigh-Ritz procedure (Bathe, 1996) or the discrete bifurcation theory of Thompson & Hunt (1973; 1984) are useful for determining the critical buckling load and post-buckling behaviour for structures with a supercritical response. However, for structures with an unstable bifurcation point, their application is limited because periodic modes provide a poor basis for representing localized buckle patterns.

In this section a perturbation method is used to generate post-buckling solutions for the problem of a strut on a nonlinear elastic foundation. Variations of both amplitude and phase are achieved using a double-scale analysis in which the amplitude is defined as a function of a length scale which is in turn a function of the distance from the critical point. The approach is derived from the total potential energy of the system, unlike traditional perturbation schemes which are based on the governing differential equation (Potier-Ferry, 1983; Hunt *et al.*, 1989). It has the advantage that the suppression of secular terms and elimination of passive coordinates are guaranteed automatically. Secular terms are those which become

unbounded as $x \to \pm\infty$. When seeking localized solutions, which are by definition bounded for all x, it is necessary to suppress such terms. A more detailed explanation of perturbation methods, including the role of secular terms and the elimination of passive coordinates, may be found in texts on the subject (see Murdock (1991), for example).

The method presented here is an extension of the perturbation procedures presented by Wadee (1993) for a strut on a quadratic foundation. Although the formulation is much the same, the method is continued to a higher order and is therefore capable of describing features further into the post-buckling regime. The earlier method was hampered by an inconsistency in the formulation which gave rise to anomalous mode forms in the asymptotic solution. This problem has been eliminated by expanding all variables in terms of a perturbation parameter. A further difference between the two methods is the choice of foundation reaction. The work here is for a cubic foundation, having the same resistance to upward and downward displacement, where as the previous work involved a quadratic foundation which has a bias favouring upward deflections. The new perturbation procedure is to be published shortly (Wadee *et al.*, 1996).

3.3.1 Description of method

The small, but finite, amplitude response for a strut on a cubic foundation may be described by the total potential energy

$$V = \int_{-\infty}^{\infty} \left\{ \frac{1}{2} EI\, \ddot{w}^2 - \frac{1}{2} P\, \dot{w}^2 + \frac{1}{2} k\, w^2 - \frac{1}{4} c\, w^4 \right\} \mathrm{d}x, \tag{3.18}$$

where $\dot{()} \equiv \mathrm{d}/\mathrm{d}x$. As with traditional harmonic analyses the deflected shape w is expanded as a Fourier series in x,

$$w = \sum_{i=0}^{\infty} \{ A_i(X) \cos i\beta x + B_i(X) \sin i\beta x \}, \tag{3.19}$$

with the difference that the amplitudes, A_i and B_i, are not constant. Instead, they are permitted to vary with X, the so-called slow-space variable (Potier-Ferry, 1983).

This is a linear function of x and the perturbation parameter s, and is defined as

$$X = sx. \tag{3.20}$$

The choice of this particular expression is based on previous descriptions of localized buckling as a slowly varying phenomenon (Hunt *et al.*, 1989). The inclusion of both sine and cosine modes allows a variation in the wavelength, which is important in the vicinity of the centre of localization (Wadee, 1993), as well as a modulation of the amplitude. The selection of a suitable perturbation parameter requires some knowledge of the nature of the solution being sought. In problems of elastic stability the point of bifurcation provides a convenient reference. The perturbation parameter is therefore defined as the distance from this point (Hunt *et al.*, 1989),

$$s = \sqrt{P^c - P}. \tag{3.21}$$

When $s = 0$ the linear eigenvalue problem is retained.

The derivatives of w are readily evaluated

$$\begin{aligned} \dot{w} &= \sum_{i=0}^{\infty} \{ sA_i' \cos i\beta x - A_i i\beta \sin i\beta x \\ &\qquad + sB_i' \sin i\beta x + B_i i\beta \cos i\beta x \}, \end{aligned} \tag{3.22}$$

$$\begin{aligned} \ddot{w} &= \sum_{i=0}^{\infty} \left\{ s^2 A_i'' \cos i\beta x - 2sA_i' i\beta \sin i\beta x - A_i i^2\beta^2 \cos i\beta x \right. \\ &\qquad \left. + s^2 B_i'' \sin i\beta x + 2sB_i' i\beta \cos i\beta x - B_i i^2\beta^2 \sin i\beta x \right\}, \end{aligned} \tag{3.23}$$

where a prime ($'$) denotes differentiation with respect to X[1]. The series representations for w and its derivatives are then fed into the energy expression (3.18). The result is

$$\begin{aligned} V &= \frac{1}{2} \sum_{i=0}^{\infty} \left(V_{ii} \int_{-\infty}^{\infty} A_i{}^2 \mathrm{d}x + V_{i'i'} \int_{-\infty}^{\infty} A_i'^2 \mathrm{d}x \right. \\ &\qquad \left. + V_{ii''} \int_{-\infty}^{\infty} A_i A_i'' \mathrm{d}x + V_{i''i''} \int_{-\infty}^{\infty} A_i''^2 \mathrm{d}x \right. \end{aligned}$$

[1]Note, in this section $\dot{()} \equiv \mathrm{d}/\mathrm{d}x$ and $()' \equiv \mathrm{d}/\mathrm{d}X$ whereas in all other parts of this thesis $\dot{()} \equiv \mathrm{d}/\mathrm{d}t$ and $()' \equiv \mathrm{d}/\mathrm{d}x$.

$$
\begin{aligned}
&+ V_{i''i'} \int_{-\infty}^{\infty} A_i'' B_i' \mathrm{d}x + V_{i'i''} \int_{-\infty}^{\infty} A_i' B_i'' \mathrm{d}x \\
&+ V_{i'i} \int_{-\infty}^{\infty} A_i' B_i \mathrm{d}x + V_{ii'} \int_{-\infty}^{\infty} A_i B_i' \mathrm{d}x \\
&+ V_{ii} \int_{-\infty}^{\infty} B_i{}^2 \mathrm{d}x + V_{i'i'} \int_{-\infty}^{\infty} B_i'{}^2 \mathrm{d}x \\
&+ V_{i''i''} \int_{-\infty}^{\infty} B_i''{}^2 \mathrm{d}x + V_{ii''} \int_{-\infty}^{\infty} B_i B_i'' \mathrm{d}x \Big) \\
&+ \frac{1}{24} V_{ijkl}^{\mathrm{cc}} \int_{-\infty}^{\infty} A_i A_j A_k A_l \, \mathrm{d}x \\
&+ \frac{1}{4} V_{ijkl}^{\mathrm{cs}} \int_{-\infty}^{\infty} A_i A_j B_k B_l \, \mathrm{d}x \\
&+ \frac{1}{24} V_{ijkl}^{\mathrm{ss}} \int_{-\infty}^{\infty} B_i B_j B_k B_l \, \mathrm{d}x, \qquad (3.24)
\end{aligned}
$$

where the Einstein convention is used to imply summation over repeated indices and the coefficients $V_{ii}, V_{i'i'}$, etc. are listed in Appendix A. These coefficients contain a constant part and an oscillatory part. The latter is neglected in order to render the analysis tractable. This simplification introduces an error which is negligible for small s (close to the critical point), but which becomes increasingly significant further into the post-buckling regime (Hunt & Wadee, 1991). The contribution of these terms is examined in Chapter 5 using other methods of solution. The constant coefficients in Equation (3.24) are brought outside the integral sign while the amplitudes, being functions of the slow-space variable X, must remain inside.

The calculus of variations is applied to the integral (3.24), with appropriate boundary conditions being employed to eliminate unwanted terms. The precise details of the procedure are described by Wadee (1993). The important results are the final Euler-Lagrange equations:

$$
\begin{aligned}
&V_{i''i''} A_i'''' + \frac{1}{2}\left(V_{i''i'} - V_{i'i''}\right) B_i''' + \left(V_{ii''} - V_{i'i'}\right) A_i'' + \frac{1}{2}\left(V_{ii'} - V_{i'i}\right) B_i' \\
&\qquad + V_{ii} A_i + \frac{1}{6} V_{ijkl}^{\mathrm{cc}} A_j A_k A_l + \frac{1}{2} V_{ijkl}^{\mathrm{cs}} A_j B_k B_l = 0, \qquad (3.25) \\
&V_{i''i''} B_i'''' + \frac{1}{2}\left(V_{i'i''} - V_{i''i'}\right) A_i''' + \left(V_{ii''} - V_{i'i'}\right) B_i'' + \frac{1}{2}\left(V_{i'i} - V_{ii'}\right) A_i' \\
&\qquad + V_{ii} B_i + \frac{1}{2} V_{jikl}^{\mathrm{cs}} A_j A_k B_l + \frac{1}{6} V_{jikl}^{\mathrm{ss}} B_j B_k B_l = 0. \qquad (3.26)
\end{aligned}
$$

Note that the classical periodic analysis of Thompson & Hunt (1973) is recovered when the amplitudes are fixed because all coefficients and terms with primes are

then zero. The former analysis may, therefore, be considered a special case of this more general localized procedure.

The steps required to generate approximate solutions to these Euler-Lagrange equations are listed in Appendix A and a summary of the results is presented next.

3.3.2 Ordered expansions

The solution of the Euler-Lagrange equations requires a great deal of algebraic manipulation and is best performed using a package such as Mathematica (Wolfram, 1991). The asymptotic form of the deflected shape for a compressed strut on a nonlinear elastic foundation is

$$\begin{aligned} w &= sA_{1,1}\cos\beta x + s^2 B_{1,2}\sin\beta x + s^3(A_{1,3}\cos\beta x + A_{3,3}\cos 3\beta x) \\ &\quad + s^4(B_{1,4}\sin\beta x + B_{3,4}\sin 3\beta x) + O(s^5), \end{aligned} \tag{3.27}$$

where the amplitudes $A_{i,j}$ and $B_{i,j}$ are

$$\begin{aligned} A_{1,1} &= \frac{4}{\sqrt{6c}}\beta^c \operatorname{sech}\Omega X, \\ B_{1,2} &= \sqrt{\frac{3}{c}}\frac{\beta^c}{\sqrt{P^c}}\operatorname{sech}\Omega X\tanh\Omega X, \\ A_{1,3} &= \frac{1}{36\sqrt{6c}}\frac{\beta^c}{P^c}\left(-317\operatorname{sech}\Omega X + 307\operatorname{sech}^3\Omega X\right), \\ A_{3,3} &= \frac{1}{12\sqrt{6c}}\frac{\beta^c}{P^c}\operatorname{sech}^3\Omega X, \\ B_{1,4} &= \frac{1}{432\sqrt{3c}}\frac{\beta^c}{P^{c3/2}}\left(-2389\operatorname{sech}\Omega X\tanh\Omega X + 5524\operatorname{sech}^3\Omega X\tanh\Omega X\right), \\ B_{3,4} &= \frac{\sqrt{3}}{8\sqrt{c}}\frac{\beta^c}{P^{c3/2}}\operatorname{sech}^3\Omega X\tanh\Omega X, \end{aligned} \tag{3.28}$$

in which the following substitution has been made:

$$\Omega = \frac{\beta^c}{\sqrt{2P^c}}. \tag{3.29}$$

In principle, perturbation results may be extended to any level of accuracy desired. However, in this instance their applicability is limited because the oscillatory components of the coefficients V_{ii}, etc. in Equations (3.25) and (3.26) were ignored.

At each level of s, the solutions of the equations corresponding to δA_1 and δB_1 yield a non-homogeneous second-order equation with non-constant coefficients. While by no means obvious, it appears that a closed-form solution will exist at all levels of s and is likely to have a similar form to the solutions already found. Obtaining these solutions, however, is likely to become increasingly more difficult at each level of s.

3.3.3 Discussion of results

The perturbation analysis generates an ordered sequence of solutions which are expected to approximate well the shape of the deformed strut close to the point about which the scheme is expanded, with a progressive loss of accuracy as the value of s increases. The method presented here takes into account modulation of phase as well as amplitude and should, therefore, be valid further into the post-buckling regime than the more restrictive schemes of Hunt *et al.* (1989). The accuracy of the perturbation analysis cannot be determined by comparison with an exact solution (because it does not exist), so instead a comparison is made with an accurate numerical solution. These numerical solutions were obtained independently using the methods outlined in Chapter 4.

Three solutions for the buckled strut are shown in Figure 3.5 at different levels of load. Overall, the perturbation method is seen to model the localized solution well, especially in the vicinity of P^c. As the load decreases, the general features of the solution are still identified, with the maximum amplitude increasing and the profile becoming increasingly localized. The deflection at the centre of the localization ($x = 0$) is consistently overestimated, as recorded by Figure 3.6, with a marginal improvement at the s^3 level. An improvement in the peak amplitude does not occur at the s^2 and s^4 levels because the associated amplitudes $B_{i,j}$ are zero at $x = 0$, although they do affect the profile elsewhere.

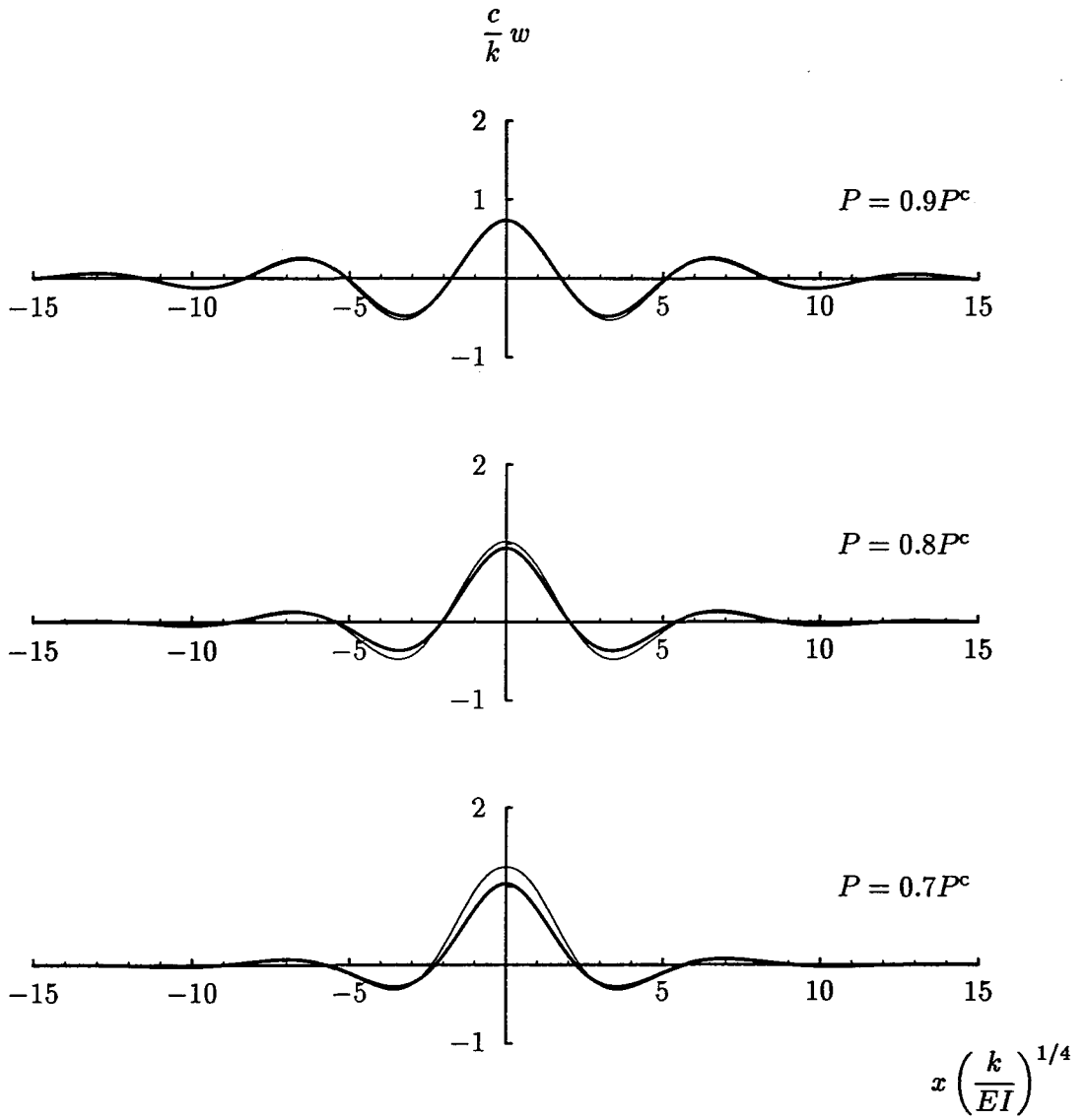

Figure 3.5 Comparisons of s^4 perturbation solutions (thin lines) with numerical solutions (thick lines).

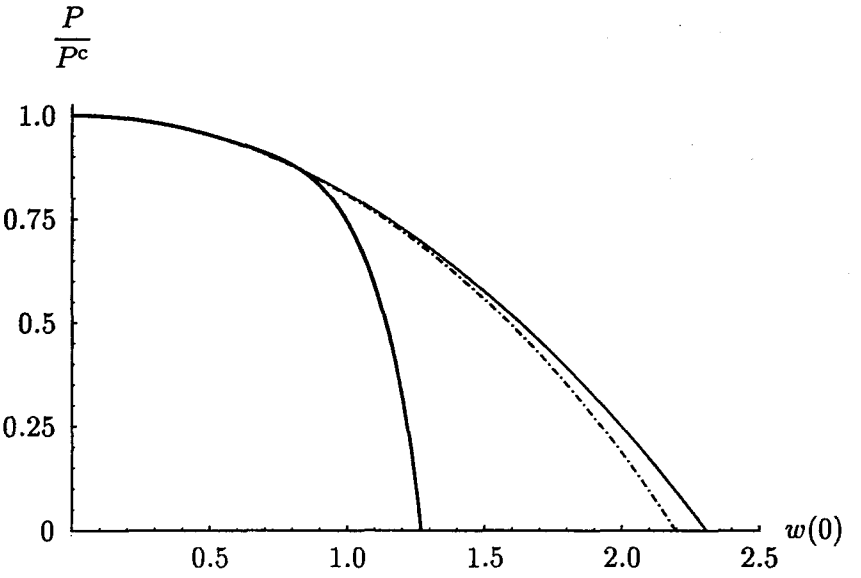

Figure 3.6 Load versus amplitude for perturbation solutions at various orders of s with a numerical solution (solid line): s, s^2 — thin solid line; s^3, s^4 — dot-dashed.

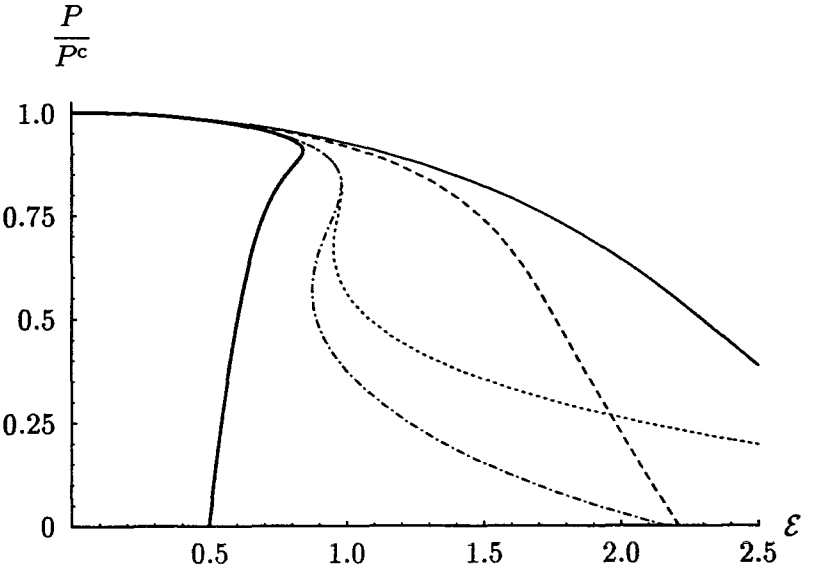

Figure 3.7 Load versus end-shortening for perturbation solutions at various orders of s with a numerical solution (solid line): s — thin solid line; s^2 — short dashed; s^3 — dot-dashed; s^4 — dotted.

Phase modulation, where the wavelength is allowed to vary along the length of the strut, is successfully modelled by including sine modes in addition to cosine modes in the Fourier expansion of w. The effect of $B_{i,j}$ terms is apparent in the end-shortening plot of Figure 3.7. The end-shortening, being an integral along the length of the strut, provides an *average* measure of the error of the solution. The inclusion of further terms arising at the s^3 and s^4 levels enables the turning point in the end-shortening (at $P \approx 0.92P^c$) to be approximated. This qualitative feature of the solution is not evident when an approximation of order s^2 is used and illustrates the asymptotic nature of the perturbation results with new features of the solution emerging at successive levels of s. However, the s^4 approximation for end-shortening is worse than the s^3 solution for $P < 0.8P^c$. The reason for this discrepancy is not clear — it may be related to the absence of the oscillating components of the coefficients V_{ii}, etc.

The results presented here are an improvement on those obtained by Wadee (1993). The main reason for their superior performance is the consistent formulation in which both load and wavelength are expanded as power series in terms of the perturbation parameter s.

3.4 Concluding remarks

The general nonlinear treatments of elastic stability (Koiter, 1945; Thompson & Hunt, 1973) are based on the total potential energy of the system and help to explain the reserve post-buckling strength of plates and the catastrophic failure of shell structures under conservative loading. When nonconservative loads are present a potential energy function does not exist and it is necessary to resort to the equations of equilibrium. An example of a continuous nonconservative elastic system is the cantilever with follower force (Plaut, 1978). The equilibrium equations, or equations of motion, are also important starting points for visco-elastic systems where energy is dissipated.

Chapter 4

Numerical methods

The objective of this chapter is to describe the numerical methods employed in this thesis to solve the problem of localized buckling in a strut-on-foundation model. The chapter begins with a review of methods for solving boundary-value problems numerically and goes on to discuss various theoretical aspects of these problems, and of procedures for their numerical solution. Two different approaches are distinguished: initial-value methods and boundary-value methods. The numerical procedure implemented in this thesis, which is based on the latter approach, is then described in detail. Finally, the numerical methods are verified by comparison with an analytical solution and an alternative numerical procedure.

4.1 Introduction

The success of a numerical process depends on a combination of two factors: a well-conditioned problem and a stable algorithm with which to solve it. These concepts are explored in the following sections. The treatment here is intentionally brief and descriptive rather than mathematically rigorous, a detailed account of the theory of ordinary and partial differential equations and of numerical methods is available elsewhere (see Ascher *et al.* (1995) or Ames (1992), for example).

4.1.1 Theory of boundary-value problems

The theory of boundary-value problems involves the existence and uniqueness of solutions and conditioning of the problem. An *existence* theorem proves there is a solution to be found — after all, it would be pointless to spend time and effort looking for a solution which did not exist. Having found a solution, it would be equally futile to discover later that there is more than one solution to the problem and that the solution found was the wrong one. This is the value of *uniqueness.* In addition to being assured that a problem has a solution, it is also worth establishing whether or not the problem is *well-conditioned* (or well-posed). According to Duchateau (1986), a boundary-value problem is well-posed if: a solution to the problem exists; the solution is unique; and the solution depends continuously on the data.

Existence and uniqueness theory for boundary-value problems is considerably more complicated and not as comprehensively developed as for initial-value problems. For an initial-value problem represented by an nth-order ordinary differential equation, a unique solution is guaranteed when n (initial) conditions are specified at a single point. In the case of a boundary-value problem, however, boundary conditions are specified at more than one point which gives rise to the possibility that a differential equation may have many solutions, one solution or no solutions. This is illustrated by the following example.

Example 4.1.1 *Consider the linear second-order eigenvalue problem*

$$w'' + w = 0, \tag{4.1}$$

with boundary conditions $w(0) = 0$ *and* $w(b) = w_b$. *The general solution of this problem is* $w(x) = A \sin x$, *where* A *is a constant determined by* w_b. *Thus, for* $b = n\pi$, *where* n *is an integer, Equation (4.1) has no solutions if* $w_b \neq 0$ *and an infinite number of solutions when* $w_b = 0$. *Alternatively, if* $b \neq n\pi$, *the problem has a unique solution.*

The difficulty of ascertaining the existence and uniqueness of solutions for boundary-value problems was succinctly expressed by Keller (1968) when he said:

> "...(existence theory for boundary-value problems) is far from sufficient to cover most problems that arise in practice. However, solutions of boundary-value problems and roots of transcendental systems can exist without formal proofs of these facts. Thus in many of the difficult and important applied problems leading to boundary-value problems we may use the (standard numerical) techniques (for boundary-value problems) without the benefit of existence theorems."

4.1.2 Numerical procedures for boundary-value problems

Methods for the numerical solution of boundary-value problems can be divided into two distinct classes: shooting methods (or initial-value methods) and finite difference methods (or boundary-value methods). The prime difference between these approaches is that shooting methods generate solutions to boundary-value problems by solving related initial-value problems, while finite difference methods generate solutions directly by an explicit treatment of the boundary-value problem. Important properties of numerical methods for boundary-value problems (and initial-value problems) are accuracy, consistency, stability, and convergence. These are summarised below.

Accuracy

The solution of a differential equation by computer requires certain approximations which inevitably introduce small errors. There are two main sources of error. The first is *roundoff error* which results from the computation being performed in finite precision on a digital computer. In this thesis 64-bit (double precision) floating-point variables were used for all calculations. The second is *discretization* or *truncation error* which arises because a numerical method is designed only to approximate the solution to a problem. This is the error that arises in the absence of roundoff error and any errors in the input data resulting, for example, from imperfect physical measurements. Roundoff error accumulates when an ordinary differential equation is integrated using discretized derivatives. Although the discretization error tends to zero as the integration step size is refined, the roundoff error increases. For optimum results there is a need to balance the effects of these two error sources.

Consistency

A finite difference method is said to be consistent (or compatible) with the original differential equation if the local truncation error tends to zero more rapidly than the step size. This property ensures that the *difference* operator is inherently capable of representing the *differential* operator.

Stability

Another important property of numerical methods for the solution of boundary-value problems is that of stability. A numerical method is unstable if small errors in the input data are propagated by the method to produce errors that eventually dominate the output data. Stability, therefore, is solely a property of the numerical method rather than of the problem it is used to approximate. The importance of stability for shooting methods is discussed further in § 4.2 in the context of localized buckling problems.

Convergence

A final concept, often related to stability, is that of convergence. Differential equations are usually solved on a mesh which is defined in terms of one or more interval sizes. A numerical method is said to be convergent if the discrete solution converges to the true solution of the differential equation as the interval size decreases to zero. In general, if the properties of stability and consistency are satisfied, the property of convergence will follow automatically (Ames, 1992).

4.2 Initial-value methods

Initial-value methods are a useful tool for solving boundary-value problems. These methods require a succession of initial-value problems to be solved, each with different initial conditions. The objective is to find and solve the initial-value problem which corresponds to the original boundary-value problem. The *simple shooting method*, illustrated in Figure 4.1, is the simplest initial-value approach. In this method solutions are obtained for various initial conditions (indicated by the angle

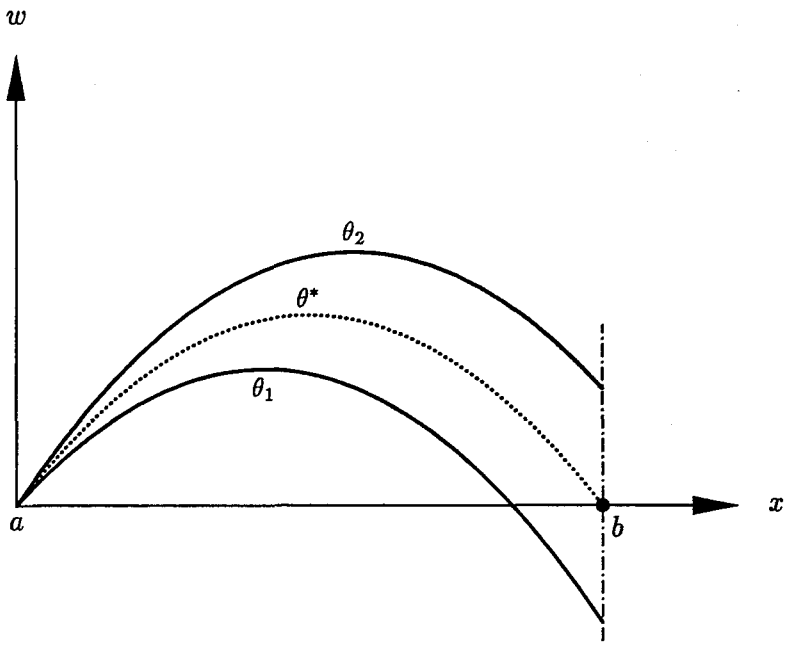

Figure 4.1 Schematic of shooting method. Trial solutions are integrated from point a to point b. The discrepancy in the boundary conditions at the end point are used to adjust the starting conditions until the conditions at both ends are satisfied.

θ) by integrating (shooting) over the interval $[a, b]$. The aim is to find the starting conditions (of an initial-value problem) at $x = a$ which cause the boundary conditions (of the corresponding boundary-value problem) to be satisfied at $x = b$. The intuitive appeal of this approach is strengthened by the advanced state of numerical tools for initial-value problems. Efficient and flexible general-purpose codes are readily available for such problems in most mathematical software libraries.

Although the simple shooting method is a relatively straightforward and practical method for solving boundary-value problems, its effectiveness is often hampered by stability restrictions. Numerical stability is particularly important in shooting methods for localized elastic buckling problems because the linearized eigenvalues of the governing differential equation indicate the presence of both exponentially growing and decaying solutions. This means that while integrating from specified initial conditions towards the linearized inset (decaying solution), a combination of roundoff and discretization error may cause the solution to drift onto the outset, making the solution diverge to infinity instead of decaying to the flat state. These types of stability drawbacks can be alleviated by using more complicated initial-value techniques such as the *multiple shooting method* and *stabilized march* (Ascher *et al.*, 1995).

Two different shooting strategies are reported in the literature for solving localized buckling problems. Hunt & Wadee (1991) used a shooting method to reveal a multiplicity of localized solutions which had not been detected using traditional boundary-value techniques. Champneys & Spence (1993) also used an initial-value approach to track localized solutions in the problem of a strut on an elastic foundation. Both of these strategies are outlined below.

4.2.1 Search algorithms

In order to implement a shooting method, a search algorithm is required to determine initial conditions for successive initial-value problems. The procedure described here is that of Hunt & Wadee (1991) who investigated localized buckling in the model of a strut on a quadratic softening foundation. The fourth-order governing equation,

$$EIw'''' + Pw'' + kw - cw^2 = 0, \tag{4.2}$$

is first decomposed into a system of first-order equations:

$$\begin{aligned} w' &= v, \\ v' &= u, \\ u' &= t, \\ t' &= -\frac{1}{EI}\left(Pu + kw - cw^2\right). \end{aligned} \tag{4.3}$$

This system of equations is treated as an initial-value problem, requiring four initial conditions to determine a unique solution. In fact, Wadee (1993) has shown that two initial conditions are sufficient to capture the essential characteristics of the solution. Hunt & Wadee (1991) and Hunt *et al.* (1993) used a self-refining algorithm to search amongst the reduced two-dimensional space for small, non-zero, initial conditions that define solutions which satisfy the symmetry conditions, $w' = w''' = 0$, at some point. The procedure minimizes the quantity $\sqrt{w'^2 + w'''^2}$ until a predetermined value is achieved. Blackmore (1995) used a similar approach based on energy conservation criteria.

These types of search routines may be implemented in the absence of formal existence theorems. Naturally though, it is not possible to conclude that a particular solution does not exist if an algorithm fails to find it. Wadee (1993) performed extensive numerical experiments using such methods and revealed the robust nature of various localized forms which were not apparent from earlier perturbation analyses. These buckling solutions were obtained for specific load values. The major drawback of this shooting method becomes apparent when it is used to determine the complete post-buckling response of a model, requiring multiple runs at different values of load. The problem is that the search algorithm does not make use of information obtained about a solution at adjacent load values, nor is there any guarantee that a solution will be found at all. Another drawback is that for low loads it becomes increasingly difficult to find localized solutions, as virtually all starting conditions lead to divergence.

4.2.2 Automatic continuation

Champneys & Spence (1993) also developed a strategy for the numerical approximation of localized solutions for a strut model. Their method uses continuation and a shooting approach, based on Newton's method, to compute the first solution. Continuation is the computation of solutions to a differential equation as a parameter is varied. This is readily implemented using a standard continuation package and allows a complete post-buckling response to be established in a single run. The method is described here in some detail because it is used in § 4.6.2 as an independent check of the boundary-value method employed throughout this thesis. The principal steps of this initial-value procedure, which is illustrated in Figure 4.2, are:

1. *Investigation of linear system*

   For a given load P, the eigenvalues of the linearized system are evaluated. The eigenvectors corresponding to the eigenvalue with the least positive real part are sought, these corresponding to the weakest outset conditions. The real and imaginary parts of this vector span the unstable eigenspace of the linearized system.

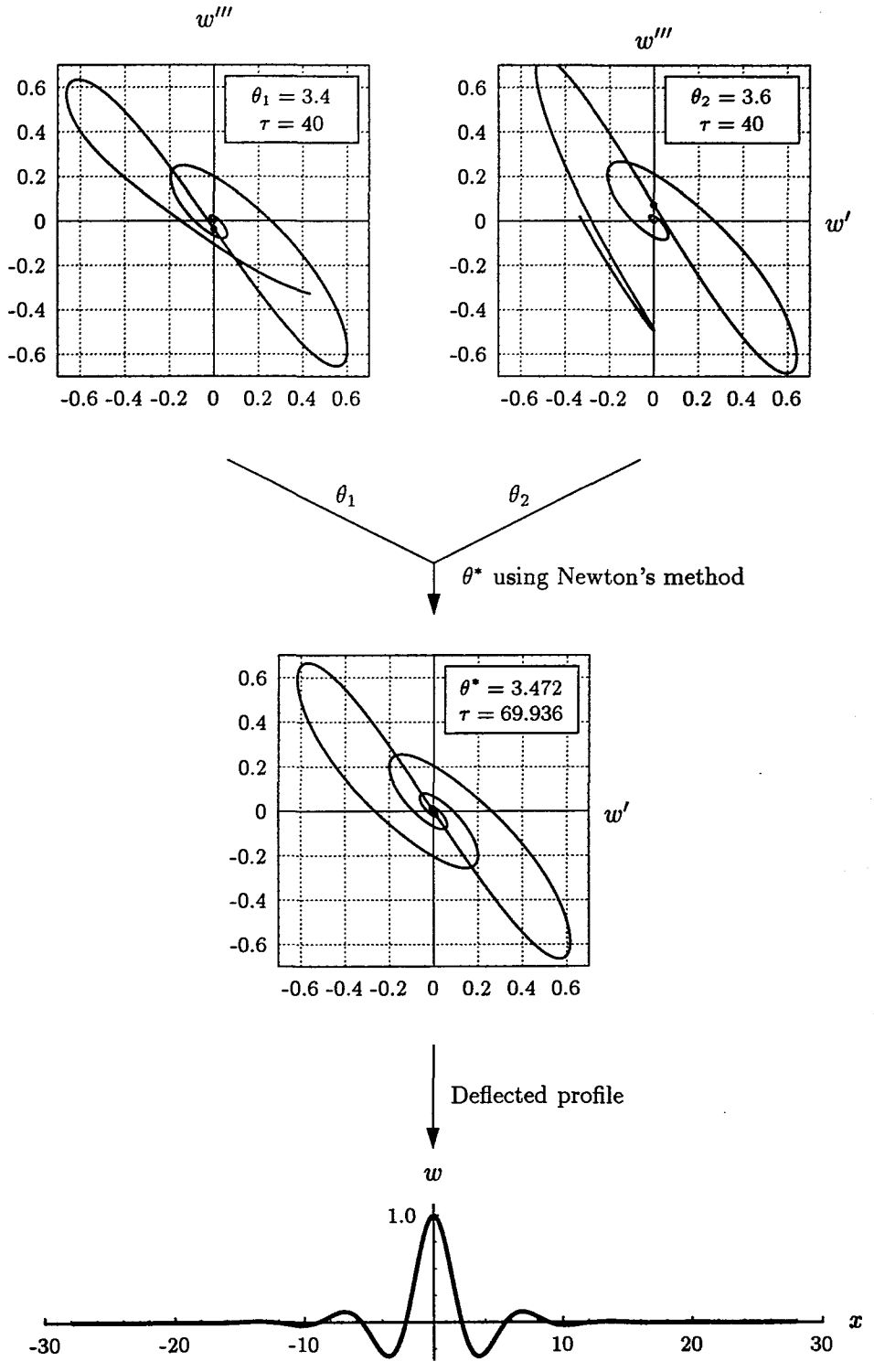

Figure 4.2 Procedure for the shooting method of Champneys & Spence (1993) used to locate localized solutions for the elastic buckling equation (4.17) ($EI = k = c = 1$, $P = 1.5$).

2. *Initial conditions*

   The two-dimensional unstable eigenspace of the origin is parameterized using polar coordinates (r, θ). For a sufficiently small radius r the angle θ parameterizes all possible solutions.

3. *Shooting method*

   A variable-order variable-step size Adam's method is used to perform the integration from the initial conditions. Plotting the trajectory in w'–w''' space, the solution is seen to spiral outwards, much like the linear solution, until the nonlinear component forces the trajectory back towards the origin. In general, the solution will not satisfy the symmetry conditions, $w' = 0$ and $w''' = 0$, simultaneously. It is possible, however, to find two adjacent starting conditions, denoted θ_1 and θ_2, which pass close to the origin. The points on these trajectories where $w' = 0$ is marked in Figure 4.2 by a dot ($\bullet$). Newton's method is then used to generate successive guesses for the shooting angle θ. Quadratic convergence is achieved towards θ^*, the initial conditions which satisfy the symmetry conditions within a numerical tolerance. The solution of this initial-value problem is then the solution of the original boundary-value problem.

4. *Automatic continuation*

   A standard continuation package, in this case AUTO (Doedel, 1981), is then used to compute solutions of the buckling equation (4.2) as the parameter P is varied between two limiting values.

4.3 Boundary-value methods

Boundary-value methods are conceptually different from the shooting methods of the previous section. Instead of solving a series of initial-value problems, an approximate solution is sought simultaneously over the whole domain, as shown in Figure 4.3. For this reason boundary-value methods are often referred to as *global methods*. Given an initial approximate profile $\bar{w}(x)$, a boundary-value method refines the approximate solution iteratively until it resembles the exact solution $w(x)$ for all

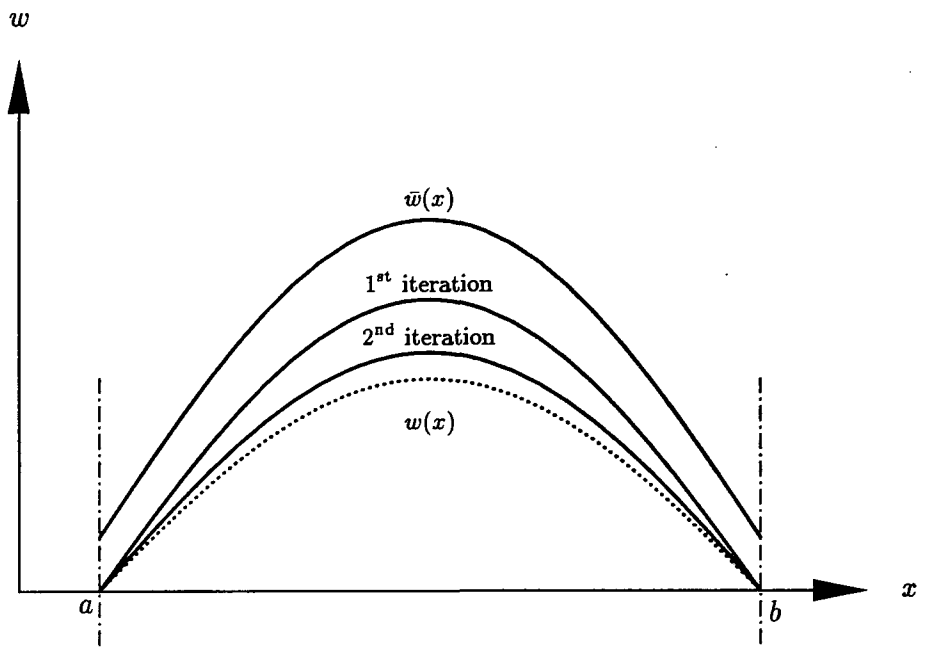

Figure 4.3 Schematic of relaxation method. An initial approximation $\bar{w}(x)$ is refined iteratively until it agrees closely with the true solution $w(x)$.

x in the domain within a prescribed tolerance. Boundary-value methods are particularly useful for solving ordinary differential equations when difficulties of stability arise with initial-value methods (Fox, 1961). There are other circumstances when a boundary-value method is the only practical alternative, as for example, in the case of boundary-value problems in partial differential equations. The main disadvantage of using boundary-value methods is that *a priori* knowledge of the solution is required in order to provide a sufficiently accurate initial profile. It is unlikely that these methods would have been used to discover the variety of multi-peaked localized solutions if their presence had not already been detected using initial-value methods. Nevertheless, for specific solutions, like the primary localized forms in this thesis, boundary-value methods are a powerful tool.

Finite difference methods are one of the most widely used boundary-value methods. Their application involves three fundamental steps:

- The selection of a mesh of the form $a = x_1 < x_2 < \cdots < x_{n+1} = b$ on the interval $[a, b]$. An approximate solution is then sought at these mesh points.
- Setting up a system of algebraic equations by replacing derivatives in the differential equation by difference quotients and specifying boundary conditions.

- Solving the system of algebraic equations to produce an approximate solution at discrete mesh points. Interpolation may then be used to construct the solution for any point $x \in [a, b]$.

These steps are common to all finite difference methods. Thus, a good finite difference method must not only utilize an appropriate discretization method but also a suitable mesh selection procedure and algorithms for the solution of systems of algebraic equations.

The main criterion for selecting a mesh is to achieve a sufficiently accurate solution as inexpensively as possible. Since the computational effort for a given discretization method increases with the number of mesh points, the coarsest possible mesh is sought which at the same time yields an approximate solution with tolerable error. In general, the mesh must be fine in regions where the desired solution changes rapidly but relatively coarse elsewhere, provided that the resulting scheme is sufficiently stable. A good mesh is especially important for problems with localized solutions which, by their very nature, involve small regions of rapid change.

4.4 Strut on a visco-elastic foundation

The numerical methods used to solve the equations of an elastic strut on a Maxwell foundation are described in this section. For convenience the method is outlined for the linear form of the governing equations which are common to all visco-elastic models in this thesis. These are:

- the strut buckling equation,

$$EIw'''' + Pw'' + F = 0, \tag{4.4}$$

- and the Maxwell relation,

$$\frac{1}{k}\dot{F} + \frac{1}{\eta}F = \dot{w}. \tag{4.5}$$

The solution of this system of partial differential equations proceeds by first reducing it to a series of ordinary differential equations. These are solved at each time step for specified boundary conditions and load conditions. These procedures, including truncation from an infinite to a finite domain, are described below.

4.4.1 Temporal discretization

The problem of buckling of a strut on a visco-elastic foundation is represented by Equations (4.4) and (4.5) involving two independent variables, the spatial variable x and time t. A reduction of these partial differential equations to a system of ordinary differential equations is achieved by discretizing the problem in terms of one of the independent variables. Replacing the time derivative by a difference scheme results in a system of boundary-value problems. Alternatively, if the spatial derivative is replaced with a difference scheme, the outcome is a system of initial-value problems. These are both examples of the *method of lines*. The method of discretizing in time, and then solving a boundary-value problem, is called the *transverse* method of lines, while discretizing in x, and then solving an initial-value problem, leads to the *longitudinal* method of lines. For localized buckling the main feature of interest occurs in the x direction, so a temporal discretization method is implemented to reduce the governing equation in time. A backward difference scheme is used in preference to a forward difference because it is generally acknowledged as being more stable (Smith, 1985). The resulting ordinary differential equations have the form

$$EIw_n'''' + P_n w_n'' + \frac{k}{1+r\Delta t} w_n = \frac{G(x)}{1+r\Delta t}, \tag{4.6}$$

where $w_n(x)$ is the displacement of the strut at the nth time step, Δt is the time step, $r = k/\eta$, and

$$G(x) = EIw_{n-1}'''' + P_{n-1}w_{n-1}'' + kw_{n-1}, \tag{4.7}$$

involves quantities evaluated at the previous time step. $G(x)$ varies with position along the strut and may therefore be considered as a forcing function. It is not, however, a forcing function in the usual sense of being a well defined function of x, rather it is defined in terms of data from the previous time step. The system of partial differential equations (4.4) and (4.5) has now been reduced to a fourth-order ordinary differential equation involving a free parameter P. The supplementary conditions required to solve this problem on a finite interval are described next.

4.4.2 Boundary conditions

The fourth-order differential equation (4.6) requires four boundary conditions to define a solution. Two of these follow directly from the conditions of symmetry,

$$w' = w''' = 0, \tag{4.8}$$

which are imposed, for convenience, at $x = 0$. This ensures that only half of the spatial domain need be considered, $x \in [0, \infty)$. For a localized solution the remaining boundary conditions must ensure the flat state is achieved as $x \to \infty$. For the initial elastic state these are the conditions which prohibit the positive exponential solutions described in § 3.2.2. Upon differentiating the general solution (3.16) and eliminating the trigonometric terms, the following expressions are found for the boundary conditions as $x \to \infty$:

$$\begin{aligned} w'' + 2\alpha w' + \left(\alpha^2 + \beta^2\right) w &= 0, \\ 2\alpha w''' + \left(3\alpha^2 - \beta^2\right) w'' - \left(\alpha^2 + \beta^2\right)^2 w &= 0. \end{aligned} \tag{4.9}$$

As the localized solutions evolve in time the issue of boundary conditions becomes more complicated. Under displacement control, the end-shortening at each step is restrained, requiring the evaluation of a nonlinear expression. Hence, the starting boundary conditions (4.9), determined from the linearized equation of the initial elastic state, are not sufficient. To understand better this problem, numerical experiments are performed in § 4.6.3 using three different boundary conditions for evolving solutions: clamped conditions, $w = w' = 0$; pinned conditions, $w = w'' = 0$; and the linearized elastic conditions (4.9) maintained for all time. For a sufficiently long strut, no significant difference was found in the profile of the localized solution. The semi-infinite interval is further truncated to $[0, L]$, with the length L chosen to be sufficiently large that the amplitude of the linearized deflection at $x = L$ is very small ($w \approx 10^{-6}$).

4.4.3 Rigid loading

The majority of buckling theories for geological folding concern the evolution of an instability in a layer under conditions of constant load (Biot (1961), Mühlhaus (1993), for example). One of the principal differences between these theories and the work presented in this thesis is the consideration of buckling under rigid load conditions (controlled axial displacement). In this case, the load is a free parameter whose value is determined by the integral constraint

$$\mathcal{E} = \int_{-\infty}^{\infty} \left\{ 1 - \sqrt{1 - w'^2} \right\} \mathrm{d}x, \tag{4.10}$$

representing the exact end-shortening of the strut (Thompson & Hunt, 1973). This integral may be transformed into a differential equation by introducing the function

$$v(x) = \int_{-\infty}^{x} \left\{ 1 - \sqrt{1 - w'^2} \right\} \mathrm{d}s, \tag{4.11}$$

and differentiating it with respect to x to give

$$v' = 1 - \sqrt{1 - w'^2}, \tag{4.12}$$

with boundary conditions $v(0) = \mathcal{E}/2$ and $v(\infty) = \mathcal{E}$ on the semi-infinite interval. The contribution to end-shortening beyond $x = L$ is assumed to be negligible, so that $v(L) \approx v(\infty)$. Constant *rate* of end-shortening is achieved in a similar fashion with the value of end-shortening incremented by a constant value at each time step.

4.5 General purpose software

The solution of each visco-elastic system was performed numerically using the program COLPAR (Ascher *et al.*, 1995). This is a FORTRAN code for solving mixed-order systems of boundary-value problems in ordinary differential equations. It belongs to a group of general-purpose codes which have been successful in solving a large class of problems due, in part, to the stable nature of the discretization method and efficient algorithms for error estimation and mesh selection. A historical review of the development of this group of programs is presented next.

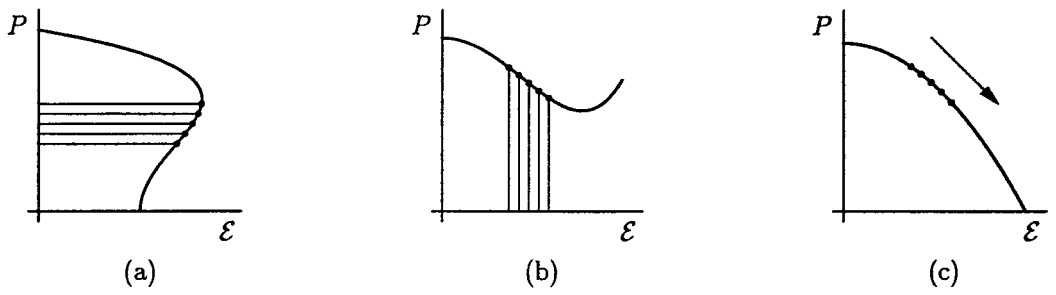

Figure 4.4 Schematic illustrating the potential of subroutines based on COLSYS: (a) COLNEW for different but constant values of load; (b) COLPAR for different but constant values of end-shortening; and (c) COLCON for automatic continuation.

4.5.1 Historical development

In 1980 Ascher *et al.* (1981) developed a program called COLSYS for systems of boundary-value problems in ordinary differential equations. This code uses a global method, based on collocation, to approximate the solution at discrete mesh points. A number of improvements have been made to the original code to enable a wider class of problems to be solved. Applications for the different versions of the code are illustrated in Figure 4.4 for a sequence of hypothetical buckling problems. COLNEW (Bader & Ascher, 1987) is capable of solving ordinary differential equations with constant coefficients. In a buckling context, this means the post-buckling curve (P versus $\mathcal{E}$) may be constructed by solving the governing equation at different, but fixed, values of load. This is particularly valuable for buckling problems which exhibit "snap back". An extension of this code, known as COLPAR, was made by Bader & Kunkel (1989) to solve parameter-dependent boundary-value problems. This enables the post-buckling response to be determined by evaluating the buckle solutions at different, but constant, values of end-shortening. A further extension of the code, known as COLCON, was made by the same authors to facilitate automatic continuation in parameter-dependent problems. This means an entire post-buckling response can be evaluated from a single run. The load is free to vary between specified upper and lower limits.

Amongst the group of subroutines based on COLSYS, the extension COLPAR is best suited to solve the problem of buckling in a strut-on-foundation model under rigid load control.

4.5.2 Implementation

COLPAR is a general-purpose code used to solve mixed-order systems of d nonlinear differential equations of orders $1 \leq m_i \leq 4$ with the form

$$w_i^{(m_i)} = f_i\left(x; \boldsymbol{z}(\boldsymbol{w}, \mathbf{par})\right), \quad 1 \leq i \leq d, \tag{4.13}$$

on the interval $a \leq x \leq b$. The exact solution vector is

$$\boldsymbol{w}(x) = (w_1(x), w_2(x), \cdots, w_d(x)), \tag{4.14}$$

par is a vector of unknown parameters, and

$$\boldsymbol{z}(\boldsymbol{w}(x), \mathbf{par}) = \left(w_1(x), w_1'(x), \cdots, w_1^{(m_1-1)}(x), \cdots, w_d(x), \cdots, w_d^{(m_d-1)}(x), \mathbf{par}\right)$$

is the vector of unknowns that would result from converting Equation (4.13) to a first-order system. The system is subject to $m^* = q + \sum_{j=1}^{d} m_j$ boundary conditions

$$g_j(\zeta_j; \boldsymbol{z}(\boldsymbol{w}(\zeta_j), \mathbf{par})) = 0, \quad 1 \leq j \leq m^*, \tag{4.15}$$

where q is the number of unknown parameters and ζ_j is the location of the jth boundary condition, $a = \zeta_1 \leq \zeta_2 \leq \cdots \leq \zeta_{m^*} = b$.

Unlike other codes, COLSYS is designed to handle mixed-order systems without explicitly converting them to a first-order system. For collocation, this direct treatment is more efficient both in terms of storage requirements and execution time (Ascher *et al.*, 1995).

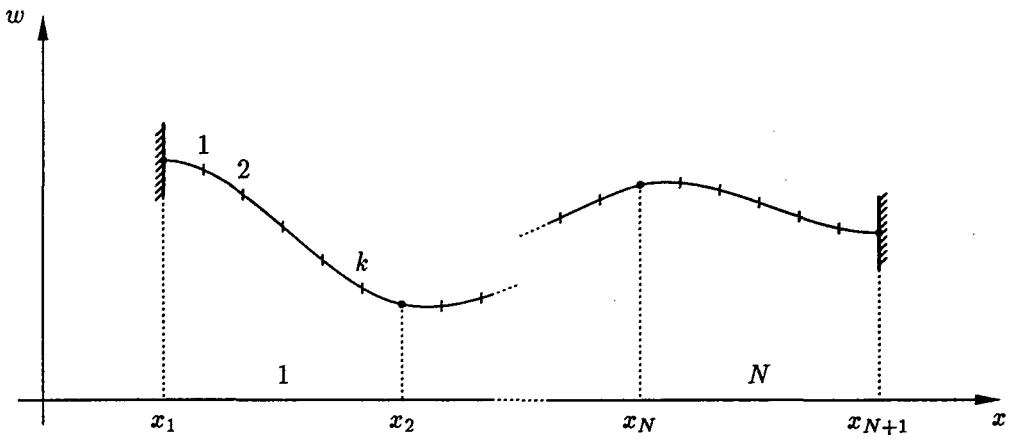

Figure 4.5 Schematic of collocation procedure.

4.5.3 Method of solution

COLPAR uses a collocation method to approximate the solution at Gaussian points as described in detail by Ascher *et al.* (1995). Approximate solutions are computed at mesh points which are automatically redistributed and refined until the solution at these mesh points satisfies a set of predefined tolerances. The facility for automatic mesh generation is especially important for localized solutions where the significant deformation is concentrated over a fraction of the spatial domain. A damped Newton's method is used for the nonlinear iteration.

The collocation method is depicted in Figure 4.5. An approximate solution is sought of the form

$$w_\pi(x) = \sum_{j=1}^{N} c_j \phi_j(x), \qquad a \le x \le b, \tag{4.16}$$

where $\phi_j(x)$ are linearly independent functions defined on $[a, b]$ and c_j are unknown constants. Using a piecewise polynomial $w_\pi(x)$ to approximate the solution on the interval $[a, b]$ reduces to a polynomial on each subinterval $[x_i, x_{i+1}]$. There are k collocation points per subinterval. For each of the N subintervals, $k + m_i$ constants are needed to define uniquely the local polynomial, resulting in $N(k+m_i)$ unknowns for each differential equation. These unknown quantities are determined by requiring that $w_\pi(x)$ satisfy: (i) m_i boundary conditions; (ii) the ordinary differential equation exactly at k points in each of the N subintervals of the mesh; and (iii) m_i matching constraints at each internal mesh point (corresponding to w and $m_i - 1$ continuous derivatives). The total number of equations is $(N-1)m_i + m_i + Nk = N(k + m_i)$,

which corresponds exactly to the number of unknowns. The advantage of using piecewise polynomials to approximate the function is that local use of low-degree polynomials is usually more accurate and more efficient than using a high-degree polynomial globally (Ascher *et al.*, 1995).

The implementation of the collocation procedure relies on a number of other features including error estimation, automatic mesh generation and an initial approximation. These issues are addressed below.

Error estimation

A standard extrapolation technique is used for the purpose of reliably estimating the accuracy of the collocation solution. For a given mesh and solution the subintervals are halved and the solution re-evaluated and compared with the original solution (on the undoubled mesh). This process is continued until a user-prescribed tolerance is satisfied at all positions along the length of interest, $x \in [a, b]$.

Mesh refinement and redistribution

A particular strength of COLPAR, and the other codes based on COLSYS, is their automatic mesh generation algorithm. This procedure places more mesh points in regions where the profile of the solution changes rapidly and less in other regions, thus capturing the essence of the solution with as few subintervals as possible. Mesh refinement, which involves both redistribution of mesh points and mesh halving, is illustrated in Figure 4.6 for an elastic buckling problem. The basis of the criterion for mesh refinement is an approximation of the local error. The reason that this error estimate is used for mesh selection is that it has the advantage of being cheaper to compute than the extrapolated error estimate. A *monitor function* is used to refine the mesh and ensure the error is approximately equal in each subinterval. Despite the power of automatic mesh selection, a good initial mesh can improve performance considerably. The nonlinear iteration may not converge for an inadequate initial mesh, causing repeated mesh halving without obtaining convergence until storage limitations are reached.

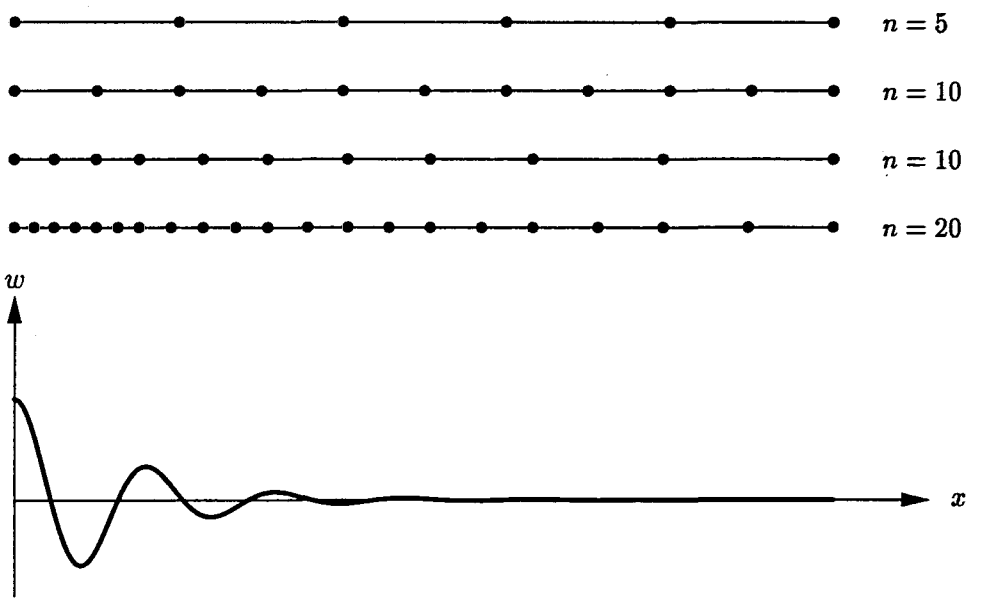

Figure 4.6 Automatic mesh refinement, including mesh redistribution and mesh halving, in the solution of buckling equation (4.17) ($EI = k = c = 1$, $P = 1.80$).

Initial approximation

At each time step the differential equation solver COLPAR requires an initial guess of the nonlinear solution with which to begin its iteration process. Beyond the first time step this is achieved simply by using the solution from the previous time step as the initial guess for the next time interval. However, at the first time step a previous solution does not exist and a different approach is required. In this case, a sufficiently accurate starting solution can usually be obtained using a trial function with a single term. Two such methods, based on weighted residual procedures, are discussed in Chapter 5. The difficulty with this approach is that these methods are not practical for equations containing general nonlinear terms such as the elastica on a linear foundation given by Equation (3.9). However, Wadee (1993) has shown that qualitatively similar localized solutions exist in elastic buckling equations irrespective of the source of softening nonlinearity. In this thesis trial solutions of the nonlinear differential equation

$$EIw'''' + Pw'' + kw - cw^3 = 0, \tag{4.17}$$

were found to provide an adequate starting solution for more general nonlinear systems. In the few instances where this procedure was insufficient for COLPAR to achieve convergence, simple continuation was used to start from a nearby solution. In this process a chain of intermediate problems is solved, with the final mesh and solution from the preceding problem used as the initial mesh and approximation for the next.

4.6 Validation of numerical procedure

The numerical techniques outlined in this chapter play a leading role in subsequent chapters for evaluating solutions to a range of nonlinear problems. It is essential, therefore, to investigate the accuracy of these methods. Three different approaches are used to confirm the suitability of COLPAR, and other aspects of the solution procedure, for tracing localized buckling solutions. First, the ability of the code to solve nonlinear differential equations is examined by considering a classic buckling problem for which closed-form solutions are available. Secondly, localized solutions obtained using the boundary-value method of the previous section are checked using the shooting method of Champneys & Spence (1993). Finally, a series of numerical experiments are carried out to examine the effect of boundary conditions, length and time step on the solution of the buckling problem represented by a strut on a Maxwell foundation.

4.6.1 Elastica column

Consider a slender column of length $2L$ simply-supported at each end and subjected to an axial force P. As a result of the symmetrical nature of the problem, only half of the structure need be considered, as shown in Figure 4.7. To determine the large-amplitude solutions which exist when the load exceeds the critical load P^{c}, the exact expression for curvature must be used. Adopting the intrinsic coordinate system $x - \theta$ shown in the figure, and measuring the distance x along the column from the free end, the exact expression for curvature is $\frac{\mathrm{d}\theta}{\mathrm{d}x}$, the first derivative of the slope. The column is considered to be inextensible, so that the change in length

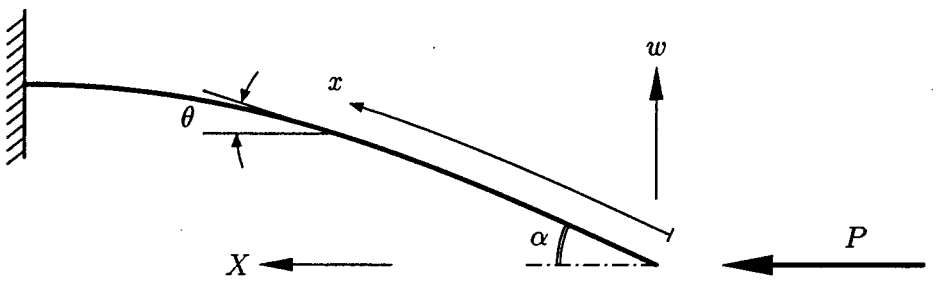

Figure 4.7 Elastica column.

of the column due to compression is neglected. The resulting differential equation (Timoshenko & Gere, 1963) is

$$EI\frac{\mathrm{d}^2\theta}{\mathrm{d}x^2} + P\sin\theta = 0, \tag{4.18}$$

the solution of which is referred to as the *elastica* (Love, 1944).

Theoretical solution

The theoretical solution for the elastica column, involving elliptic integrals, is well known (Timoshenko & Gere, 1963). It was discovered originally by Kirchhoff (1859) for the analogous problem involving large oscillations of a pendulum, and is known as "Kirchhoff's dynamical analogy". The horizontal and vertical coordinates (X, w) of a point along the column are given as:

$$\begin{aligned} X &= \frac{2}{p}E(\gamma) - \frac{1}{p}K(\gamma), \\ w &= \frac{2\gamma}{p}(1-\cos\phi), \end{aligned} \tag{4.19}$$

where the elliptic integrals of the first and second kind are

$$\begin{aligned} K(\gamma) &= \int_0^{\phi} \frac{\mathrm{d}\phi}{\sqrt{1-\gamma^2\sin^2\phi}}, \\ E(\gamma) &= \int_0^{\phi} \sqrt{1-\gamma^2\sin^2\phi}\,\mathrm{d}\phi, \end{aligned} \tag{4.20}$$

and $p = \sqrt{P/EI}$ is a load parameter, $\gamma = \sin(\alpha/2)$ is a deformation parameter, and

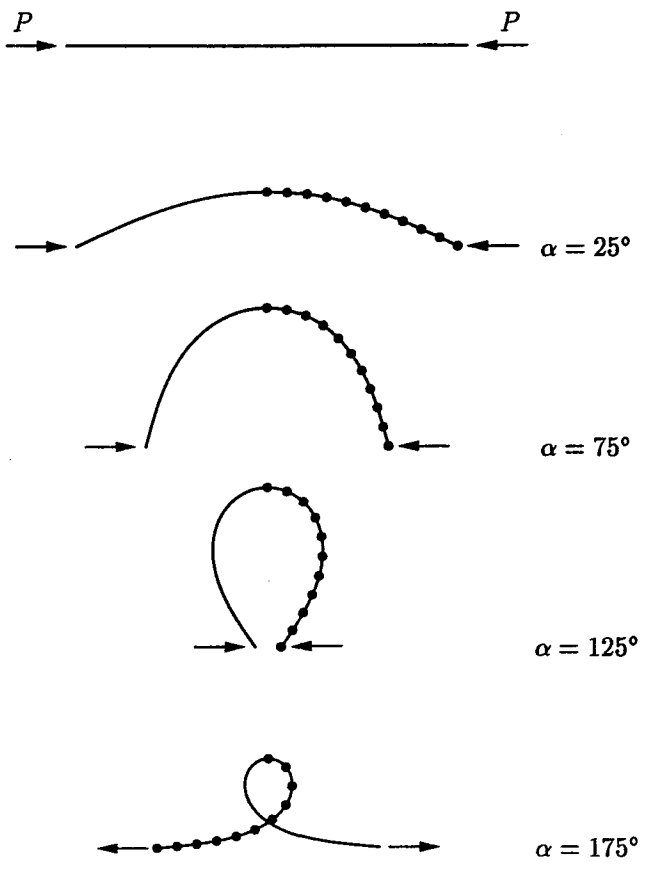

Figure 4.8 Comparisons of large-deflection solutions for a simply-supported elastica column: —— analytical solutions; and • numerical solutions (COLPAR).

ϕ is a location parameter which varies $0 \leq \phi \leq \pi/2$ as $0 \leq \theta \leq \alpha$. The axial load P can be calculated from the following relationship between the deformation and load parameters

$$p = \frac{1}{L}\int_0^{\frac{\pi}{2}} \frac{\mathrm{d}\phi}{\sqrt{1-\gamma^2\sin^2\phi}}. \tag{4.21}$$

The deflected shape of the column can be calculated by first selecting a value of α (or γ), then determining p, and hence P, from Equation (4.21), and the profile from Equation (4.19).

Numerical solution

COLPAR is used to solve the second-order differential equation (4.18) subject to the boundary conditions $\frac{\mathrm{d}\theta}{\mathrm{d}x} = 0$ at $x = 0$ and $\theta = 0$ at $x = L$. The deflected profile is found for various α values, by allowing the load to vary subject to the additional boundary condition $\theta = \alpha$ at $x = 0$. These profiles are shown in Figure 4.8. As with

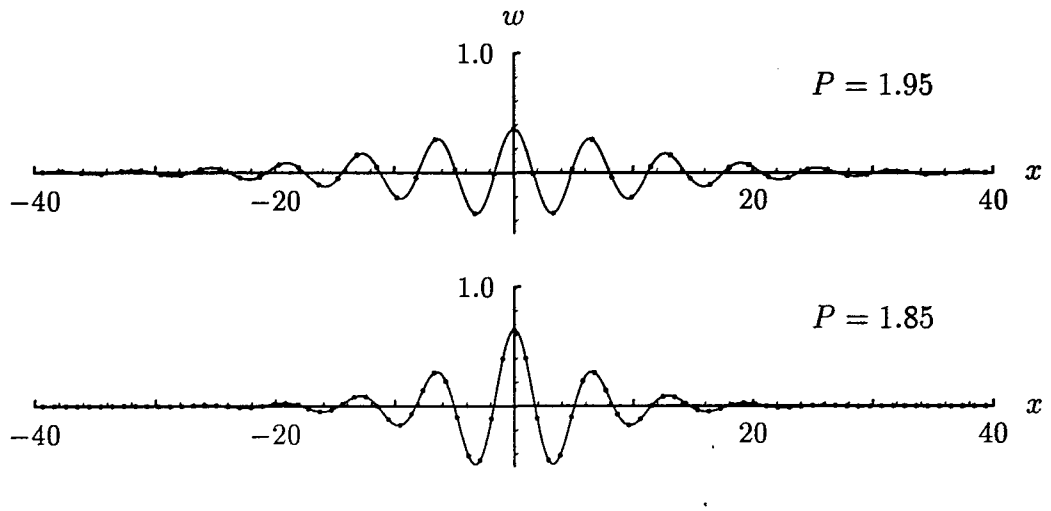

Figure 4.9 Comparisons of solutions for Equation (4.17): —— initial-value solutions; and • boundary-value solutions ($EI = k = c = 1$).

the theoretical solution, only half of the column need be analysed, the problem being symmetric about $x = L$. A mesh comprising 10 subintervals was required to satisfy a prescribed tolerance of 10^{-6} in the solution at mesh points. The numerical solution displays excellent agreement with analytical results evaluated at 100 equidistant points using Mathematica.

4.6.2 Comparison with shooting method

Closed-form solutions are generally not available for localized buckling problems. The next best check of the ability of COLPAR to approximate localized solutions is by comparison with an independent method. An obvious candidate for this role is the shooting method presented by Champneys & Spence (1993). The potential of this initial-value method for revealing localized solutions has already been proven for strut-on-foundation problems (Champneys & Toland, 1993; Champneys, 1994). The details of this procedure are described in § 4.2.2 and summarised by the flow chart in Figure 4.2. A comparison of results obtained using this method with the results from COLPAR is shown in Figure 4.9. For load values $P = 1.95$ and $P = 1.85$, the agreement between solutions is within the tolerances prescribed for each method (10^{-10}).

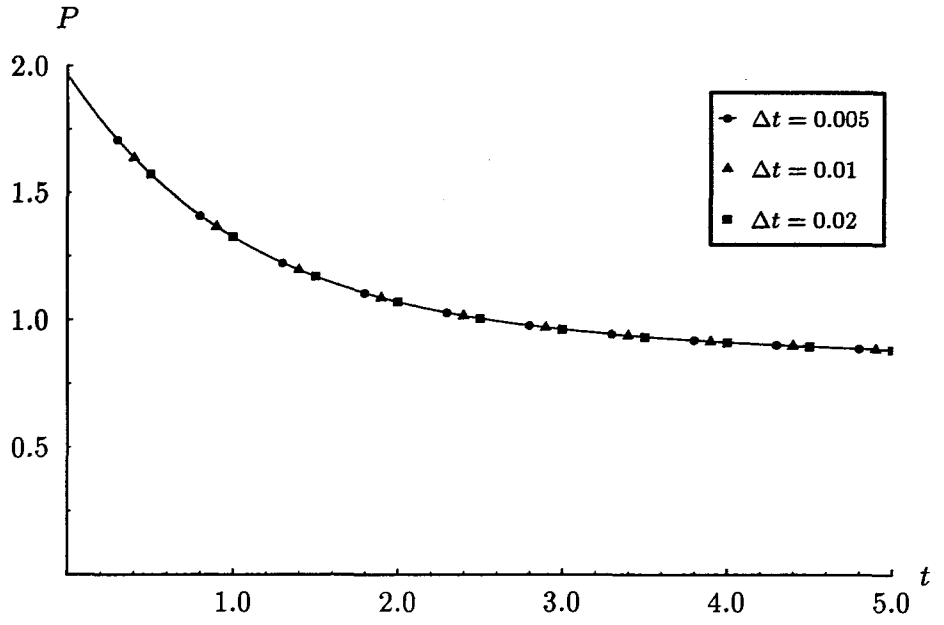

Figure 4.10 Effect of time step on the solution for an elastica strut on a linear Maxwell foundation under constant end displacement ($\mathcal{E} = 1.50$, $L = 50$, $EI = k = \eta = 1$, pinned end conditions).

4.6.3 Numerical experiments

The preceding sections have confirmed the ability of the techniques described in this chapter to solve specific problems. It is also desirable to investigate the effect of the various assumptions made in § 4.4 on the solution to the problem of a strut on a foundation. This includes truncation of the infinite problem to a finite domain, the temporal discretization procedure, and the choice of boundary conditions. These effects are not addressed theoretically; instead a parametric study is used. The penalty for this approach is that the effect of each assumption must be investigated separately for each problem.

The effect of the size of time step Δt on the axial load of an evolving localized solution is shown in Figure 4.10. There is no discernible difference in the solutions obtained for each of the time steps shown. While this suggests that a larger time step could be used, difficulties were encountered with convergence of the numerical scheme at the first time step for $\Delta t \geq 0.03$. The need for a small time step is confined to the early period where the rate of change of load (and profile) is greatest. After this time the evolution proceeds more slowly and a larger time step would suffice.

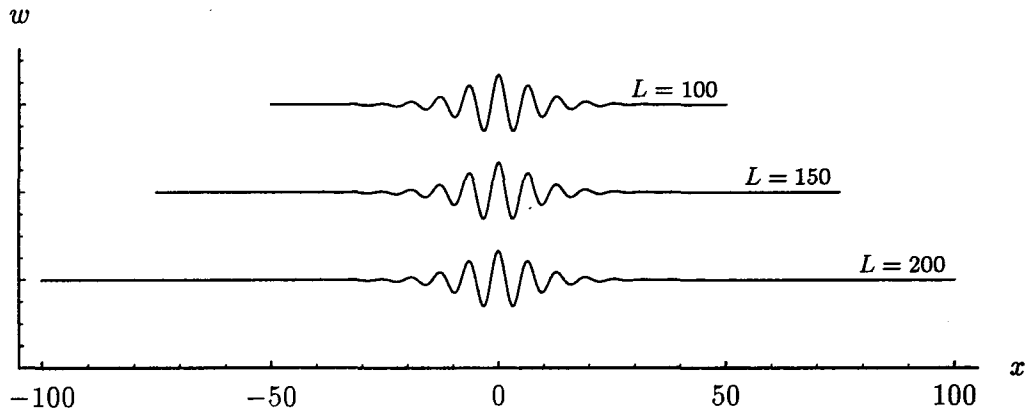

Figure 4.11 Effect of length on the solution for an elastica strut on a Winkler foundation ($P = 1.90$, $EI = k = 1$, pinned end conditions).

Perhaps the most efficient approach would be to incorporate a variable time step, just as there is a variable mesh, Δx. However, while computational efficiency is certainly a laudable goal it is not the principal objective here. For all time-dependent results presented in this thesis at least three numerical runs were performed for different values of Δt. The usual method of repeated reduction of time step was employed to ensure convergence of the numerical scheme.

In the context of geological folding, the model of a strut on a foundation is regarded as being infinitely long. In practice, however, it is impossible to analyse such a structure; it must instead be transformed into a finite structure, either by truncation or mapping. The former method is adopted here with boundary conditions imposed at the ends to ensure a good approximation to the solution of the corresponding infinite problem is obtained. Confirmation that the truncation length is adequate is provided in Figure 4.11 where no visible difference between localized solutions is recorded for $L = 50$, 100 and 200 in the buckling of an elastica strut supported by a linear Winkler foundation.

Appropriate boundary conditions for the truncated problem are those that ensure the solution of the approximate problem converges to the actual solution of the "infinite" problem as the length of the finite interval tends to infinity. Rigorous methods for solving boundary-value problems posed on infinite intervals are discussed by

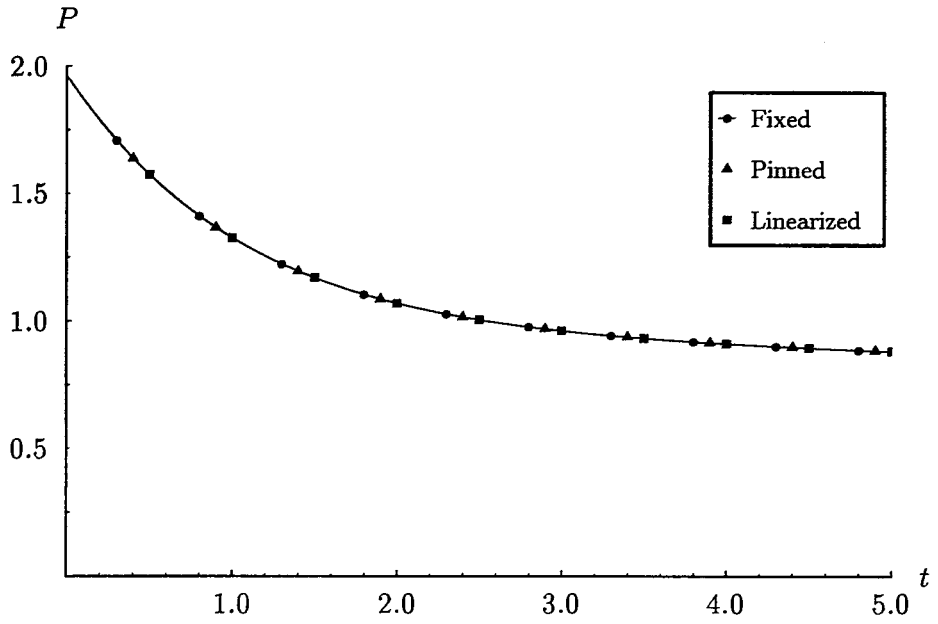

Figure 4.12 Effect of boundary conditions on the solution for an elastica strut on a linear Maxwell foundation under constant end displacement ($\mathcal{E} = 1.50$, $L = 50$, $\Delta t = 0.01$, $EI = k = \eta = 1$).

cussed by Markowich (1982) and Lentini & Keller (1980). An alternative method, albeit crude, is to make the domain of the problem sufficiently large that the boundary conditions have negligible impact on the solution. In Figure 4.11 this method was used to demonstrate that the solution is unaffected by the length of the strut for the same boundary conditions. In Figure 4.12 the effect of three different boundary conditions at $x = L$ are shown for an evolving localized solution. The boundary conditions considered are: clamped conditions, $w = w' = 0$; pinned conditions, $w = w'' = 0$; and the linearized elastic conditions (4.9) maintained for all time. Again there is no visible difference between each of the solutions for the end conditions shown. For a strut on a Maxwell foundation under conditions of constant end displacement, the localized buckle profile has a tendency to become less localized with time. It is inevitable, therefore, that the boundaries will ultimately affect the solution. However, the time before the boundary conditions have a significant effect on the solution can be delayed by choosing a longer strut.

4.7 Concluding remarks

The validity of the boundary-value method of this chapter has been confirmed using a three-pronged approach involving a comparison with a closed-form solution for the large deflections of a simply-supported column and an independent numerical (shooting) method. The effect of approximating the infinite boundary-value problem by a series of finite ordinary differential equations has also been established through a series of numerical experiments. In combination, these checks engender confidence that the behaviour reported is a genuine characteristic of the problem, rather than of the numerical method. Further confidence is gained in the following chapter by comparison with solutions obtained using the method of weighted residuals.

Although shooting methods are perfectly adequate for solving ordinary differential equations of elastic buckling systems, they cannot be applied practically to solve partial differential equations of visco-elastic systems. For this reason the method outlined in this chapter is better suited to localized buckling of an elastic strut on a Maxwell foundation than are the published methods of Champneys & Spence (1993) and Hunt & Wadee (1991).

Chapter 5

Weighted residual methods

This chapter explores the potential of classical techniques for determining localized buckle patterns in strut-on-foundation models. It commences with an overview of the method of weighted residuals and variational principles and a discussion of suitable trial functions. A Galerkin method is then used to approximate localized solutions to the equation of a linearized strut on a nonlinear Winkler foundation. This is followed by a collocation method which is used to study a related viscoelastic system. In both cases, results are compared with solutions obtained using the numerical methods outlined in the previous chapter.

5.1 Introduction

Classical methods of analysis were developed originally for the manual solution of problems with simple geometries and material properties. More recently, the advent of computers has led to general numerical methods capable of solving more difficult problems involving complex geometry and nonlinear material behaviour. Today the stability of almost any structure could, at least in principle, be analysed using a geometrically nonlinear finite element code with incremental loading. Powerful though this approach may be, the value of simple analytical methods must not be underestimated, for these methods enhance our understanding of the solution and provide important checks of the more complicated numerical schemes.

5.1.1 Discretization of continuous structures

Models of struts on foundations are continuous problems with an infinite number of degrees of freedom. For their solution, it is customary to reduce such problems to corresponding problems with finite degrees of freedom. This may be performed in one of two ways: (i) by expressing the deflected shape as the sum of specified displacement patterns which are referred to as generalized coordinates, as for example in the Rayleigh-Ritz method; or (ii) by subdividing the structure into segments and using the displacement at nodes to represent the generalized coordinates, as for example in the finite element method (Bathe, 1996). In either case, a set of algebraic equations is derived, the solution of which approximates the deformed shape of the structure. Clough & Penzien (1993) suggest that for uniform struts the first method provides a better approximation for the same number of degrees of freedom while the latter is best for discrete (lumped mass) systems.

5.1.2 Benefits of classical methods of solution

Numerical methods, such as the finite difference and finite element methods, are applicable to broad classes of one-, two- and three-dimensional problems. In many cases, however, it is preferable to perform analyses using specialized approaches which are not burdened by rigid methods and excessive generality. These simple methods enable knowledge gained from previous mathematical studies to be incorporated in the solution and often lead to approximations which embody many of the essential features of the true solution using only a few modes. In contrast, numerical methods generally make no assumptions about the solution to a specific problem, hence their universal application.

The one-dimensional nature of the strut-on-foundation model makes it an ideal candidate for solution by classical means. In particular, the infinite length of the strut model, which is the bane of many numerical schemes, is dealt with easily using infinite mode shapes. Initial-value methods (Champneys & Spence, 1993) and boundary-value methods (Whiting & Hunt, 1996) become increasingly difficult to use when tracking localized buckling solutions towards the critical point because the truncation length increases without bound. By comparison, it is in this vicinity,

where the amplitudes and slopes are small, that classical solution procedures are most accurate.

Perhaps the most important contribution of classical methods of analysis is their ability to generate approximate solutions which can be used as initial approximations for numerical boundary-value solvers. These tools require an initial profile of a solution in much the same way that Newton's method can be used to determine a root of a polynomial provided a sufficiently close starting value is specified. An approximate solution with a single mode is often sufficient to enable a boundary-value procedure to achieve numerical convergence and, with the inclusion of additional terms, may provide an independent check of the numerical solution.

5.2 Weighted residual and variational methods

Methods for approximating solutions to differential equations fall into two broad categories: weighted residual methods and variational methods. The former operate directly on the differential equation while the latter use a functional related to the differential equation. A comprehensive description of these methods may be found in various books (Finlayson (1972) and Ames (1992), for example).

5.2.1 Weighted residual methods

In the method of weighted residuals, the solution of a differential equation,

$$D[w] = 0, \tag{5.1}$$

is approximated by a trial solution $\bar{w}(x)$ in the form of a series,

$$\bar{w} = \sum_{i=1}^{n} A_i \, \phi_i, \tag{5.2}$$

where $\phi_i(x)$ are linearly independent trial functions (or modes) chosen to satisfy the boundary conditions and A_i are adjustable constants (or amplitudes). The

amplitudes[1] are chosen to give the best solution to the differential equation (5.1) by substituting for the approximate form (5.2) and minimizing the residual, or error,

$$R(A_i, x) = D[\bar{w}]. \tag{5.3}$$

If the trial solution is the *exact* solution, the residual is zero at every point. In general, this will not be the case, and the residual $R(A_i, x)$ is a function of the unknown amplitudes A_i and spatial variable x. The objective of the method of weighted residuals is to minimize the error with respect to the unknown amplitudes A_i. This is achieved by first multiplying the residual by a weighting function $W_i(x)$ and integrating over the domain. The result is then set to zero:

$$\int R W_i \, \mathrm{d}x = 0 \qquad i = 1, 2, ..., n. \tag{5.4}$$

Thus, the amplitudes A_i are determined by requiring the *weighted average* of the residual to be zero, giving rise to the title of this class of solution methods. The choice of weighting functions W_i is unlimited and can be used to place emphasis on different parts of the solution. Each family of weighting functions corresponds to a different criterion of the method of weighted residuals, some of which are discussed next.

Method of least squares

In this technique the integral of the square of the residual is minimized with respect to each of the amplitudes,

$$\frac{\partial}{\partial A_i} \int R^2 \, \mathrm{d}x = 2 \int R \frac{\partial R}{\partial A_i} \mathrm{d}x = 0 \qquad i = 1, 2, ..., n. \tag{5.5}$$

The weighting functions are, in effect, the derivatives $\partial R / \partial A_i$. A disadvantage of this method is that it often leads to rather cumbersome equations making it awkward to apply in practice (Finlayson, 1972).

[1] Note that the amplitudes A_i in Equation (5.2), and used throughout this chapter, should not be confused with the slowly varying amplitudes $A_i(X)$ and $B_i(X)$ of the perturbation scheme in Chapter 3.

Galerkin method

The Galerkin method uses trial functions as weighting functions, $W_i = \phi_i$, thus penalising the residual error according to the mode shape. The unknown amplitudes A_i are then determined from the algebraic equations

$$\int R\,\phi_i\,\mathrm{d}x = 0 \qquad i = 1, 2, ..., n, \tag{5.6}$$

which indicate that the work done by the residual (out of balance) forces over the displacements $\phi_i(x)$ is zero. This method has been applied successfully to many well known problems, including Couette flow between rotating cylinders (Finlayson, 1972).

Collocation method

The collocation method uses the Dirac delta function, $W_i = \delta(x - x_i)$, as the weighting function. No integration is required because the approximate solution is forced to satisfy the differential equation at selected collocation points. The location of these points is arbitrary although *a priori* knowledge of the form of the solution can be used to determine a suitable distribution for them. This method forms the basis of the numerical procedure outlined in Chapter 4 and is used later in this chapter to analyse the problem of a strut on a visco-elastic foundation.

These methods and others not described here were unified by Crandall (1956) and are known collectively as the *method of weighted residuals.* They have been applied to numerous problems on structural stability involving rods, plates and shells (Galerkin, 1915; Leissa *et al.*, 1969; Ames, 1992; Duxbury, 1988). A first approximation, achieved by retaining only the first term of the series, is often sufficient to achieve a qualitative description of the solution, while the accuracy can often be improved by including additional terms.

5.2.2 Variational principles

Differential equations are not the only basis upon which approximate solutions can be founded. A functional may also be used, but only for problems with an underlying variational principle, such as the total potential energy in the case of an elastic system. The variational method is similar in many respects to the method of weighted residuals with the solution expanded in terms of a set of trial functions. The undetermined amplitudes are found by making the variational integral stationary with respect to each degree of freedom. An example of a variational approach is the Rayleigh-Ritz method (Stephenson & Radmore, 1990), which has recently been applied to the problem of a strut on a nonlinear elastic foundation (Wadee *et al.*, 1996). For this problem of elastic stability the total potential energy function,

$$V = U - P\mathcal{E}, \tag{5.7}$$

is used as the basis of the method, where U is the potential energy and $\mathcal{E}$ is the end displacement of the strut due to the applied load P. The amplitudes A_i of the approximate solution are found by solving the equations

$$\frac{\partial V}{\partial A_i} = 0. \tag{5.8}$$

Wadee *et al.* (1996) obtained results which agree closely with those presented in § 5.4 using a Galerkin method. The equivalence between the Rayleigh-Ritz method, applied to the total potential energy, and the Galerkin method, applied to the differential equation, is well known and has been proven on many occasions (Galerkin, 1915; Finlayson, 1972).

The principal disadvantage of variational methods is that they can be applied only to problems which have a variational function. In contrast, the Galerkin method and other weighted residual methods are always applicable because they operate on the differential equation and do not depend on the existence of a variational principle. The differential equation governing the time-dependent response of a strut on a visco-elastic foundation is readily derived from consideration of the equations

of motion while, in general, a functional does not exist because of the dissipation of energy within the foundation. This was the deciding factor in using weighted residual methods in favour of a variational approach for the problem discussed in this thesis.

5.2.3 Choice of trial functions

An important advantage in using weighted residual methods over more general numerical methods is the ability to choose trial functions enabling information obtained from other sources to be incorporated in the trial solution. These trial functions must satisfy two criteria to ensure that the approximation converges, in the limit as $n \to \infty$, to the exact solution: they must be linearly independent and belong to a *complete* set of functions. A set of functions is complete if any function of a given class can be expanded in terms of that set, for example, the set of harmonic Fourier components. Together these conditions ensure the approximate solution is inherently capable of representing the exact solution provided enough terms are used.

The closed-form solutions generated by the perturbation method outlined in Chapter 3 are used as the family of trial functions in the methods which follow. The trial functions are

$$\begin{aligned} \phi_1 &= \operatorname{sech} \alpha x \cos \beta x, \\ \phi_2 &= \operatorname{sech} \alpha x \tanh \alpha x \sin \beta x, \\ \phi_3 &= \operatorname{sech}^3 \alpha x \cos \beta x, \\ \phi_4 &= \operatorname{sech}^3 \alpha x \tanh \alpha x \sin \beta x, \end{aligned} \tag{5.9}$$

and are shown in Figure 5.1. The first function, ϕ_1, is revealed at the s^3 level of the perturbation study, while the others become apparent at successively higher levels of s. Passive terms, such as $\cos 3\omega x$ and $\sin 3\omega x$, arising from the cubic form of the nonlinearity in the foundation stiffness, are ignored owing to their meagre contribution to the deflected shape of the strut. This is justified by comparing the magnitudes of the coefficients of the $\operatorname{sech}^3 \Omega X$ terms in Equation (3.28). The ratio

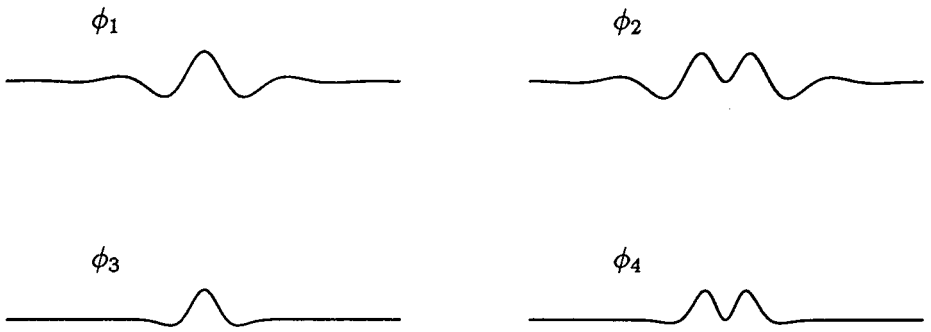

Figure 5.1 Trial functions $\phi_i(x)$.

of the magnitude of the active mode $A_{1,3}$ to the passive mode $A_{3,3}$ is $307/3 \approx 100$, while the ratio of $B_{1,4}$ to $B_{3,4}$ is $2762/81 \approx 34$. In either case, the contribution of the active modes far outweighs that of the passive modes.

The trial functions (5.9) apparently belong to an infinite set which satisfy the conditions of linear independence and completeness as defined above. The first criterion is a natural consequence of the combined trigonometric and hyperbolic mode shapes and the second follows from the formal perturbation procedure which revealed the significant modes in an ordered sequence. The modes ϕ_i also satisfy the flat boundary conditions for a localized solution as $x \to \pm\infty$, although this is not strictly necessary for weighted residual methods (Finlayson, 1972). The principal advantage of one set of trial functions over another is the rate of convergence to the exact solution. An improvement in the accuracy of an approximate solution can also be achieved by increasing the number of modes, though naturally at the expense of a corresponding increase in the number of equations to be solved.

5.3 Strut-on-foundation model

Localized behaviour in strut models involving geometric and material nonlinearities of arbitrary complexity is examined in the next chapter using numerical methods. In contrast, the types of differential equations amenable to analysis by weighted residual methods are restricted to those containing relatively simple nonlinear terms. In the case of a strut on an elastic foundation, for example, they are best applied to models with foundation reactions of the form $F = kw + c_1 w^2 + c_2 w^3 + \cdots + c_{n-1} w^n$.

The types of partial differential equations which can be tackled using weighted residual methods are even more limited. The restriction arises because of the compatibility relation for the Maxwell response which relates the displacements of the spring and dashpot to the total displacement, $w = w_s + w_d$. In order to eliminate the internal coordinates w_s and w_d from the compatibility relation they are expressed in terms of the total force acting on the Maxwell element, which is common to both the spring and dashpot. However, functions describing spring and dashpot responses are usually expressed as $F_s = f(w_s)$ and $F_d = f(\dot{w}_d)$, and may not necessarily have corresponding inverse functions. For example, a spring which obeys the relation $F_s = kw_s - cw_s{}^3$ does not have a genuine inverse function of the form $w_s = f(F_s)$, although it can be approximated locally by

$$w_s = \frac{1}{k}F_s + \frac{c}{k^4}F_s{}^3 + O(F_s{}^5). \tag{5.10}$$

Using a truncated form for w_s and replacing F_s with F, which involves a fourth derivative of w, can lead to long and unwieldy equations which negate the simplicity of weighted residual methods. This means that only certain types of models of struts on visco-elastic foundations can be practically analysed using these methods.

In this chapter, a model proposed by Hunt *et al.* (1996a) is used to demonstrate the potential of weighted residual methods for revealing localized solutions. The model is based on the linearized strut equation

$$EIw'''' + Pw'' + F = 0, \tag{5.11}$$

and visco-elastic foundation behaviour

$$\frac{1}{k}\dot{F} + \frac{1}{\eta}F = \frac{\partial}{\partial t}\left[w - cw^3\right]. \tag{5.12}$$

This foundation displays the same force-displacement characteristics as a Maxwell unit: an instantaneous elastic response followed by a period of viscous flow, although it cannot easily be described by an arrangement of springs and dashpots.

5.3.1 Nondimensionalization

For an elastic strut on a visco-elastic foundation there is a choice of nondimensional parameters; either the elastic buckle wavelength of the purely elastic system or the dominant wavelength of the purely viscous system may be used (Hunt *et al.*, 1996a). The latter introduces a time-dependence to the nondimensional spatial parameters, which effectively restricts the analysis to the case of constant load. As the intention here is to study the behaviour of the system under conditions of rigid load, the critical load and wavenumber of the purely elastic foundation are used. By using the transformations

$$\begin{aligned} x &= \left(\frac{EI}{k}\right)^{1/4} \tilde{x}, \\ w &= \left(\frac{1}{c}\right)^{1/2} \tilde{w}, \\ t &= \left(\frac{\eta}{k}\right) \tilde{t}, \\ P &= (kEI)^{1/2}\, \tilde{P}, \end{aligned} \tag{5.13}$$

it is possible to simplify the governing equations (5.11) and (5.12) into a single nondimensional form

$$\frac{\partial}{\partial \tilde{t}} \left[\tilde{w}'''' + \tilde{P}\tilde{w}'' + \tilde{w} - \tilde{w}^3\right] + \tilde{w}'''' + \tilde{P}\tilde{w}'' = 0. \tag{5.14}$$

From here on the tildes above each term will not be shown and the nondimensional form will be implicitly assumed. The effect of these transformations is to introduce a scaling which enables solutions to be determined without consideration of the values of the material constants. Solutions for specific values of EI, k, c and η may be retrieved by reversing the original transformations. For governing equations containing more general material or geometric nonlinearities, nondimensionalization may not be so straightforward and individual solutions may need to be found for different values of the material constants. This point was illustrated in § 2.6 for a rigid link model.

5.4 Galerkin method

The Galerkin[2] method is one of the best known weighted residual methods and bears the name of the Russian engineer who developed it early this century. This method is used here to describe solutions of the instantaneous elastic response of a strut on a visco-elastic foundation whose behaviour is governed by Equation (5.14). Although problems involving buckling have been tackled in the past using Galerkin procedures (Ames (1992) and Duxbury (1988), for example), it appears that no such treatments have been made of localized deformations.

The initial response, obtained by equating the contents of the square brackets in Equation (5.14) to zero, is governed by the equation

$$w'''' + Pw'' + w - w^3 = 0, \tag{5.15}$$

which is identical to the problem of a strut on a nonlinear (cubic) elastic foundation. In choosing an approximate solution $\bar{w}$ for the deflected shape of the strut, the differential equation (5.15) will not be satisfied exactly. A residual,

$$R(x, \bar{w}) = \bar{w}'''' + P\bar{w}'' + \bar{w} - \bar{w}^3, \tag{5.16}$$

remains which depends on the form of the approximate solution and varies with the position along the length of the strut.

5.4.1 Modal analysis

Single mode

The deflected shape of the strut is approximated by the modal form $\bar{w} = A_1 \phi_1$, with the single mode $\phi_1 = \operatorname{sech} \alpha x \cos \beta x$ corresponding to the first term in the ordered perturbation analysis (3.27). The values of α and β are assumed to be the

[2]Ironically, it was while he was imprisoned for his political views in 1906 that Galerkin published his first technical paper — on the buckling of rods and bars!

eigenvalues (3.13) of the linearized system which, in nondimensional form, are

$$\alpha = \sqrt{\frac{1}{2} - \frac{P}{4}}, \qquad \beta = \sqrt{\frac{1}{2} + \frac{P}{4}}. \tag{5.17}$$

According to the Galerkin method, the amplitude A_1 is found from the equation

$$\int_{-\infty}^{\infty} R(x, \bar{w})\ \phi_1\, \mathrm{d}x = 0. \tag{5.18}$$

After substituting for $\bar{w}$ and integrating over the infinite domain, the result is the nonlinear algebraic equation

$$\begin{aligned} &\frac{1}{2} f_1 A_1 I_2 + \frac{1}{2} f_1 A_1 I_{c22} + \frac{1}{2} f_2 A_1 I_{s22} - \left[2\alpha^2 \left(5\alpha^2 - 3\beta^2 + P\right) A_1 + \frac{3}{8} {A_1}^3\right] I_4 \\ &\quad - \left[2\alpha^2 \left(5\alpha^2 - 3\beta^2 + P\right) A_1 + \frac{1}{2} {A_1}^3\right] I_{c42} - 12\alpha^3 \beta A_1 I_{s42} - \frac{1}{8} {A_1}^3 I_{c44} \\ &\quad + 12\alpha^4 A_1 I_6 + 12\alpha^4 A_1 I_{c62} = 0, \end{aligned} \tag{5.19}$$

where f_1 and f_2 are given by the relations

$$\begin{aligned} f_1 &= 1 + \alpha^4 - 6\alpha^2\beta^2 + \beta^4 + P\left(\alpha^2 - \beta^2\right), \\ f_2 &= 2\alpha\beta\left(2\alpha^2 - 2\beta^2 + P\right). \end{aligned} \tag{5.20}$$

The integrals I_j, which are denoted

$$\begin{aligned} I_n &= \int_{-\infty}^{\infty} \operatorname{sech}^n \alpha x\, \mathrm{d}x, \\ I_{cnm} &= \int_{-\infty}^{\infty} \operatorname{sech}^n \alpha x \cos m\beta x\, \mathrm{d}x, \\ I_{snm} &= \int_{-\infty}^{\infty} \operatorname{sech}^n \alpha x \tanh \alpha x \sin m\beta x\, \mathrm{d}x, \end{aligned} \tag{5.21}$$

are evaluated in Appendix B. After substituting for these integrals and reordering, the expression

$$k_1 A_1 - k_{111} {A_1}^3 = 0 \tag{5.22}$$

is found in terms of the modal amplitude A_1, with coefficients

$$\begin{aligned} k_1 &= \frac{1}{15\alpha}\left[15+7\alpha^4+30\alpha^2\beta^2+15\beta^4-10P\left(\alpha^2+3\beta^2\right)\right] \\ &\quad +\frac{\beta\pi}{15\alpha^2}\left[15+7\alpha^4+10\alpha^2\beta^2+3\beta^4-10P\left(\alpha^2+\beta^2\right)\right]C_1, \\ k_{111} &= \frac{1}{2\alpha}+\frac{2\beta\pi}{3\alpha^4}\left(\alpha^2+\beta^2\right)C_1+\frac{\beta\pi}{3\alpha^4}\left(\alpha^2+4\beta^2\right)C_2, \end{aligned} \tag{5.23}$$

in which

$$C_1 = \operatorname{cosech}\left(\frac{\beta\pi}{\alpha}\right), \qquad C_2 = \operatorname{cosech}\left(\frac{2\beta\pi}{\alpha}\right). \tag{5.24}$$

For a given value of P, the nontrivial amplitude A_1 is therefore

$$A_1 = \sqrt{\frac{k_1}{k_{111}}}. \tag{5.25}$$

The ability to derive a closed-form solution for the modal amplitude is a unique property of the single-mode approximation as coupled nonlinear equations result when the deflected shape is represented by two or more modes.

Two modes

A second mode, $\phi_2 = \operatorname{sech}\alpha x \tanh\alpha x \sin\beta x$, corresponding to the s^2 coefficient in the perturbation analysis of Chapter 3, is incorporated in the trial solution so that $\bar{w} = A_1\,\phi_1 + A_2\,\phi_2$. The first term allows a modulation of the amplitude and the second an adjustment of the wavelength of the buckle profile (phase modulation) which is especially important around the centre of localization where the effect of the cubic nonlinearity is greatest (Wadee, 1993). The amplitudes A_1 and A_2 are defined by the pair of Galerkin equations:

$$\begin{aligned} \int_{-\infty}^{\infty} R\left(x, A_1, A_2\right)\,\phi_1\,\mathrm{d}x &= 0, \\ \int_{-\infty}^{\infty} R\left(x, A_1, A_2\right)\,\phi_2\,\mathrm{d}x &= 0. \end{aligned} \tag{5.26}$$

The evaluation of these equations involves considerable algebraic manipulation which is performed most simply using a mathematical package capable of symbolic manipulation, in this case, Mathematica (Wolfram, 1991). After substituting for the

integrals (5.21), the Galerkin equations may be simplified to

$$\begin{aligned} k_i A_i + k_{ijk} A_i A_j A_k &= 0, \\ l_i A_i + l_{ijk} A_i A_j A_k &= 0, \end{aligned} \tag{5.27}$$

where the Einstein convention is used to imply summation over repeated indices and the coefficients k_i, k_{ijk}, l_i and l_{ijk} are listed in Appendix C. These expressions were solved iteratively using a Newton-Raphson algorithm (Press *et al.*, 1988).

Higher modes

The earlier perturbation analysis is again used as a guide for selecting higher-order mode shapes with the third and fourth modes chosen to be $\phi_3 = \text{sech}^3\alpha x \cos\beta x$ and $\phi_4 = \text{sech}^3\alpha x \tanh\alpha x \sin\beta x$. Like the first mode, ϕ_3 affects the amplitude of the approximation while ϕ_4 influences the wavelength. The modal approximation now has the form

$$\bar{w} = \sum_{i=1}^{4} A_i \phi_i. \tag{5.28}$$

The corresponding Galerkin equations are not presented because of their length but have the same form as Equation (5.27) and may be derived using Mathematica.

5.4.2 Results

The numerical procedure outlined in Chapter 4 provides possibly the best reference with which to assess the quality of the Galerkin solutions. A visual check of the results is offered by Figure 5.2. The amplitude of the modal solutions at the centre of localization is progressively overestimated as the axial load drops to zero. The single-mode approximation provides the worst agreement, while the four-mode solution is indistinguishable to the naked eye from the numerical solution for all load values presented. The existence of a nontrivial buckled shape at $P = 0$ does not indicate an initial imperfection in the strut geometry; rather it represents an equilibrium point on the post-buckling curve of the perfect system, albeit far from the initial buckling load.

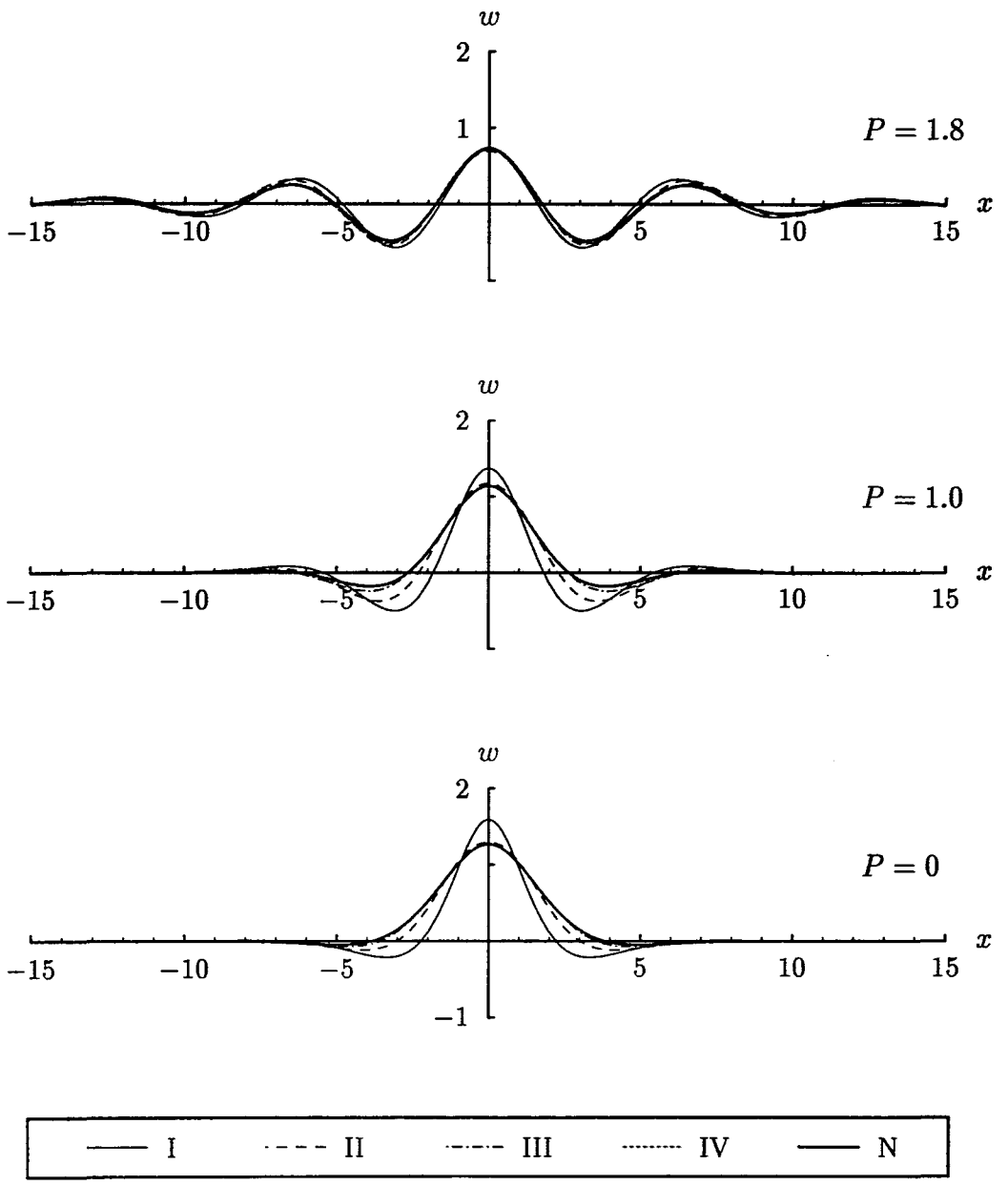

Figure 5.2 Comparison of numerical and Galerkin solutions for a strut on a nonlinear elastic foundation as represented by Equation (5.15): I — one mode; II — two modes; III — three modes; IV — four modes; N — numerical solution. The four-mode solution is indistinguishable from the numerical solution for all load levels.

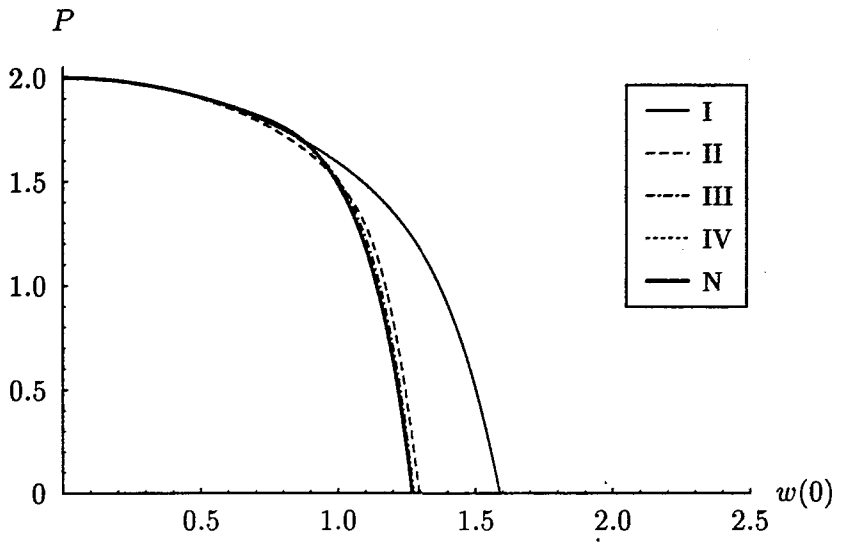

Figure 5.3 Comparison of load versus peak amplitude for numerical and Galerkin solutions: I — one mode; II — two modes; III — three modes; IV — four modes; N — numerical solution.

A closer inspection of the quality of the collocation solutions may be made by comparison with the numerical solution at specific locations or by averaging some quantity over the entire domain. Consider first the amplitude of the localized solution at the point of symmetry ($x = 0$) which is shown in Figure 5.3. For a single trial function, the amplitude is predicted well in the vicinity of P^c with a deterioration as $P \to 0$. For most load values a significant improvement is obtained following the introduction of a second and third mode, and when four modes are included the Galerkin approximation is obscured by the numerical solution.

An alternative measure of the error is provided by the average residual, defined here as

$$R_{\text{av}} = \sqrt{\int_{-\infty}^{\infty} R^2 \, \mathrm{d}x}. \tag{5.29}$$

This quantity is plotted in Figure 5.4; the smaller the error, the better the approximate shape. The exact solution has zero error and therefore represents the vertical axis. Perhaps inevitably, the error of the Galerkin solutions grows as the load decreases from P^c, for this is the point of expansion of the perturbation scheme which spawned the mode shapes. Although this method quantifies the error, it does so in an averaged sense which is only useful when comparing one approximate form with

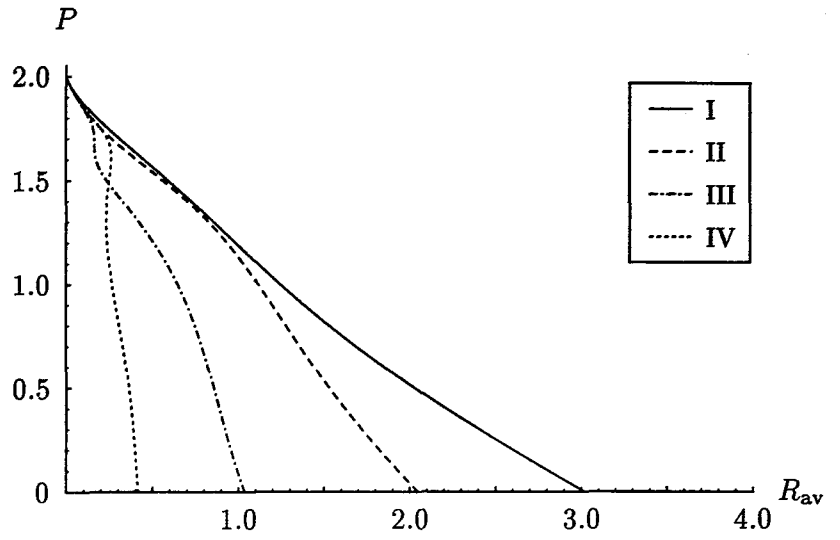

Figure 5.4 Load versus average residual for Galerkin solutions: I — one mode; II — two modes; III — three modes; IV — four modes.

another. An interesting feature of the average residual shown in the figure is that the four-mode solution is worse than the three-mode solution in the region $P \approx 1.6$. This result is not supported by direct comparisons of amplitude and end-shortening between Galerkin and numerical solutions.

Another measure of error is given by the end-shortening $\mathcal{E}$ of the deformed strut. For an inextensional strut, the first-order end-shortening for the approximate form $\bar{w} = A_1 \phi_1$ is

$$\begin{aligned}
\mathcal{E} &= \frac{1}{2}\int_{-\infty}^{\infty} w'^2 \,\mathrm{d}x \\
&= \frac{1}{4}\left(\alpha^2+\beta^2\right) {A_1}^2 \int_{-\infty}^{\infty} \operatorname{sech}^2 \alpha x \,\mathrm{d}x \\
&\quad + \frac{1}{4}\left(\alpha^2-\beta^2\right) {A_1}^2 \int_{-\infty}^{\infty} \operatorname{sech}^2 \alpha x \cos 2\beta x \,\mathrm{d}x \\
&\quad - \frac{1}{4}\alpha^2 {A_1}^2 \int_{-\infty}^{\infty} \operatorname{sech}^4 \alpha x \,\mathrm{d}x \\
&\quad - \frac{1}{4}\alpha^2 {A_1}^2 \int_{-\infty}^{\infty} \operatorname{sech}^4 \alpha x \cos 2\beta x \,\mathrm{d}x \\
&\quad + \frac{1}{2}\alpha\beta {A_1}^2 \int_{-\infty}^{\infty} \operatorname{sech}^2 \alpha x \tanh \alpha x \sin 2\beta x \,\mathrm{d}x \\
&= \frac{1}{6\alpha}\left(\alpha^2+3\beta^2\right) {A_1}^2 + \frac{\beta\pi}{6\alpha^2}\left(\alpha^2+\beta^2\right) {A_1}^2 C_1, \qquad (5.30)
\end{aligned}$$

where C_1 is given by Equation (5.24). The end-shortening is plotted in Figure 5.5

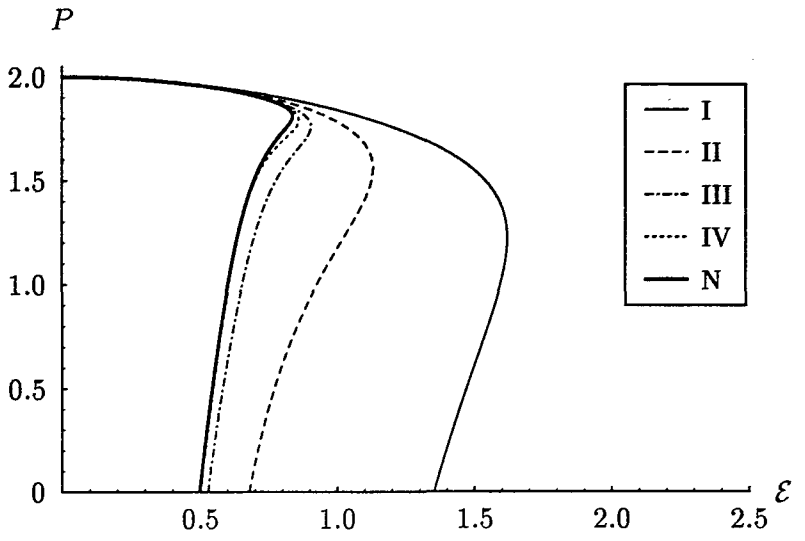

Figure 5.5 Comparison of load versus end-shortening for numerical and Galerkin solutions: I — one mode; II — two modes; III — three modes; IV — four modes; N — numerical solution.

and reveals that for all Galerkin approximations the qualitative behaviour of the numerical solution is duplicated with end-shortening initially increasing and then decreasing as the load falls from the critical point. Better approximations of end-shortening are obtained when additional modes are included. The actual load versus end-shortening response is unusual with a turning point developing at $P \approx 1.8$. It is reminiscent of the classic "snap back" post-buckling curve for a cylinder (Bažant & Cedolin, 1991) but differs qualitatively in at least two respects. Firstly, it involves a smooth transition at a position some distance from the critical point and secondly it does not involve a cusp bifurcation. However, it is the ability of the approximate solution to mimic the behaviour of the accurate numerical solution and not the appropriateness of the nonlinear elastic foundation to model real behaviour that is of concern here. In any case, this figure represents the load versus end-shortening for a specific set of equilibrium solutions and is independent of the type of loading applied. Under rigid load conditions, for example, the deflected shape may change from a primary localized profile into an alternative localized form with two or more peaks as the load snaps downwards. The precise response of this system is an open question at this time.

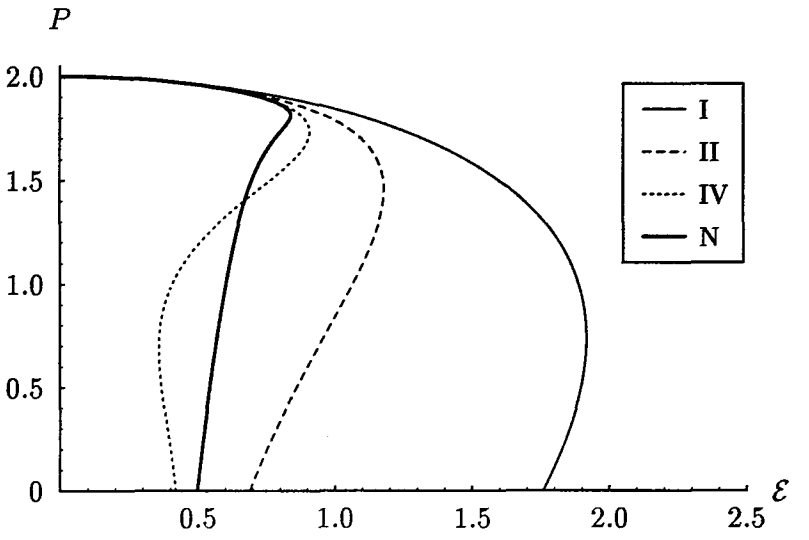

Figure 5.6 Effect of omission of contour integrals on the load versus end-shortening response of Galerkin solutions.

5.4.3 Effect of contour integrals

The Galerkin method described here is an improvement over the perturbation method of Chapter 3 because of its ability to account for the so-called contour integrals, I_{cnm} and I_{snm} of Equation (5.21). Hunt & Wadee (1991), in their perturbation analysis, argued that the contribution of these integrals is negligible because they can be repeatedly integrated by parts to reveal terms of ever decreasing magnitude. Although their reasoning was not entirely correct (they neglected an increasing contribution of the integrand) their conclusion that contour integrals have little effect on the solution is true in the vicinity of P^c in an asymptotic sense. When seeking approximate solutions over the complete range $0 \leq P \leq P^c$ these integrals should be included to ensure the solutions are consistent. The adverse effect on the load versus end-shortening response when these integrals are ignored is demonstrated in Figure 5.6. The mode IV approximation is particularly affected whereas previously it was virtually eclipsed by the numerical solution. Another contrasting feature is that the results overestimate the end-shortening for some values of P and underestimate it at others. When contour integrals were included in the analysis the results (see Figure 5.5) displayed a consistent trend to overestimate the end-shortening but by a progressively smaller amount as the number of trial functions increased.

5.5 Collocation method

For the problem of a strut embedded in a visco-elastic medium, as represented by Equation (5.14), the buckled shape of the strut is expected to change with time owing to the viscous nature of the Maxwell foundation. One way of ensuring a solution method is capable of reflecting this behaviour is by using a large number of trial functions with fixed shape but time-varying amplitudes, $A_i(t)\,\phi(x)$. Another option, which has the potential for generating a better solution with the same number of modes, is to allow both amplitude and shape of the trial functions to change with time, $A_i(t)\,\phi(x,t)$. The latter option is implemented here by using the same trial functions as for the elastic analysis and permitting $\alpha(t)$ and $\beta(t)$ to vary with time. The Galerkin method of the previous section relied on the fixed values of α and β from the linearized elastic state and apparently cannot be extended to the visco-elastic problem. Another possibility is the method of least squares. This has the capacity to allow α and β to vary by introducing them as extra variables and establishing the additional algebraic equations

$$\frac{\partial}{\partial\alpha}\int R^2\,\mathrm{d}x = 0 \quad \text{and} \quad \frac{\partial}{\partial\beta}\int R^2\,\mathrm{d}x = 0. \tag{5.31}$$

However, the length of the resulting equations makes this method awkward to apply in practice. Instead, a collocation method is proposed for both the initial elastic state and the subsequent period of visco-elastic evolution. The method was born out of the publication by Hunt *et al.* (1996a), where the possibility for non-periodic forms and localization within a geological framework was discussed.

5.5.1 Buckle initiation

As for the Galerkin analysis, the buckling of the initial elastic phase is governed by Equation (5.15). Approximate solutions with one and two modes are considered.

Single mode

A trial solution of the form $\bar{w} = A_1\,\phi_1$ is assumed, where ϕ_1 is the same as for the previous Galerkin analysis. Replacing w in the differential equation (5.15) by the

approximate form $\bar{w}$ leaves a residual

$$\begin{aligned} R(x, \alpha, \beta, P, A_1) &= \bar{w}'''' + P\bar{w}'' + \bar{w} - \bar{w}^3 \\ &= \sum_{i=1}^{6} M_i \psi_i, \end{aligned} \tag{5.32}$$

in which the coefficients M_i are

$$\begin{aligned} M_1 &= f_1 A_1, \\ M_2 &= -2\alpha^2 \left(10\,\alpha^2 - 6\,\beta^2 + P\right) A_1 - \frac{3}{4} {A_1}^3, \\ M_3 &= 24\alpha^4 A_1, \\ M_4 &= f_2 A_1, \\ M_5 &= -24\alpha^3 \beta A_1, \\ M_6 &= -\frac{1}{4} {A_1}^3, \end{aligned} \tag{5.33}$$

the quantities f_1 and f_2 are defined in Equation (5.20), and the functions ψ_i are

$$\begin{aligned} \psi_1 &= \operatorname{sech} \alpha x \cos \beta x, \\ \psi_2 &= \operatorname{sech}^3 \alpha x \cos \beta x, \\ \psi_3 &= \operatorname{sech}^5 \alpha x \cos \beta x, \\ \psi_4 &= \operatorname{sech} \alpha x \tanh \alpha x \sin \beta x, \\ \psi_5 &= \operatorname{sech}^3 \alpha x \tanh \alpha x \sin \beta x, \\ \psi_6 &= \operatorname{sech}^3 \alpha x \cos 3\beta x. \end{aligned} \tag{5.34}$$

The collocation procedure requires that the differential equation (5.15) be satisfied exactly at three distinct points: one for each of the unknown quantities α, β and A_1. Although the location of these points is arbitrary, the analysis can be greatly simplified by selecting collocation points where some of the functions ψ_i are zero. For the purely elastic problem, solutions are found in this way for different but constant values of load. Consider the analysis for the points x_1, x_2 and x_3 shown in Figure 5.7. The first two points are chosen far from the centre of localization to coincide with the node and peak of the oscillating solution. The last point is

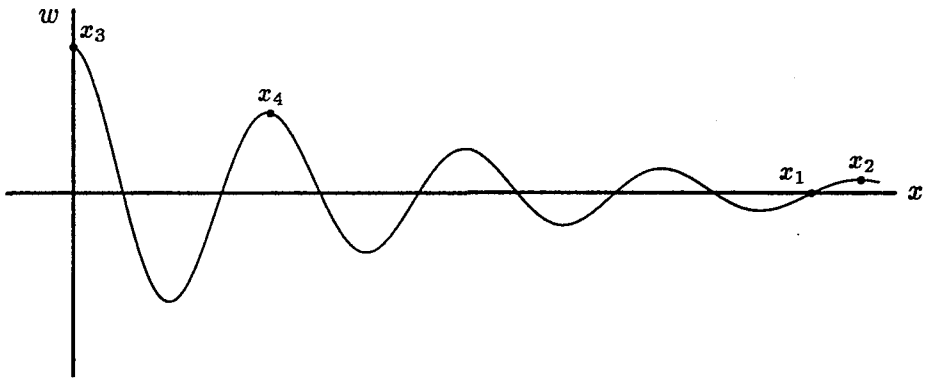

Figure 5.7 Location of collocation points.

positioned at the point of maximum amplitude and symmetry, $x = 0$.

At x_1, $\cos\beta x = 0$ and $\sin\beta x = 1$ which means that ψ_1, ψ_2, ψ_3 and ψ_6 are all zero. Setting the residual (5.32) equal to zero then simplifies to

$$M_4 \operatorname{sech}\alpha x_1 \tanh\alpha x_1 + M_5 \operatorname{sech}^3\alpha x_1 \tanh\alpha x_1 = 0. \tag{5.35}$$

For large x_1, $\operatorname{sech}^3\alpha x_1 \ll \operatorname{sech}\alpha x_1$ and $\tanh\alpha x_1 \approx 1$, so the latter term may be regarded as being of higher order. Neglecting this term enables the residual to be reduced further to $M_4 = 0$, which has the nontrivial ($A_1 \neq 0$) solution

$$f_2 = 0. \tag{5.36}$$

A similar argument at x_2, where $\sin\beta x = 0$ and $\cos\beta x = 1$, gives $M_1 = 0$, which has the solution

$$f_1 = 0. \tag{5.37}$$

Thus, the linear relations for α and β given by Equation (5.17) are retained if collocation points x_1 and x_2 are used.

The amplitude of the approximate solution is found by considering the collocation equation at the point x_3, where $\cos\beta x = \operatorname{sech}\alpha x = 1$ and $\sin\beta x = 0$. At this point the functions ψ_4 and ψ_5 are both zero and $\psi_1 = \psi_2 = \psi_3 = \psi_6 = 1$. Equating the residual to zero leaves

$$M_1 + M_2 + M_3 + M_6 = 0, \tag{5.38}$$

from which it can be determined that

$$2\alpha^2\left(2\alpha^2+6\beta^2-P\right)A_1-{A_1}^3=0. \tag{5.39}$$

After substituting for α and β from Equation (5.17), the nontrivial amplitude for the single-mode solution is found to be

$$A_1=\sqrt{4-2P}. \tag{5.40}$$

Two modes

Bearing in mind that the quality of an approximate solution is expected to improve as the number of trial functions is increased, consider the trial solution

$$\bar{w}=A_1\,\phi_1+A_2\,\phi_2, \tag{5.41}$$

with amplitudes A_i and modes

$$\begin{aligned}\phi_1 &= \operatorname{sech}\alpha x\cos\beta x,\\ \phi_2 &= \operatorname{sech}\alpha x\tanh\alpha x\sin\beta x.\end{aligned} \tag{5.42}$$

Substituting the approximate form $\bar{w}$ into the differential equation (5.15) results in the residual

$$R(x,\alpha,\beta,P,A_1,A_2)=\sum_{i=1}^{10}M_i\,\psi_i, \tag{5.43}$$

where the coefficients M_i and functions ψ_i are listed in Appendix D.

In order to determine the four unknowns α, β, A_1 and A_2, the governing differential equation must be satisfied exactly at four locations. The points x_1, x_2 and x_3 are used again, with a final point x_4 making the foursome. As for the single-mode solution, the first two points lead to the linear relations

$$f_1=f_2=0, \tag{5.44}$$

in terms of α and β. At x_3, the functions ψ_1, ψ_2, ψ_3, ψ_7 and ψ_8 are equal to one,

and the remaining functions are zero. The third collocation equation is therefore

$$M_1 + M_2 + M_3 + M_7 + M_8 = 0. \tag{5.45}$$

The final equation comes from choosing a point $x_4 = n\pi/\beta$, where n is an integer, on the peak (or trough) of the oscillating cosine solution. For even values of n, $\cos \beta x = 1$ and $\sin \beta x = 0$, and the residual is

$$\begin{aligned} M_1 \operatorname{sech} \alpha x_4 + M_2 \operatorname{sech}^3 \alpha x_4 + M_3 \operatorname{sech}^5 \alpha x_4 \\ + M_7 \operatorname{sech}^3 \alpha x_4 + M_8 \operatorname{sech}^5 \alpha x_4 = 0. \end{aligned} \tag{5.46}$$

Using the condition $M_1 = 0$, implied by Equation (5.44), the third and fourth collocation equations (5.45) and (5.46) may be rearranged to give

$$\begin{aligned} (M_2 + M_7) + (M_3 + M_8) &= 0, \\ (M_2 + M_7) + (M_3 + M_8) \operatorname{sech}^2 \alpha x_4 &= 0, \end{aligned} \tag{5.47}$$

for which a solution, independent of the value of x_4, is

$$M_2 + M_7 = 0 \qquad \text{and} \qquad M_3 + M_8 = 0. \tag{5.48}$$

This result is equivalent to equating to zero terms of the same "order" in Equation (5.46), where the order of a term is defined by the power of the accompanying $\operatorname{sech} \alpha x_4$ term. After substituting for M_i, the following expressions are obtained for the modal amplitudes A_1 and A_2:

$$\begin{aligned} A_1 &= \alpha \sqrt{10\beta^2 - P}, \\ A_2 &= \frac{\alpha}{4\beta} A_1. \end{aligned} \tag{5.49}$$

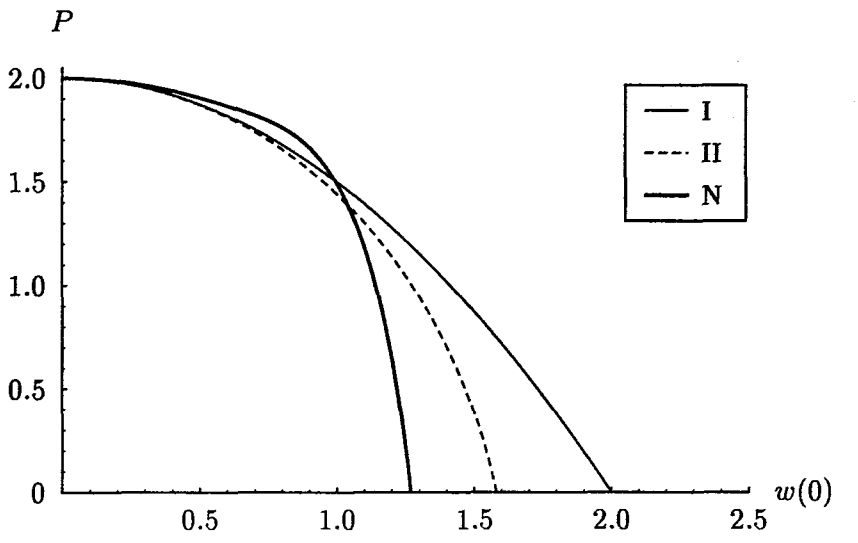

Figure 5.8 Load versus peak amplitude for collocation solutions.

Results

The collocation approximations are assessed by comparison with independent numerical solutions. An inspection of the peak amplitude of the primary localized solution, as shown in Figure 5.8, reveals the single-mode solution is closer to the numerical solution than the two-mode approximation in the region $P \geq 1.5$, while the reverse is true elsewhere. The most important feature is that the amplitude of the collocation solutions, like the numerical solution, increases monotonically as $P \to 0$. A comparison with the perturbation results obtained in Chapter 3 (see Figure 3.6) shows that the asymptotic solutions are better in the immediate vicinity of the critical point but that the collocation solutions are better elsewhere.

Instead of concentrating on the amplitude of the solution at a specific point, a more useful comparison is that of the load versus end-shortening shown in Figure 5.9. Although it is possible to calculate the exact end-shortening of the approximate solutions by numerical means, the first-order expression (5.30) is used here in order to retain the analytical nature of the solution procedure. The figure shows that the single-mode solution is best in the region $P \geq 1.8$ and that two modes are required to detect the presence of the turning point in the end-shortening. A comparison with Figure 3.7 reveals that the collocation method generates better approximations of end-shortening than the perturbation method everywhere except close to P^c.

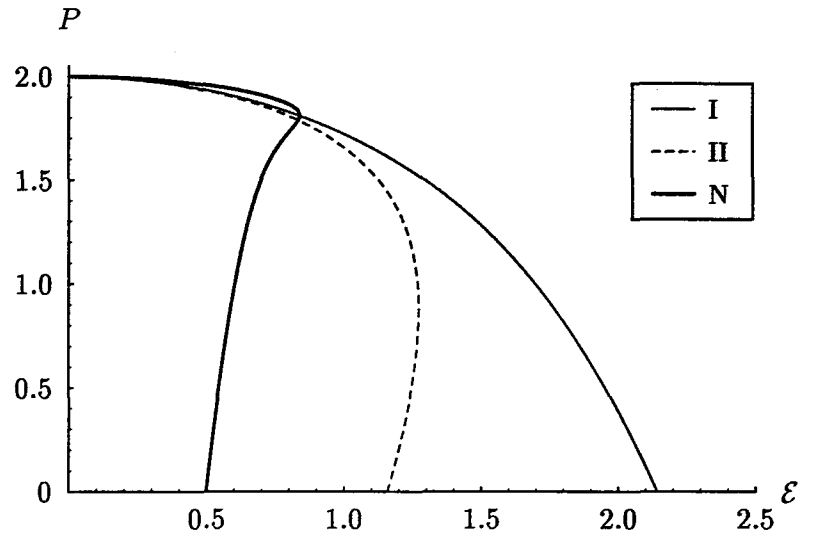

Figure 5.9 Load versus end-shortening for collocation solutions.

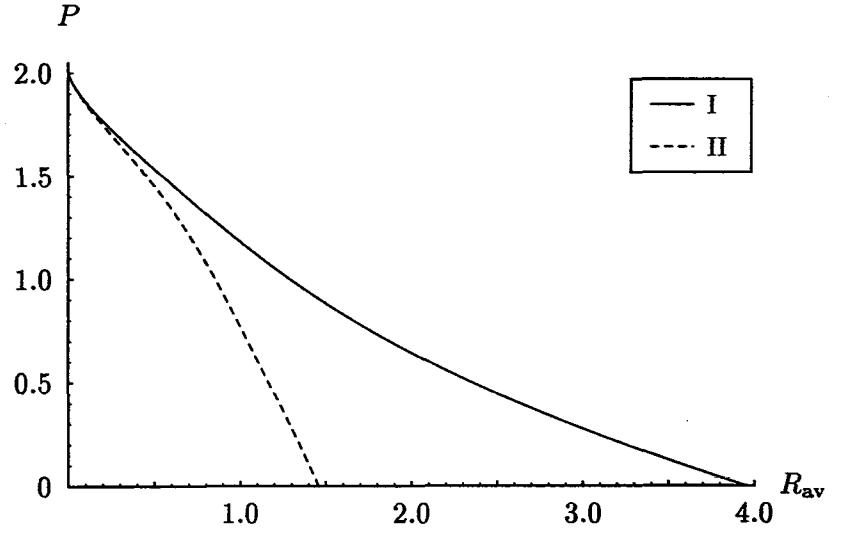

Figure 5.10 Load versus average residual for collocation solutions.

The average residual is depicted in Figure 5.10 and shows that the quality of the collocation solutions decreases almost linearly as the load falls from P^c, a feature shared with the Galerkin solutions of the previous section. It is also apparent that the two-mode solution is better, albeit in an average sense, than the single-mode solution for all values of P. As demonstrated in the earlier analysis, the inclusion of additional trial functions is expected to lead to a more accurate approximation of a localized solution.

5.5.2 Time evolution

The significance of the localized form at the start of the evolutionary process is that, in contrast with the purely viscous foundation (Biot, 1965), solutions display more than just a growth of periodic amplitudes. The procedure for following the evolution takes much the same course with Equation (5.14) as the elastic analysis did with Equation (5.15). An assumed form for the deflected shape is substituted into the governing differential equation and equated to zero at a number of collocation points. In contrast to the earlier elastic analyses, the growth of the buckle pattern is controlled by the end displacement $\mathcal{E}$. The partial differential equation is reduced to a system of four simultaneous first-order ordinary differential equations in terms of the unknown variables $\alpha(t)$, $\beta(t)$, $P(t)$ and $A_1(t)$. The following formulation is limited to a single mode on the basis that a qualitative description of the solution can be achieved in this way.

Diffusion equations

The first three rate equations of the visco-elastic system stem from a collocation method which is virtually identical to that used for the analysis of the purely elastic system. The difference now is that the residual not only varies with x but also with time t. For the evolving solution, collocation points located close to the centre of localization were found to yield optimum results. The following analysis is for collocation points at $x_1 = 0$, $x_2 = \pi/8\beta$ and $x_3 = \pi/4\beta$.

The residual at x_1 is

$$R[x_1, \alpha(t), \beta(t), A_1(t), P(t)] = M_1 + M_2 + M_3 + M_6. \tag{5.50}$$

After inserting the quantities M_i and equating the residual at this point to zero, the resulting equation may be manipulated into the form

$$K_{11}\,\dot{\alpha} + K_{12}\,\dot{\beta} + K_{13}\,\dot{P} + K_{14}\,\dot{A}_1 = L_1, \tag{5.51}$$

where the coefficients K_{1j} are

$$\begin{aligned} K_{11} &= 2\alpha\left(10\alpha^2 + 6\beta^2 - P\right) A_1, \\ K_{12} &= 2\beta\left(6\alpha^2 + 2\beta^2 - P\right) A_1, \\ K_{13} &= -\left(\alpha^2 + \beta^2\right) A_1, \\ K_{14} &= 1 + 5\alpha^4 + 6\alpha^2\beta^2 + \beta^4 - P\left(\alpha^2 + \beta^2\right) - 3{A_1}^2, \end{aligned} \tag{5.52}$$

and the right-hand side is

$$L_1 = -\left[5\alpha^4 + 6\alpha^2\beta^2 + \beta^4 - P\left(\alpha^2 + \beta^2\right)\right] A_1. \tag{5.53}$$

Performing the same procedure at x_2 and x_3 generates two further rate equations:

$$\begin{aligned} K_{21}\,\dot{\alpha} + K_{22}\,\dot{\beta} + K_{23}\,\dot{P} + K_{24}\,\dot{A}_1 &= L_2, \\ K_{31}\,\dot{\alpha} + K_{32}\,\dot{\beta} + K_{33}\,\dot{P} + K_{34}\,\dot{A}_1 &= L_3. \end{aligned} \tag{5.54}$$

The coefficients K_{2j} and K_{3j} are derived simply by manipulating the coefficients M_i and functions ψ_i listed in Appendix D and are therefore not specified here.

Rigid loading

Localized buckling is unstable under conditions of constant load for the current system so evolution is considered under the control of end displacement. The rate of end-shortening is obtained by differentiating the first-order expression (5.30) with

respect to time t,

$$\dot{\mathcal{E}} = \frac{\partial \mathcal{E}}{\partial \alpha}\,\dot{\alpha} + \frac{\partial \mathcal{E}}{\partial \beta}\,\dot{\beta} + \frac{\partial \mathcal{E}}{\partial A_1}\,\dot{A}_1. \tag{5.55}$$

Like the previous rate equations, this has an equivalent form

$$K_{41}\,\dot{\alpha} + K_{42}\,\dot{\beta} + K_{43}\,\dot{P} + K_{44}\,\dot{A}_1 = L_4, \tag{5.56}$$

where L_4 is the rate of applied end-shortening and the coefficients K_{4j} are found by evaluating the appropriate derivatives. The coefficient K_{43} is zero because the end-shortening is a geometric property of the deflected shape $\bar{w}$ and is not an explicit function of the axial load P.

5.5.3 Results

The process for tracing the buckled shape of the strut as it evolves in time is as follows. A starting value of P is chosen, from which the initial elastic profile and end-shortening $\mathcal{E}$ are determined. The equations (5.51), (5.54) and (5.56) are combined as a system of first-order equations which may be expressed in matrix form,

$$\begin{bmatrix} K_{11} & K_{12} & K_{13} & K_{14} \\ K_{21} & K_{22} & K_{23} & K_{24} \\ K_{31} & K_{32} & K_{33} & K_{34} \\ K_{41} & K_{42} & K_{43} & K_{44} \end{bmatrix} \begin{bmatrix} \dot{\alpha} \\ \dot{\beta} \\ \dot{P} \\ \dot{A}_1 \end{bmatrix} = \begin{bmatrix} L_1 \\ L_2 \\ L_3 \\ L_4 \end{bmatrix}. \tag{5.57}$$

This system is integrated forward in time using a forward difference technique with a small time step, typically $\Delta t = 0.01$. The values of α, β, P and A_1 from the initial time step are used to calculate the components of the matrices $\mathbf{K}$ and $\mathbf{L}$. After calculating the inverse $\mathbf{K}^{-1}$ and multiplying by $\mathbf{L}$, the instantaneous rates $\dot{\alpha}$, $\dot{\beta}$, $\dot{P}$ and $\dot{A}_1$ are found. These slopes are then used to calculate the new values of α, β, P and A_1 using difference relations of the form $\alpha_{\text{new}} \approx \alpha_{\text{old}} + \dot{\alpha}\,\Delta t$. The process is repeated for the desired time interval.

The results of the collocation method are plotted in Figure 5.11 together with the numerical solution for the problem of constant end-shortening, $\dot{\mathcal{E}} = 0$. The two solutions show good agreement with one another over the interval shown, thus pro-

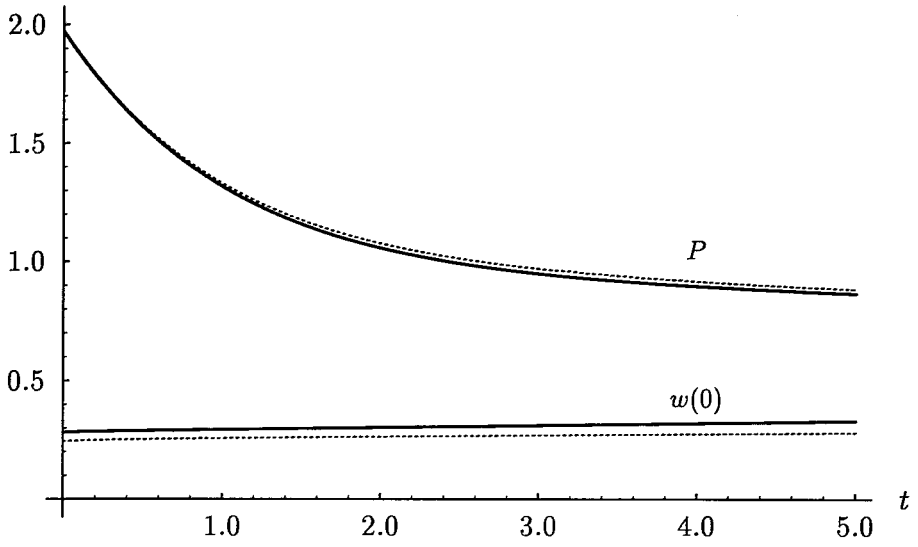

Figure 5.11 Comparison of single-mode collocation solution (dashed lines) with numerical solution (solid lines) under rigid load conditions, $P(0) = 1.97$.

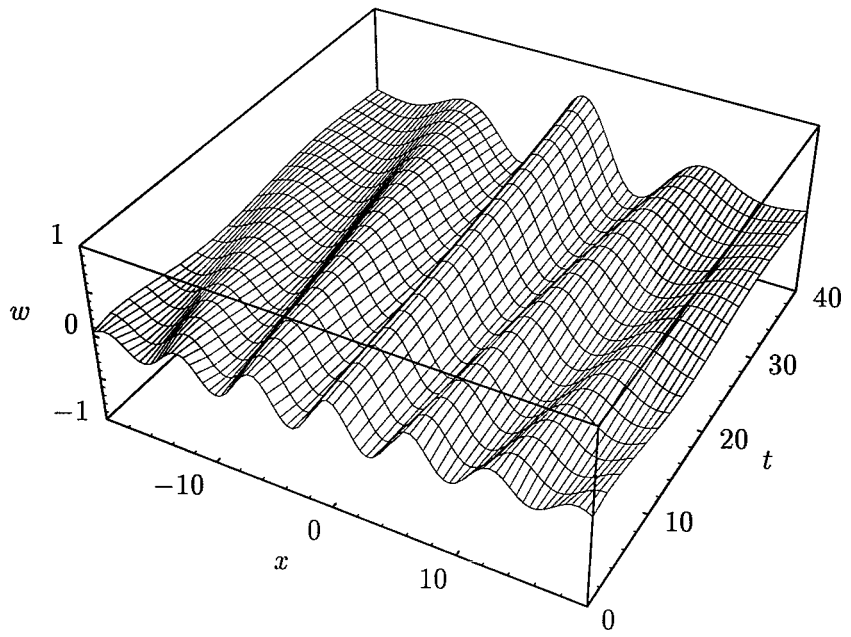

Figure 5.12 Evolution of localized profile for single-mode collocation method under rigid load conditions, $P(0) = 1.97$.

viding additional confidence in both methods, particularly the collocation method. A three-dimensional view of the evolving buckle profile is displayed in Figure 5.12 for a longer time period. It is interesting to observe the sequence of events for this nondimensionalized and hence general problem. The most salient feature is that the load drops rapidly, apparently asymptotically to zero, as the viscous part of the foundation absorbs the energy stored in the system. In common with the elastic response (Champneys & Toland, 1993), the lower the load, the more localized the buckle shape. At the same time, the wavelength of the solution increases as the elastic bending energy of the strut is released. The combined effect is to evolve towards a single long half-sine wave without ever approaching a periodic form.

5.6 Concluding remarks

The weighted residual methods demonstrated here are valuable for the improved understanding and insight which they provide into the nature of localized buckling in the model of a strut on a foundation. For the types of elastic and visco-elastic behaviour studied here these methods have proven capable of predicting all of the qualitative features of the buckling solution, often with a single degree of freedom. In this chapter these methods were used to reduce a *partial* differential equation to a system of *ordinary* differential equations and an ordinary differential equation to a set of algebraic equations, some of which have closed-form solutions. There are also occasions when these classical methods convey information that other methods cannot, for example, close to the bifurcation point where numerical methods have difficulty tracking localized solutions. In this light, weighted residual methods may be said to complement numerical methods. However, unlike the applications for classical techniques developed earlier this century, they cannot be performed practically by hand and it has required the advent of advanced algebraic manipulation packages, such as Mathematica, to implement them.

The number of problems amenable to analysis by a Galerkin method or collocation procedure is considerably less than can be solved by numerical methods. For example, they cannot be used to solve the geometrically nonlinear problem of the

elastica strut (3.9) nor problems involving general nonlinear foundation behaviour. In such cases, these methods require a Taylor expansion to approximate the nonlinear behaviour and even then it is practical only to consider the first nonlinear term. Nevertheless, the solutions provided by weighted residual methods may be used as initial profiles for more complicated boundary-value methods.

Chapter 6

Numerical experiments

In this chapter the ideas and methods of Chapter 4 are used to explore the evolution of localized patterns in visco-elastic buckling models. Unlike the previous chapter, where the types of problems amenable to analysis were restricted by the practical implementation of the method of weighted residuals, here the types of localized buckling problems which can be solved is virtually unlimited. The chapter begins by establishing the effects of geometric and material nonlinearities on the post-buckling response of a strut on an elastic foundation. Numerical results are then presented for the initiation and subsequent development of localized buckle forms in two visco-elastic models. Load conditions of constant end displacement and constant rate of change of end displacement are used to simulate tectonic plate movement. The chapter ends with a brief treatment of the myriad of other buckling solutions which exist in such systems.

6.1 Introduction

A method of solution is usually developed for a specific task and generally has limited application to other problems. In particular, this is true of the shooting methods described in § 4.2. The blanket runs by Hunt & Wadee (1991), while ideal for detecting localized solutions with multiple peaks, are a poor means of generating entire post-buckling profiles for specific localized forms. This is because their search algorithm makes no use of information regarding the solution profile at

adjacent parameter values. Similarly, the automatic continuation strategy developed by Champneys & Spence (1993), although ideal for isolating and tracing multi-modal localized solutions, is applicable only to certain types of buckling problems. Their method cannot be applied to the elastica problem because the Hamiltonian[1] cannot be conveniently separated into components of potential and kinetic energy.

By comparison, the boundary-value method described in Chapter 4 was developed specifically for the study of primary localizations (those with a single peak). For the purely elastic problem, a solution at one value of P (or $\mathcal{E}$) provides the boundary-value solver with an initial profile for the next value, thus enabling the entire family of post-buckling solutions to be generated. In a similar fashion, a solution at one time step acts as an initial profile at the next time step, thus revealing the evolving localized form of the visco-elastic system. Using the numerical tool in this manner provides answers to several fundamental questions regarding the effects of nonlinear elasticity on the buckling of strut-on-foundation models.

6.2 Nonlinear elasticity

Since the pioneering work of Koiter (1945), buckling has been regarded as an inherently nonlinear phenomenon. This does not mean that the linearized form is not important; indeed, it is the solution of the linearized equation that reveals the potential for localization. For subcritical loads, $P < P^{\mathrm{c}}$, the characteristic equation gives rise to complex eigenvalues. The corresponding eigenvectors represent oscillatory behaviour with exponentially varying amplitude. As the amplitude grows, so too does the influence of nonlinear terms and, ultimately, these terms may cause the amplitude to reverse and decay exponentially. This is the essential feature of localized buckling.

There are three main types of nonlinearity: material (or physical), geometrical, and loading nonlinearity. The first type of nonlinear behaviour is due to the physical properties of the material being used. The second arises from the consideration of large deflections and the third occurs when an axial load on a structure undergoes

[1]The Hamiltonian is a property which is constant for conservative systems such as a strut on an elastic foundation (Goldstein, 1980).

small lateral displacements thus inducing additional bending moments. For the buckling models considered in this thesis, the axial load is assumed to be applied at infinite boundaries where the amplitude is zero so the third type of nonlinearity can be discounted. The effects of the other nonlinearities are explored by including them in the governing equation one at a time. Only in special cases is it possible to reduce a buckling equation to an equivalent nondimensional form and for this reason solutions in this chapter are found for specific values of the material constants.

6.2.1 Taylor series approximation

Researchers investigating localized strut buckling have usually based their analysis on the linearized equation

$$EIw''' + Pw'' + F = 0, \tag{6.1}$$

with a nonlinearity in the foundation, typically $F = kw - cw^n$. The cases $n = 2$ (Hunt *et al.*, 1989; Hunt & Wadee, 1991; Wadee, 1993; Champneys & Spence, 1993) and $n = 3$ (Potier-Ferry, 1983; Thompson & Virgin, 1988; Whiting, 1996) have received much attention. Although it is conceivable that these foundation reactions have practical applications in the context of buckling, they can also be seen as attempts by the authors to introduce a softening nonlinearity into the governing equation by approximating a more general nonlinear function. Consider a Winkler foundation with springs governed by the inverse hyperbolic sine function

$$F(w) = \frac{k}{n}\sinh^{-1} nw, \tag{6.2}$$

where k is the tangent stiffness of an undeformed spring and n is a measure of the degree of nonlinearity whose influence is examined later in the chapter. This function increases monotonically with w as shown in the upper part of Figure 6.1. It has the essential softening ingredient necessary for localization without the negative stiffness of the above polynomial. In the vicinity of the origin, the Taylor series

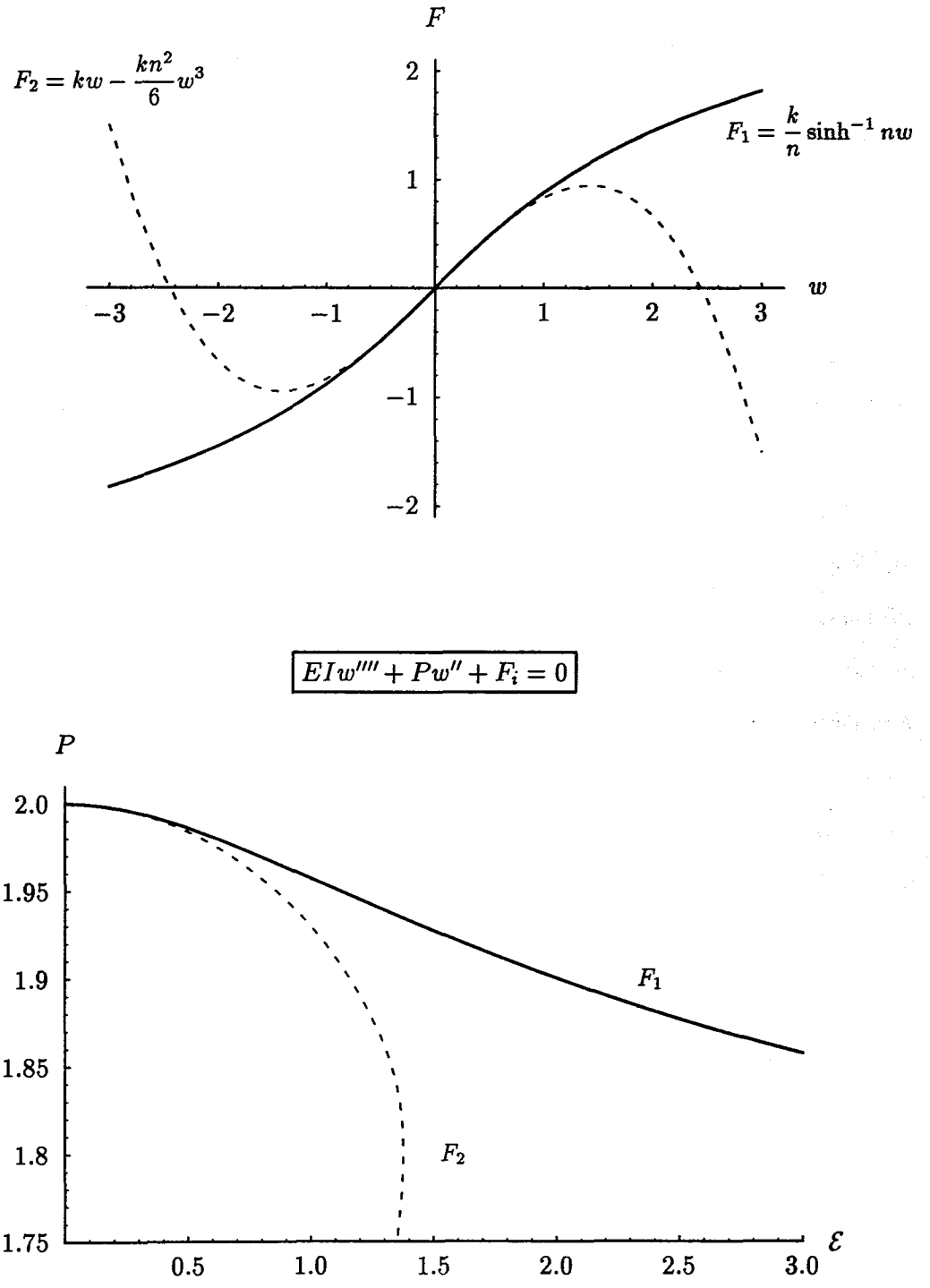

Figure 6.1 Foundation behaviours (top figure) and associated post-buckling responses (bottom figure) for a linearized strut on a nonlinear elastic foundation ($EI = k = 1$, $n = 2$).

expansion of this function is

$$\frac{k}{n}\sinh^{-1} nw = kw - \frac{kn^2}{6}w^3 + O(w^4). \tag{6.3}$$

A question which seems not to have been addressed in the literature is: what is the effect on the post-buckling response of the system arising from truncation of higher-order terms $O(w^4)$ in the foundation reaction?

In order to answer this question, two buckling equations are solved: one incorporating the general nonlinear function (6.2) and the other its truncated form. These results are presented in the lower part of Figure 6.1. For the truncated foundation reaction, the post-buckling response is characterized by a turning point at $P \approx 1.81$, though naturally this position depends on the value of the material parameters. This behaviour is also present in the model of a strut on a quadratic foundation (Wadee *et al.*, 1996). Beyond the turning point, the post-buckling response is unstable for conditions of both dead load and rigid load and is unlikely to be observed in practice. Nevertheless, such behaviour is an integral part of the response of the model and is, therefore, practically relevant. A qualitatively different behaviour is exhibited by the hyperbolic foundation relation (6.2). For the range of values presented, the end-shortening continues to increase with load, a behaviour which is stable under displacement control.

6.2.2 Effect of geometric nonlinearities

When the deflected shape of a strut is obtained from the exact differential equation its configuration is called the *elastica* (Timoshenko & Gere, 1963). All kinematically admissible deflections then have the potential to exist, including the looping behaviour (Thompson & Hunt, 1984; El Naschie, 1989) described in Chapter 4. The problem of an elastica strut supported by a bed of linear springs has been treated previously in the literature by Hunt *et al.* (1993) and Wadee (1993). These authors concluded that localized forms exist in this system which are qualitatively similar to those for a linearized strut on a nonlinear elastic foundation.

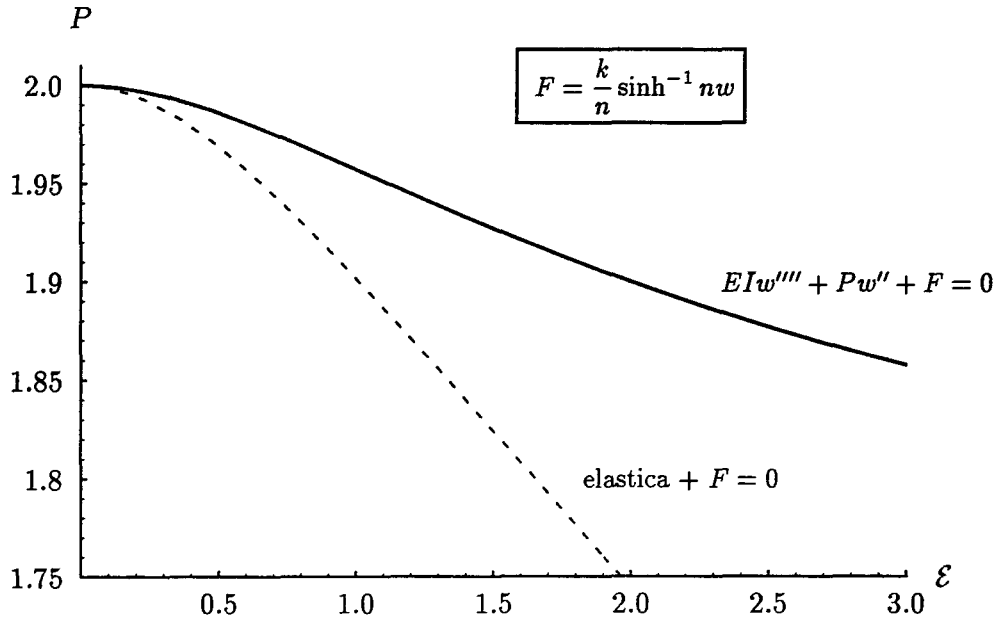

Figure 6.2 Post-buckling response for a strut on a nonlinear elastic foundation with and without geometric (elastica) nonlinearities ($EI = k = 1$, $n = 2$).

One aspect of this work which has apparently not been addressed is the quantitative influence of geometric nonlinearities. This requires a comparison of the post-buckling responses for an elastica strut and a linearized strut, both supported by the same nonlinear foundation. Unlike the works mentioned above, which consider a pure (linear) Winkler foundation, it is necessary to incorporate a nonlinear foundation reaction here because a linearized strut on a linear foundation is devoid of nonlinear terms and can, therefore, have no localized response.

The effect of elastica terms on the buckling response of a strut on the nonlinear elastic foundation (6.2) is shown in Figure 6.2. The result is a less stiff post-buckling response when geometric nonlinearities are incorporated in the equation. The removal of these nonlinear terms causes the solution to approximate more closely the neutral stability of the fully linearized equation. For the latter case, the amplitude and end-shortening are undefined and the post-buckling response is simply a horizontal line emerging from $P^c = 2$. Nonlinear terms arising from large deflections were also considered in Chapter 4, where a simply-supported column was used as a benchmark for the numerical procedure. In the absence of a foundation, the geometric nonlinearities had a stabilizing influence with an increasing load required to

induce further deformation of the column. However, the strut on a foundation is a fundamentally different structure from the simply-supported strut (as discussed in § 3.2) and it is difficult to draw comparisons between the two.

Analysis of the simply-supported elastica is aided by the use of an intrinsic coordinate system in which the length along the strut x and the angle θ, tangent to the original undeformed state, are used as coordinates. However, the problem of an elastica on a foundation requires the integral of θ along the length of the strut to calculate the deflection at every point. An alternative, involving the arc length x and vertical displacement w, was presented in Chapter 3, following the method of Thompson & Hunt (1984). This description is not without difficulties. For example, looping solutions, which can be described easily with an intrinsic coordinate system by allowing θ to vary continuously from 0 to 2π, suffer from a discontinuity at inflection points ($w' = \pm 1$) where the strut has vertical slope. A physically realisable solution exists if w'' is zero at this point, but the numerical method is unable to interpret this possibility. In physical situations where a looping solution exists, it is unlikely the Winkler hypothesis remains valid. The $x - w$ coordinate system is therefore regarded as satisfactory for the geological situations modelled here.

6.2.3 Effect of material nonlinearities

In the study of a linearized strut on a nonlinear foundation, a softening foundation results in an overall softening response of the system (see Chapter 5). A stiffening foundation, on the other hand, leads to a stable post-buckling response which apparently has no localized solutions. However, in the previous section the global softening effect of geometrically nonlinear terms was demonstrated. It is conceivable, therefore, that localized solutions may exist in a strut model with a stiffening foundation provided elastica nonlinearities are retained. Kerr (1989) considers a stiffening foundation to be a more realistic description of soil and rock behaviour than a softening model because of the densification these materials exhibit when loaded. In any case, it is likely that all types of nonlinear behaviour, including softening and hardening, exist in nature.

In Figure 6.3 various foundation reactions F are displayed with their corresponding localized post-buckling responses. The curves $F_1(x)$, $F_2(x)$ and $F_3(x)$ represent stiffening, linear and softening foundations, respectively. While the response for the linear foundation arises from purely geometrical nonlinearities, the other curves demonstrate the influence of material nonlinearity: a softening foundation leads to greater overall softening of the system; a stiffening foundation causes a reduction of the softening effect of the elastica nonlinearities by raising the post-buckling response, making it "less unstable" with respect to load.

The ability of a *system* to display localization, which involves softening, while the deforming *material* undergoes strain-hardening is also reported by Hobbs *et al.* (1990). These authors cite experimental and theoretical evidence to dispel the common misconception that material strain-softening is a prerequisite for localization in deforming rocks. In this context the following comment by Griggs & Handin (1960) is appropriate:

> "... a geologist may not infer the type of stress-strain curve from the nature of faults or flow."

6.3 Nonlinear visco-elastic models

There have been many analyses of buckling in layers of rock for conditions of constant load, for example, Biot (1965) and Kerr (1969). Laboratory experiments have also been carried out for this type of loading. Biot *et al.* (1961) immersed thin sheets of elastic material vertically in a viscous fluid and observed the deformation resulting from a load of constant mass. Perhaps a more realistic load condition of relevance to plate tectonics is the impact of an initially horizontal layer with a mass moving at constant velocity. For an infinite mass, a step velocity of the end of the layer is imposed with axial displacement increasing linearly from the moment of collision. Under these conditions total collapse of the structure is inevitable, and interest centres on the mode of collapse and the ensuing change of load with time.

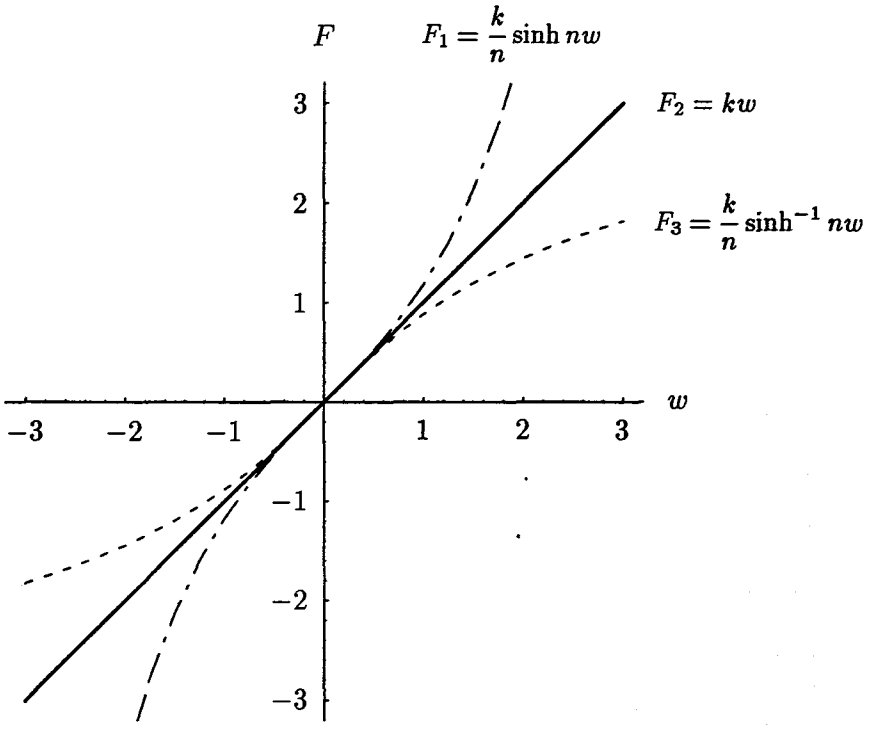

elastica + $F_i = 0$

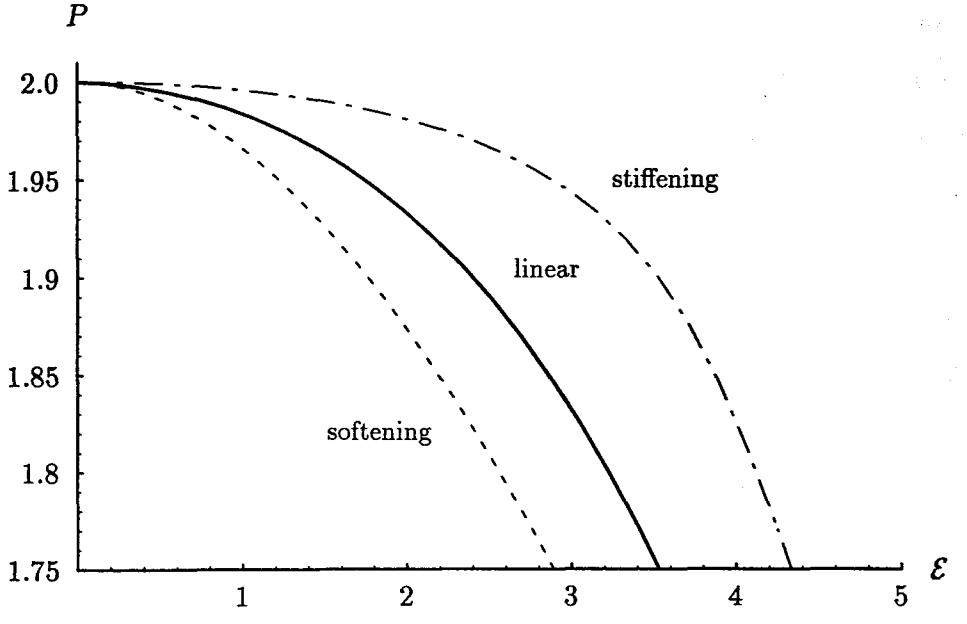

Figure 6.3 Foundation characteristics (top figure) and associated post-buckling responses (bottom figure) for an elastica strut on an elastic foundation ($EI = k = n = 1$): F_1 — stiffening, F_2 — linear and F_3 — softening.

The effect of constant axial displacement on the buckling of an elastic layer has been studied by Mühlhaus *et al.* (1994) and Hunt *et al.* (1996a). The first authors considered the evolution of periodic forms in an elastic plate embedded in a purely viscous (Newtonian) medium. They found the initial stages of fold evolution were governed by Biot's (1965) dominant wavelength, determined from a linear stability analysis, and that the fold proceeded through various transitional stages as $t \to \infty$, eventually evolving into a single half-sine wave over the full length of the plate. The latter authors drew attention to the possibility for non-periodic forms and localization within a geological framework. They focussed on the deformation of an elastic layer supported by a visco-elastic (Maxwell) foundation with a wavelength-dependent characteristic. They concluded similarly that the axial load drops asymptotically to zero, while the fold pattern progresses through a series of localized states, ultimately adopting the same half-sine wave.

In this chapter, evolving localized buckle patterns are examined in two different models. The first involves the large deflections of an elastica strut resting on a linear foundation (model A) while the second combines the linearized strut equation with a nonlinear foundation (model B). In both cases a Maxwell-type foundation is considered. Upon loading, the elastic component of the foundation leads to an instantaneous buckling of the layer, causing an end-shortening $\mathcal{E}$ to occur at $t = 0$. The initial elastic phase of both models is characterized by a falling load versus end-shortening response, which is unstable under conditions of load control. The response is stabilized by considering the evolution under conditions of controlled end displacement. This is achieved by allowing the load P to vary subject to conditions on the integral

$$\mathcal{E} = \int_{-\infty}^{\infty} \left\{ 1 - \sqrt{1 - w'^2} \right\} \mathrm{d}x, \tag{6.4}$$

representing the end-shortening of the strut, as described in Chapter 4. Two load cases are considered. In the first, end-shortening is held constant for all time, $\dot{\mathcal{E}} = 0$, and in the second end-shortening increases at a constant rate, $\dot{\mathcal{E}} = 1$.

6.4 Visco-elastic model A — geometric nonlinearity

Only the large-amplitude nonlinearities are retained in this model. The governing equations, which were derived in Chapters 2 and 3, are reproduced here for clarity. They are:

- the elastica strut buckling equation,

$$EI\left[w''''\left(1-w'^2\right)^{-1}+4w'''w''w'\left(1-w'^2\right)^{-2}+w''^3\left(1+3w'^2\right)\left(1-w'^2\right)^{-3}\right] + Pw''\left(1-w'^2\right)^{-3/2}+F=0. \tag{6.5}$$

- and the Maxwell foundation reaction,

$$\frac{1}{k}\dot{F}+\frac{1}{\eta}F=\dot{w}. \tag{6.6}$$

For this model, x is measured along the length of the strut. The small-deflection equation (6.1) is retrieved by ignoring all nonlinear terms. Evolution of the buckled shape is governed by the integral constraint (6.4) and Equations (6.5) and (6.6). The boundary conditions and method of solution for this system of partial differential equations are described in Chapter 4.

6.4.1 Fold initiation

The initial deformation of the strut occurs instantly with the viscous dashpots having no time to affect the deflected shape. This corresponds to the deformation of an elastic strut supported by a Winkler foundation of springs. Nonlinear formulations of this system have a wide range of spectacular variations which have only recently been understood (Hunt & Wadee, 1991; Champneys & Toland, 1993). It is these post-critical equilibrium solutions of the perfect elastic system which are used to trigger the time-dependent deformation. This contrasts with previous studies in which arbitrary geometric imperfections (Zhang *et al.*, 1996) or initial lateral velocities (Leu & Yang, 1989) are used.

The instantaneous load versus end-shortening response of the system is shown in Figure 6.4. Upon loading, the axial force increases from zero to the critical load,

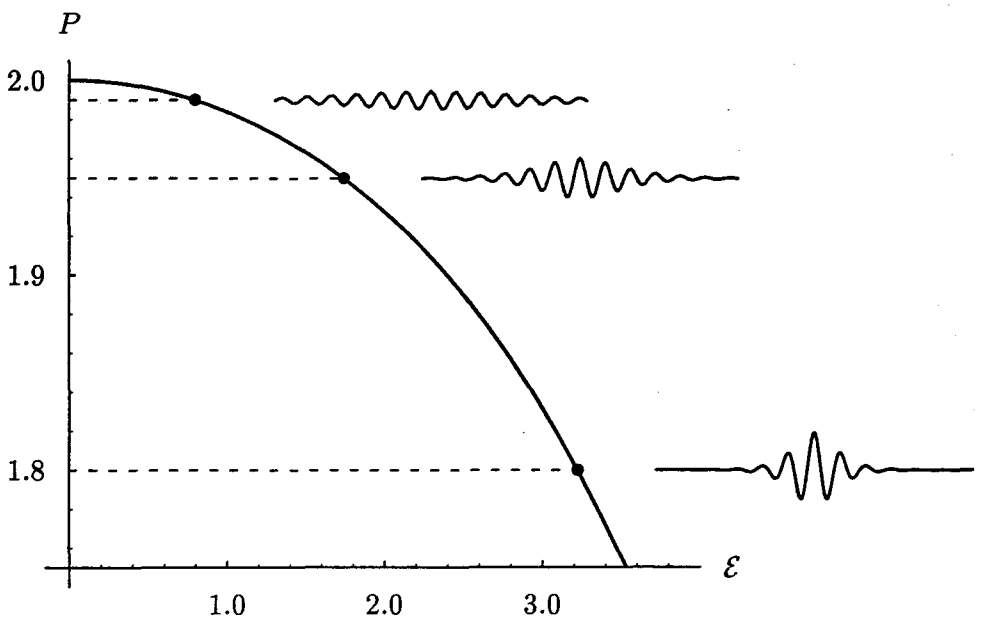

Figure 6.4 Load versus end-shortening and deflected profiles for the initial elastic response of model A ($EI = k = 1$).

$P^c = 2$, at which point a buckling instability takes place. Initially, node points develop along the strut at regular intervals corresponding to the wavelength of the linearized equation. The amplitude at this stage is zero. As the strut buckles, the amplitude and end-shortening start to grow. Further into the post-buckling regime, the wavelength and amplitude at the centre of the strut continue to grow while the deflection elsewhere decreases. The end-shortening continues to increase throughout the post-buckling regime with the result that the buckle profile becomes increasingly more localized.

6.4.2 Fold development

After the rapid initial phase of deformation, a further period of slow folding takes place under conditions of controlled end displacement. Figure 6.5 shows the response for the case of constant end-shortening, $\dot{\mathcal{E}} = 0$, corresponding to $P(0) = 1.95$. A sudden decrease in the load occurs as the dashpots alleviate the stresses in the springs, in much the same way that an isolated Maxwell unit exhibits stress relaxation under constant axial displacement (see Figure 1.4). While the end-shortening is held constant, the waveforms begin to open out and the peak amplitudes, although initially

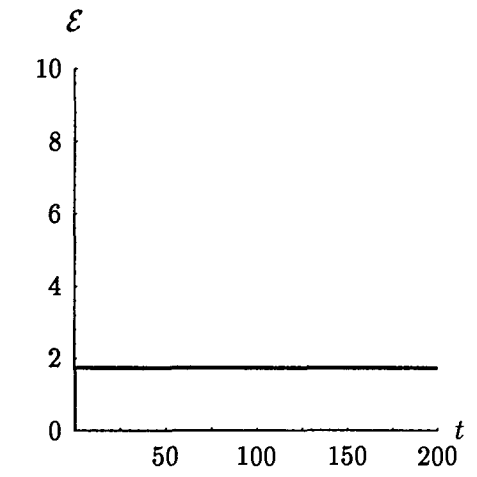

(a)

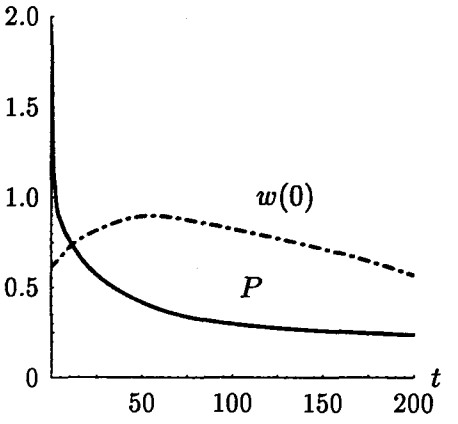

(b)

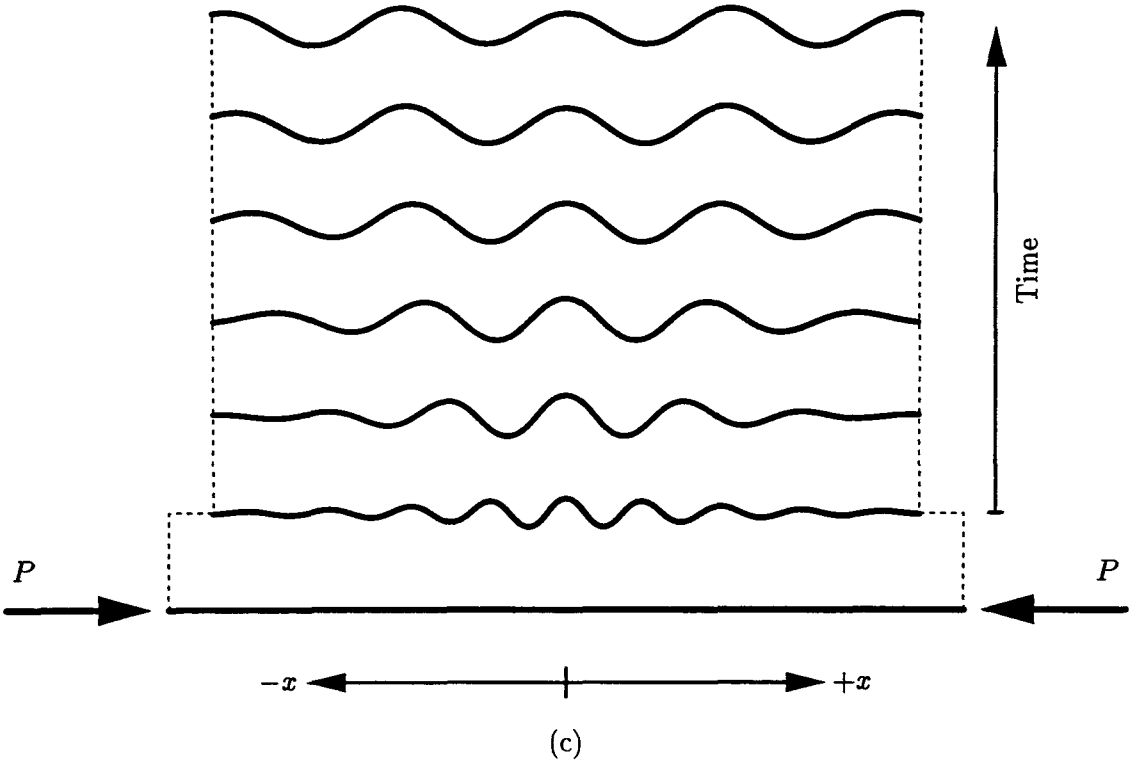

(c)

Figure 6.5 Evolution of fold pattern for model A with constant end-shortening, $\dot{\mathcal{E}} = 0$, corresponding to $P(0) = 1.95$.

increasing, eventually decay; the profile becomes increasingly less localized as time goes on. Despite the appearance of the final profile in Figure 6.5, genuine periodicity is never achieved as this implies infinite end-shortening. The numerical method was applied to a model several times longer than the range of values presented in the figure. Aspects of the numerical procedure, including the length, boundary conditions and time step, are discussed in Chapter 4. Ultimately, the flat state is attained through a succession of less localized forms. For a finite length strut, the deflected profile would adopt a wavelength corresponding to twice the length of the strut.

Figure 6.6 shows the evolution response for the case of constant *rate* of end-shortening, $\dot{\mathcal{E}} = 1$. Although the time scale is much shorter than for the previous load case, it displays a markedly different behaviour. The amplitude at the centre grows continuously and the deflected profile folds up with the wavelength becoming smaller as time progresses. The deformed shape displays a remarkable resemblance to the patterns reported by Zhang *et al.* (1996), especially those for the elasto-plastic layer and matrix reproduced in Figure 2.1. Despite their use of different materials for the layer and matrix, and the use of initial imperfections to perturb the instability, the features are qualitatively similar.

The numerical solution was traced until the maximum slope was nearly vertical, the limit of the formulation. The analysis could be extended using an intrinsic coordinate system, allowing the strut to loop back on itself. However, such extreme deflections are likely to exceed the proportional limit of the elastic strut and are deemed unnecessary.

A comparison of the evolution of load and maximum amplitude for two starting positions, under conditions of constant end-shortening and constant rate of end-shortening, is shown in Figure 6.7. Two features are immediately apparent. First, the general behaviour of both load and amplitude with time is the same for each starting position; the load decays, apparently exponentially, and the amplitude increases either slowly or rapidly depending on the rate of applied end-shortening. The second point is more intriguing. Figure 6.7 (a) shows that the initial drop in load is greater for the case of increasing end-shortening than for the case of constant end-shortening. For $P(0) = 1.8$, the load for $\dot{\mathcal{E}} = 1$ remains below that for the $\dot{\mathcal{E}} = 0$

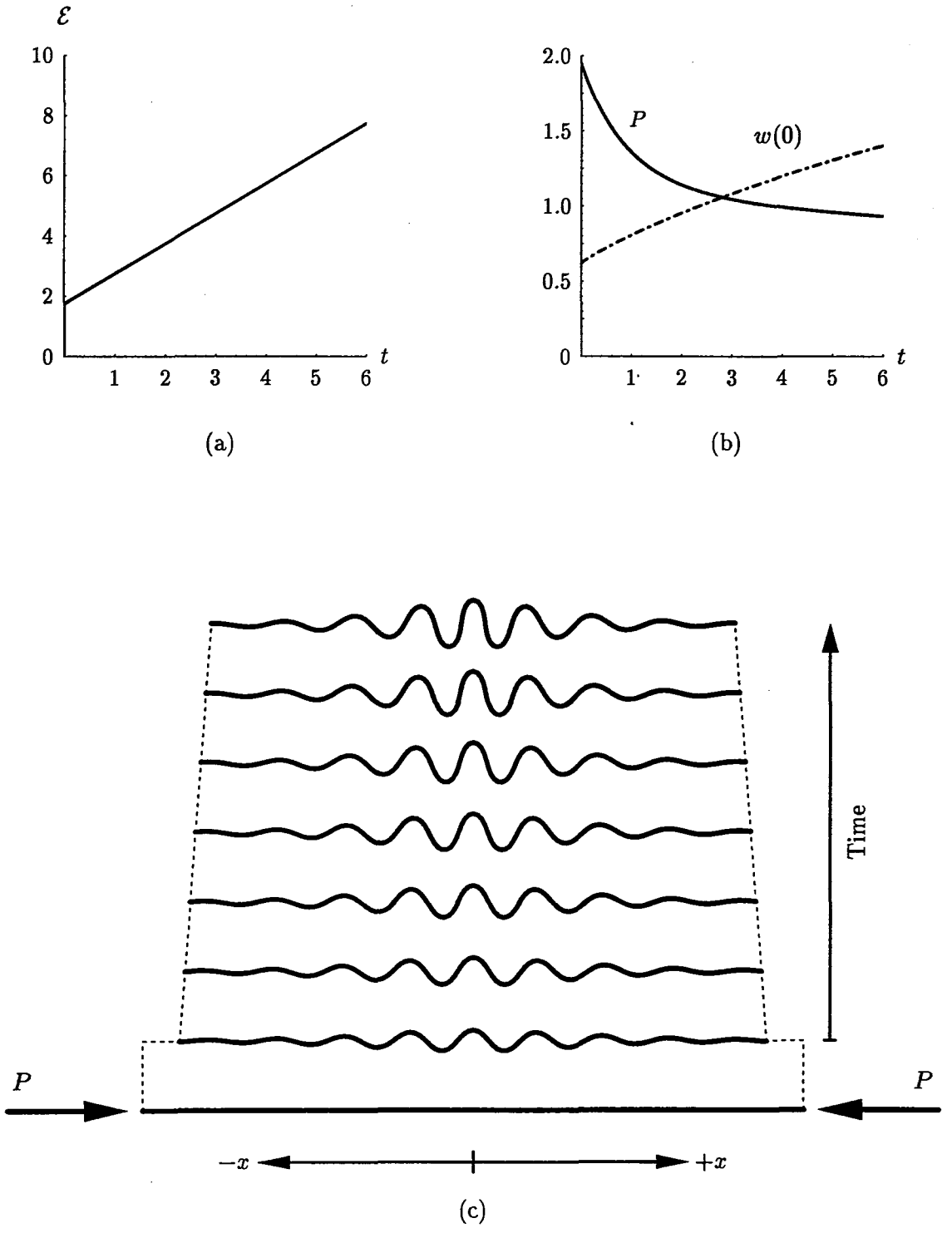

Figure 6.6 Evolution of fold pattern for model A with constant rate of change of end-shortening, $\dot{\mathcal{E}} = 1$, corresponding to $P(0) = 1.95$.

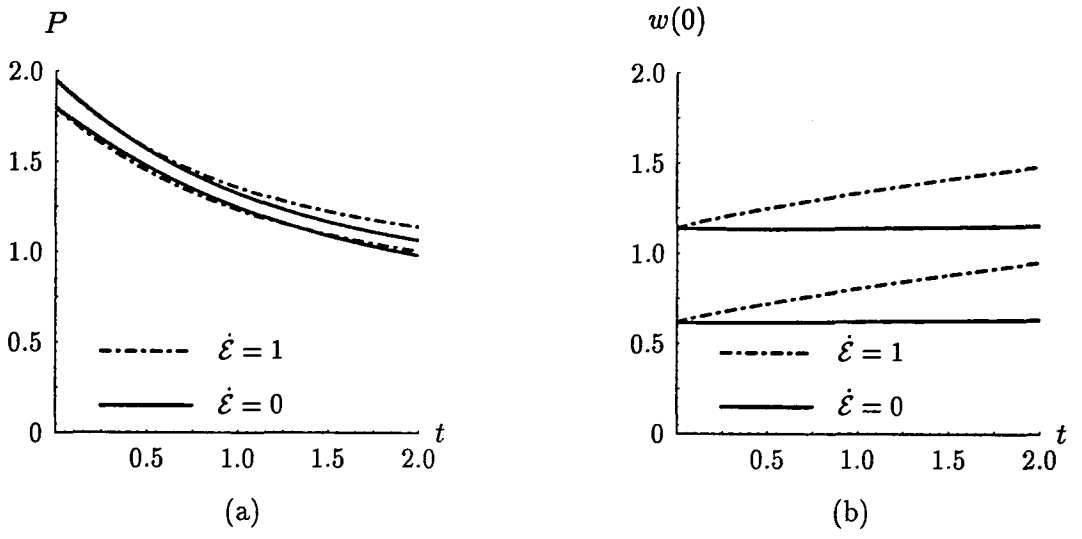

Figure 6.7 Evolution of load P and amplitude $w(0)$ for model A for starting conditions $P(0) = 1.8$ and $P(0) = 1.95$.

load case until $t \approx 1.35$. This apparent paradox is a result of the softening effect of the nonlinear terms and may be explained with reference to the initial elastic state of Figure 6.4. At $t = 0$ the initial end-shortening is the same for both load cases. However, after a small period of time the end-shortening for the $\dot{\mathcal{E}} = 1$ load case is greater than for the $\dot{\mathcal{E}} = 0$ load case, which remains constant. The negative stiffness of the post-buckling curve means that greater end-shortening is associated with lower axial load. This interpretation is valid only during the very early stages of evolution where the elastic behaviour dominates. After this time the result is overshadowed by the influence of viscous deformations.

6.5 Visco-elastic model B — material nonlinearity

For this model, the Maxwell foundation is assumed to have nonlinear spring elements, which obey the inverse hyperbolic sine function (6.2), and Newtonian dashpots. The foundation nonlinearity is assumed so strong that the linear strut equation can be used, leaving the foundation reaction as the only nonlinear component in the formulation. The evolution of the system is now controlled by the following equations:

- the linear strut equation

$$EI\,w'''' + P\,w'' + F = 0, \tag{6.7}$$

- and the nonlinear Maxwell relation

$$\frac{\partial}{\partial t}\left[w - \frac{1}{n}\sinh\left(\frac{n}{k}F\right)\right] - \frac{1}{\eta}F = 0. \tag{6.8}$$

6.5.1 Fold initiation

The differential equation governing the deformation of the initial elastic state is obtained by substituting for F from Equation (6.7) and setting the contents of the square brackets in Equation (6.8) to zero. This gives

$$EIw'''' + Pw'' + \frac{k}{n}\sinh^{-1} nw = 0. \tag{6.9}$$

If the hyperbolic function is expanded as a series and truncated after the first nonlinear term, the resulting differential equation has the same form as the equation for an elastic strut supported by a softening cubic foundation. That equation was the subject of the previous chapter and belongs to a family of equations known to exhibit a multiplicity of solutions which have been described as spatially-chaotic (Champneys, 1994). It seems reasonable to assume that many of the characteristics of the truncated differential equation are shared with the general nonlinear form of Equation (6.9).

Figure 6.8 shows the load versus end-shortening response for the initial elastic state of model B and the effect of the degree of foundation nonlinearity n on the force-displacement response of the spring. As the degree of nonlinearity n decreases, the post-buckling curve becomes progressively stiffer. In the limit as $n \to 0$, the curve tends to a horizontal line from P^c. Three localized profiles are shown for various values of n at $P = 1.95$. A greater degree of material nonlinearity results in a localized buckle pattern with smaller amplitude and end-shortening.

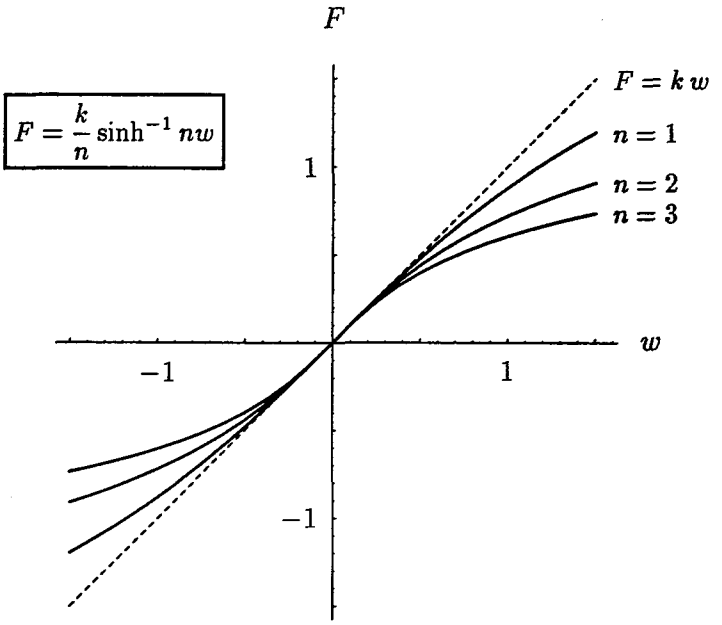

$$EIw'''' + Pw'' + F = 0$$

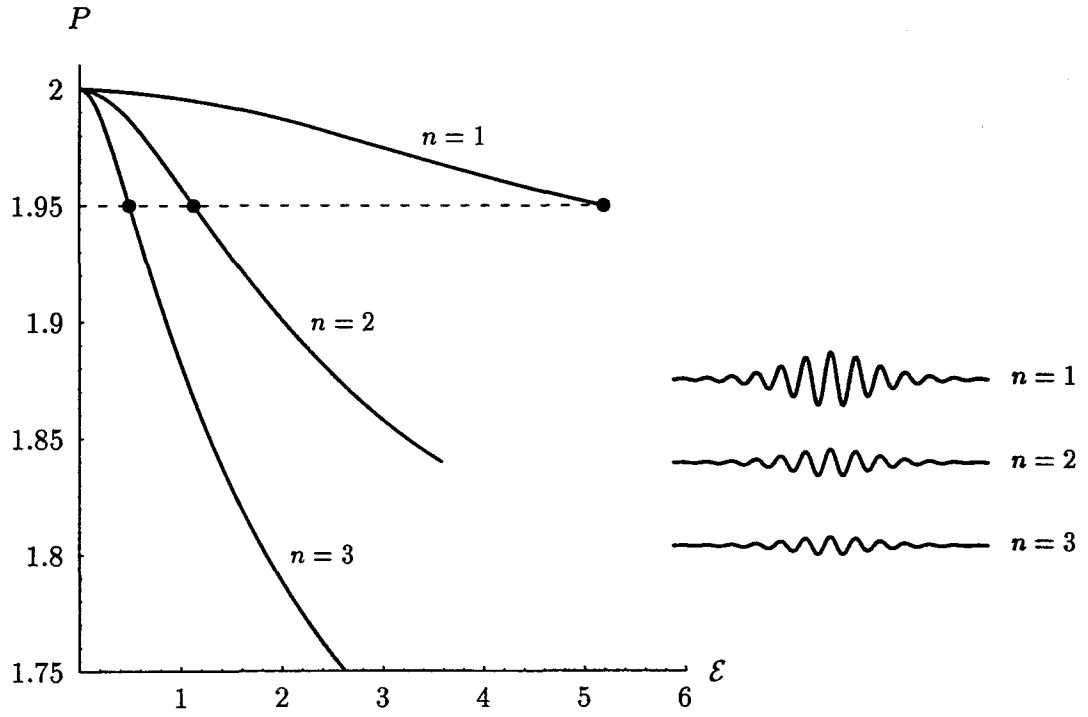

Figure 6.8 Foundation behaviours (top figure) and load versus end-shortening (bottom figure) for the initial elastic response of model B ($EI = k = 1$).

6.5.2 Fold development

As for the previous model, evolution of the buckled form is considered under load conditions of constant axial displacement. The case of constant rate of end-shortening is not considered as the formulation is not valid for the large deflections and slopes which are likely to occur. To consider such an event it would be more appropriate to solve the combined system of the nonlinear foundation (6.8) together with the elastica equation (6.5).

Figure 6.9 shows the response of the model for $\dot{\mathcal{E}} = 0$, corresponding to $P(0) = 1.95$. As with the geometrically nonlinear model, the load falls sharply and the deformed shape gradually opens out as the energy stored in the foundation springs and the internal bending energy are released. The eventual outcome is, again, the flat state through a series of less localized forms.

6.6 Multiplicity of localized solutions

Buckling solutions of a strut on a foundation are many and varied. In addition to the primary (symmetric) localized form, upside down, anti-symmetric, asymmetric, multi-peaked and periodic solutions have been found. The discovery of this spectacular variety of buckling solutions was made by Hunt & Wadee (1991) using initial-value methods and concepts from the theory of dynamical systems. From amongst the myriad of competing solutions, the one with least stored energy is likely to be preferred. In general, for a perfect strut and a homogeneous foundation, this is the primary mode. In natural systems, however, the presence of spatial or material imperfections may favour a localized form other than the primary mode. In the following sections, numerical examples of the variety of localized solutions are presented for the elastica strut on a Winkler foundation.

6.6.1 Anti-symmetric solutions

Primary localizations have a symmetric form which stems from the reversibility property of the buckling equations; replacing x with $-x$ does not affect the equation, or the solution. Anti-symmetric solutions are those with rotational symmetry

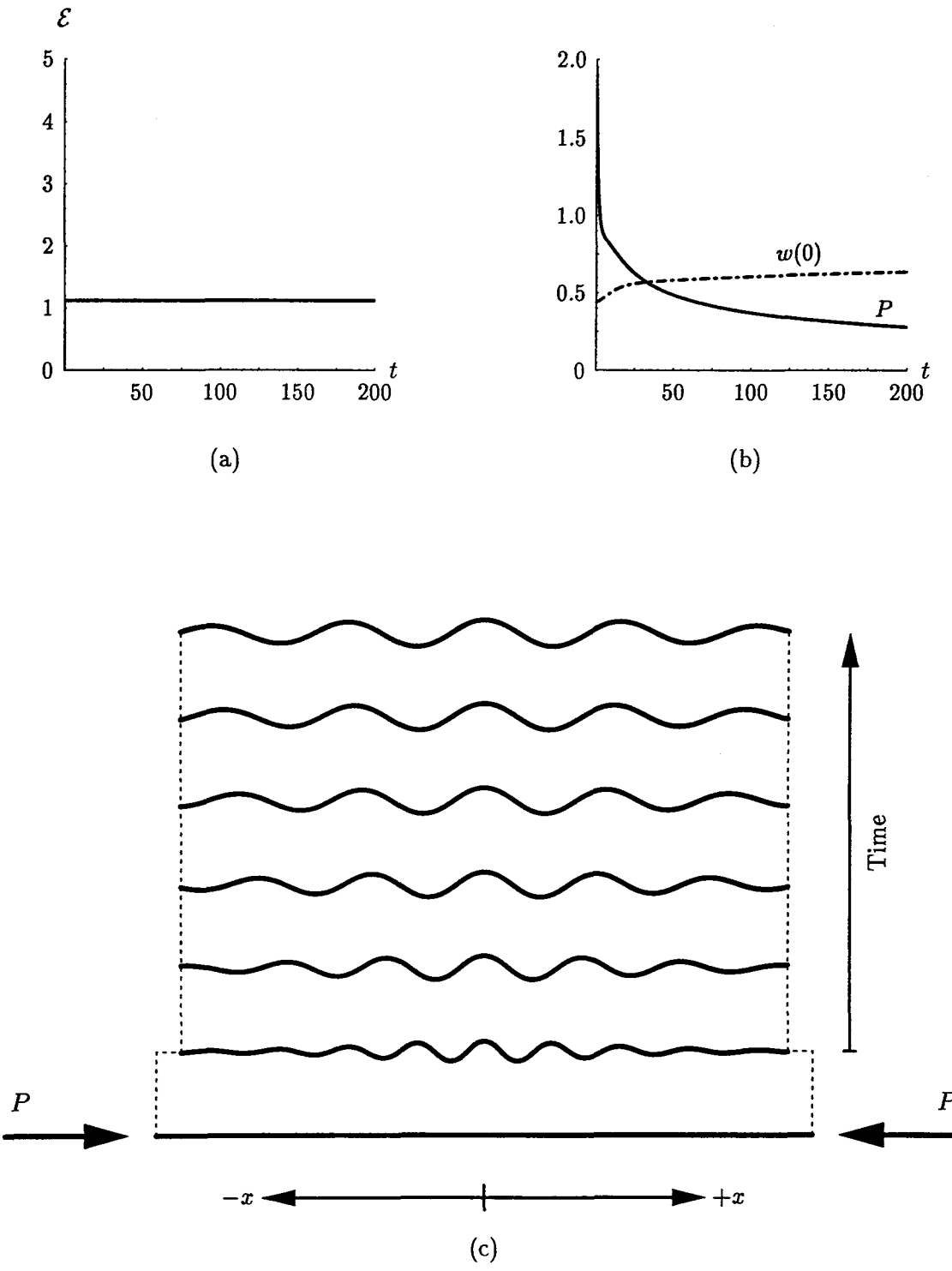

Figure 6.9 Evolution of fold pattern for model B with constant end-shortening, $\dot{\mathcal{E}} = 0$, corresponding to $P(0) = 1.95$.

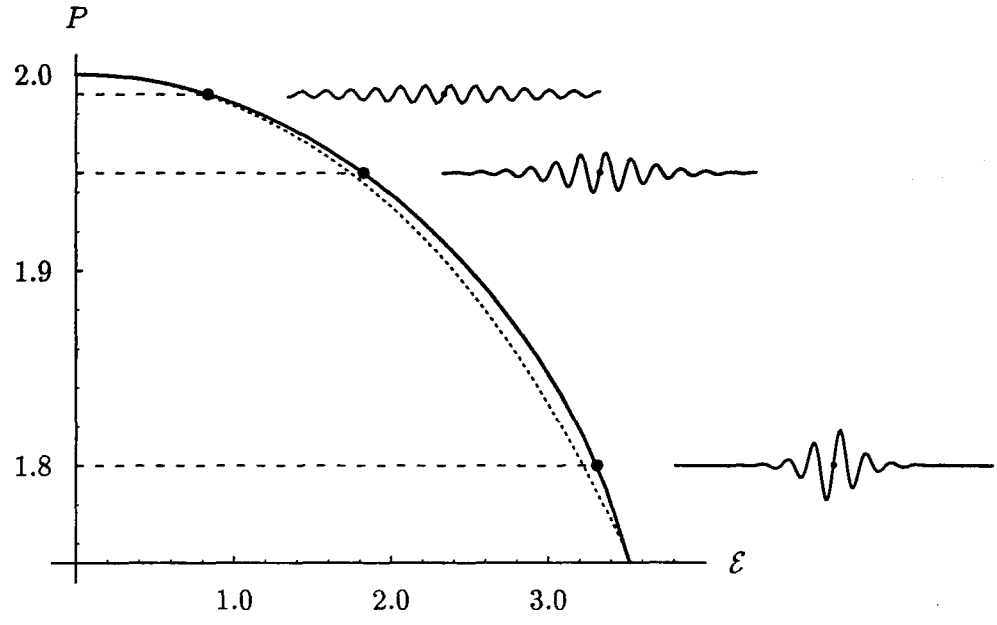

Figure 6.10 Load versus end-shortening and deflected profiles for anti-symmetric solutions of an elastica strut on a Winkler foundation ($EI = k = 1$). The dashed line represents the post-buckling response for the symmetric solutions of Figure 6.4.

about a point and exist only in buckling models for which upward and downward displacements are equally likely. The post-buckling response for the simplest anti-symmetric form of the elastica strut is shown in Figure 6.10 along with several deflected profiles. A small dot is used to highlight the point of (rotational) symmetry in these buckle patterns, which are otherwise difficult to detect at high load values. The end-shortening for anti-symmetric solutions is marginally greater than for their symmetric counterparts, suggesting the symmetric pattern is the preferred mode of deformation.

Wadee (1993) remarks on the difficulties associated finding anti-symmetric solutions numerically using a shooting approach. By contrast, the solutions generated here were obtained relatively easily and required only a small modification to the method described in Chapter 4. An initial profile $\bar{w} = A \operatorname{sech} \alpha x \sin \beta x$ was used in conjunction with boundary conditions $w = w'' = 0$ at the assumed point of anti-symmetry, $x = 0$.

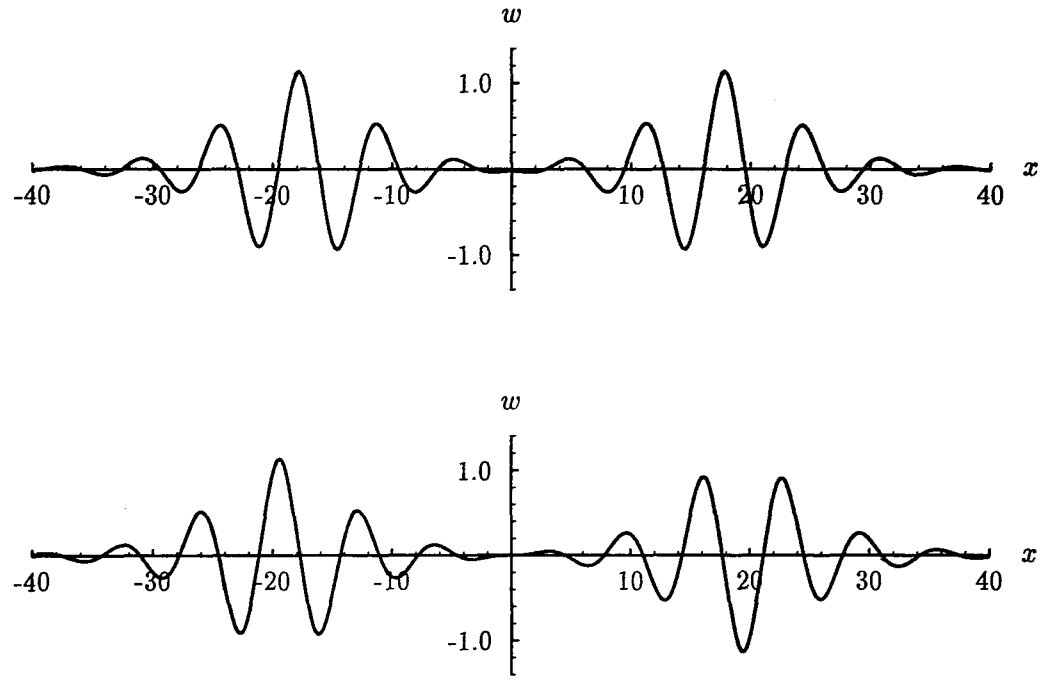

Figure 6.11 Bimodal solutions for an elastica strut on a Winkler foundation ($EI = k = 1$, $P = 1.8$).

6.6.2 Multi-modal solutions

The formal existence of multi-modal localized buckle patterns has been established for a strut on a nonlinear elastic foundation (Champneys & Spence, 1993; Champneys & Toland, 1993). These authors classified modes according to the number of quarter wavelengths between adjacent peaks in amplitude and demonstrated how the distance between peaks increases as the load changes. They concluded that there is an infinite number of symmetric localized solutions with any given number of peaks, each of which is born at the bifurcation point $-P^c$ and whose locus with respect to P forms a limit point for some $P < P^c$. This implies that the number of multi-modal solutions reduces with proximity to the critical point.

Localized solutions with multiple peaks have the appearance of a combination of primary modes. This is in spite of the fact that the buckling equations are nonlinear and are, therefore, not governed by the linear principle of superposition. Two bimodal solutions are depicted in Figure 6.11. The first gives the appearance of two primary modes offset by six wavelengths and has an end-shortening $\mathcal{E} = 6.42$.

The second is anti-symmetric and looks like a combination of a positive and negative (upside down) primary mode with end-shortening $\mathcal{E} = 6.44$. The end-shortening for the bimodal solutions is nearly twice that for the primary localization at $P = 1.8$ (Figure 6.4 indicates $\mathcal{E} = 3.23$ for the primary mode). This supports the idea that a bimodal solution is closely related to the sum of two primary modes. The interference between peaks and troughs of the localized solution suggests that as the distance between adjacent peaks increases, the end-shortening of a bimodal solution is likely to approach twice that for the corresponding primary mode. The buckling equations studied here are invariant under longitudinal translation which means that localization may occur anywhere along the strut. For convenience the point of (anti-)symmetry is always assumed to be $x = 0$.

The interaction of localized buckle patterns to form multi-modal shapes is similar in many ways to solitons, or humped travelling waves, which pass through one another preserving their original form (Drazin, 1991). Indeed, the analogy between the two has been reported on several occasions (Cowell, 1986; Hunt *et al.*, 1989; El Naschie, 1989). An important difference is that while solitons can travel smoothly in time, localized buckling modes interact only in discrete, quarter-wave, jumps. A particularly interesting paper by Konno & Jeffrey (1983) combines both analogies by considering the interaction of two large-amplitude deflections travelling at different speeds along an elastic rod.

The overall picture of localization is one of infinite variety, a feature typical of chaotic systems (Thompson & Stewart, 1986), leading some workers (Hunt *et al.*, 1993) to speculate that multi-modal solutions are a form of spatial chaos. In any case, it differs from earlier studies of chaos in the elastica (Thompson & Virgin, 1988; El Naschie, 1989) in that it is not induced by imperfections. These authors used sinusoidal imperfections of the strut in analogy with the periodically forced pendulum. Whereas their model was a one-degree-of-freedom system which cannot exhibit chaotic behaviour without external excitation, the elastica-on-foundation model is a two-degree-of-freedom system in which chaos may exist naturally (Thompson & Stewart, 1986).

6.7 Concluding remarks

In this chapter many of the techniques of the preceding chapters have been applied to the problem of a strut on a foundation. The importance of nonlinearities in the differential equations governing the instability process of folding has been highlighted through a series of numerical experiments. The work has focussed on the evolution of primary localizations from amongst the myriad of possible starting conditions. For a Maxwell bedding relation, the system settles naturally at the start of evolution into a pattern of localized buckling, contrasting sharply with the strongly-periodic trend found in purely viscous formulations (Biot, 1965; Mühlhaus *et al.*, 1994). Subsequent behaviour depends on the rate of applied end-shortening; for constant or slowly increasing end-shortening, the initial buckle pattern gives way to the flat state while rapid rates of applied end-shortening cause the localization to become more concentrated in time.

Chapter 7

Conclusions and suggestions for future work

The principal objective of this thesis has been the investigation of localized buckling in dynamic processes such as geological folding. Localized buckling in static (elastic) systems has been the subject of much research in recent years with particular application to engineering structures such as railway tracks and submarine pipelines (Blackmore, 1995; Champneys *et al.*, 1996). The inclusion of visco-elasticity in the same buckling model offers a plausible description for the formation of single-layer folds. The model is capable of a wide range of non-periodic solutions and may account for some of the diversity displayed by geological folds.

In the following sections a summary of this thesis is presented, emphasizing original contributions and indicating areas for further research.

7.1 Summary of research

Most of the family of theoretical models for folding in geological strata were inspired by Biot's (1965) linear instability analysis which apparently holds only for the very early stages of fold evolution (Johnson, 1977; Price & Cosgrove, 1990). By incorporating large-amplitude nonlinearities and foundation nonlinearities in the formulation of the problem, the results in this thesis are valid beyond the initial phase of deformation. If it is accepted that nonlinear behaviour is the norm for

natural systems, then the results presented here are more likely to account for real phenomena than those derived from infinitesimal theories. Another distinguishing feature between this and many of the earlier models is that the process of folding is simulated using rigid load conditions.

The model comprises an infinitely long elastic strut which is continuously supported along its length by discrete Maxwell elements. Linear Fourier analyses were presented in Chapter 2 for elastic, viscous and visco-elastic embedding mediums to demonstrate the effect of foundation rheology on the buckling response of the model. For the elastic foundation, a sinusoidal buckle pattern was predicted at discrete load values. In contrast, the viscous and visco-elastic foundations led to dispersion relations and the concept of a dominant wavelength (Biot, 1965). These analyses were limited to small (strictly infinitesimal) deflections and the case of constant applied load. To illustrate the effect of rigid loading and large displacements on the post-buckling response of the strut, an analogous rigid link model was used.

A double-scale perturbation technique was used in Chapter 3 to reveal the post-buckling behaviour of the instantaneous, purely elastic, response of the system. Unlike earlier post-buckling studies (Thompson & Hunt, 1973) which revealed only periodic forms, this procedure allows the modulation of both amplitude and phase of the buckle pattern. The method described here is closely related to that proposed by Wadee (1993) and is the subject of a forthcoming paper (Wadee *et al.*, 1996). In contrast to previous double-scale applications (Amazigo *et al.*, 1970; Potier-Ferry, 1983; Hunt *et al.*, 1989) which were developed from the governing differential equations, the scheme was based on the total potential energy of the elastic system. Like other perturbation analyses, the procedure is confined to special types of solutions, the earlier assumption of periodicity of the buckle pattern being replaced by a more general, localized form. Without modifications to the procedure more complex modes of buckling are denied.

Theoretical results concerning the existence and uniqueness of localized solutions in buckling problems are beyond the scope of this thesis. As with many physical problems, the solution of the governing equations is attempted without the benefit of existence theorems (Keller, 1968). The robustness of localized phenomena is not

in question, however, having been established by many authors using a variety of shooting methods (Bolt, 1989; Hunt *et al.*, 1989; Champneys & Spence, 1993). The change from a purely elastic system to a visco-elastic system results in a partial differential equation, which has necessitated the use of a boundary-value approach. The method, outlined in Chapter 4, uses solutions from adjacent parameter values and time steps as initial profiles to update the spatial form as time progresses.

The potential for alternative methods of analysis involving trial functions was the subject of Chapter 5. They were found to be suitable only for buckling problems composed of the linearized strut equation and a simple nonlinear foundation. A Galerkin method was used to generate modal solutions for the initial elastic state of a strut on a foundation with a cubic nonlinearity. This work has been accepted for publication and is to appear shortly (Whiting, 1996). Another procedure, based on a collocation method and resulting from the work of Hunt *et al.* (1996a), was found to be capable of providing solutions for both the elastic and visco-elastic phase of deformation. Despite the limitations of these weighted residual methods, they proved to be useful tools for generating initial profiles, with which to trigger the boundary-value solver COLSYS, and for determining solutions close to the critical point where numerical methods encounter problems.

In all of the visco-elastic strut models presented in this thesis a Maxwell fluid was used for the bedding material. While it is an exaggeration to suggest that any event of geological folding would happen instantly, the model does emphasize that two quite different time scales may be involved; one in which the response is *predominantly* elastic, enabling the initiation of a localization or non-periodic profile; and one in which visco-elasticity is the governing effect. It may be be more realistic to see both effects in the same geological time frame. This may be achieved by considering a *Newton-Kelvin* fluid, which exhibits delayed elasticity and flow. For this, and other types of visco-elastic behaviour, the work here may be extended simply by replacing the Maxwell unit with an alternative spring-dashpot model (Roscoe, 1950).

The numerical methods were finally unleashed in Chapter 6 to investigate the effects of geometric and material nonlinearities on the evolution of localized buckle

patterns. Controlled axial displacement was used to simulate tectonic plate movement. Under constant end-shortening, the instantaneous buckle of the strut was followed by progression through a succession of less localized forms, ultimately resulting in the flat state. For increasing end-shortening, at a constant rate, the buckled shape continued to fold up until it reached the limit of the formulation. These numerical results have recently been accepted for publication (Whiting & Hunt, 1996). Some of the variety of solutions arising from the assumption of nonlinear elasticity were also displayed. These higher modes of localization are apparently the spatial equivalent of the interaction of solitons (Drazin & Johnson, 1989).

Perhaps the main conclusion of this thesis is that a strut-on-foundation model with softening qualities, induced either through the foundation or by the inclusion of nonlinear curvature and end-shortening terms, is susceptible to localized buckle patterns. This work is only the beginning in the application of recent developments from the field of nonlinear dynamics (via structural engineering) to geological formations. It is hoped that much of the spatial variety evident in the elastic system can be transported to the visco-elastic domain to account for the incredible diversity of folded structures observed in the field. A review of this subject is currently in preparation (Hunt *et al.*, 1997).

7.2 Recommendations for future work

In spite of the large number of theoretical analyses of folding, there remain plenty of opportunities for researchers interested in nonlinear phenomena. The following areas are identified as natural extensions of the work in this thesis.

7.2.1 Visco-elastic continuum

A Winkler-type foundation, like the one used here, is essentially discontinuous with adjacent foundation elements acting independently of one another. Complete continuity, enabling non-local effects and shear, may be achieved using a continuum (Vardoulakis & Sulem, 1995). A hybrid foundation with partial continuity was investigated by Hunt *et al.* (1996a). They assumed the foundation reaction was

wavelength-dependent so that harmonic displacements with shorter wavelengths encounter greater resistance than displacements with longer wavelengths. Modelling of the supporting medium is one of the primary goals in the continuing work on localized buckling to be supported by the Engineering and Physical Sciences Research Council (EPSRC) at the University of Bath.

7.2.2 Formation of plastic hinges

For large deflections, folding of real geological structures inevitably involves *visco-elasto-plastic* behaviour. Plasticity may be regarded as a type of localization since it occurs in isolated regions where strains are sufficiently large. Once plasticity develops in the system, it can influence the location of maximum amplitude of the buckle pattern because no extra load is required to cause further deformation. Besides yielding of the strut, plasticity may also arise within the foundation. This case was studied by Blackmore (1995) and Hunt & Blackmore (1996) in relation to upheaval buckling in submarine pipelines where the foundation resistance suddenly becomes zero as the pipe lifts off its support.

7.2.3 Multi-layer strata

Attention in this thesis has focussed on models for the evolution of single-layer folds. Though such forms exist in nature, folding of multi-layers is more common and for this reason a great deal of literature exists about them (Ramsay, 1967; Price & Cosgrove, 1990). There are two distinct approaches to analysing folding in multi-layer strata and both depend on single-layer buckling theories. In the first, plate theory is used to describe the bending resistance of individual layers within the multi-layer (Ramberg, 1964). Compatibility of displacements is then used to match the solutions at the interface between adjacent layers, thereby obtaining a solution for the response of the layered media. In a quite different approach, the response of the layered material is analysed in terms of an equivalent thick plate with anisotropic (smeared) mechanical properties (Biot, 1961). In either case, single-layer theories are of fundamental importance in the formulation of a multi-layer theory. The effect of bending resistance and nonlinear material properties on the instability of multi-layered media has already received some attention by Latham (1985).

Appendix A

Perturbation equations

In this appendix the complete procedure required to obtain the perturbation solutions summarized in § 3.3.2 is presented. The method closely resembles that outlined by Wadee (1993). Recall that approximate solutions for the deflected shape of a strut on a nonlinear elastic foundation are obtained by solving the two sets of Euler-Lagrange equations (3.25) and (3.26), which are repeated here for convenience:

$$V_{i''i''}\,A_i'''' + \frac{1}{2}\left(V_{i''i'} - V_{i'i''}\right)B_i''' + \left(V_{ii''} - V_{i'i'}\right)A_i'' + \frac{1}{2}\left(V_{ii'} - V_{i'i}\right)B_i' + V_{ii}\,A_i + \frac{1}{6}V_{ijkl}^{cc}\,A_jA_kA_l + \frac{1}{2}V_{ijkl}^{cs}\,A_jB_kB_l = 0, \tag{A.1}$$

$$V_{i''i''}\,B_i'''' + \frac{1}{2}\left(V_{i'i''} - V_{i''i'}\right)A_i''' + \left(V_{ii''} - V_{i'i'}\right)B_i'' + \frac{1}{2}\left(V_{i'i} - V_{ii'}\right)A_i' + V_{ii}\,B_i + \frac{1}{2}V_{jikl}^{cs}\,A_jA_kB_l + \frac{1}{6}V_{jikl}^{ss}\,B_jB_kB_l = 0. \tag{A.2}$$

The coefficients of the linear terms in these equations are

$$V_{ii} = \begin{cases} k, & \text{for } i = 0 \\ \frac{1}{2}\left(EIi^4\beta^4 - Pi^2\beta^2 + k\right), & \text{for } i \neq 0 \end{cases}$$

$$V_{i'i'} = \begin{cases} -s^2P, & \text{for } i = 0 \\ \frac{1}{2}s^2\left(4EIi^2\beta^2 - P\right), & \text{for } i \neq 0 \end{cases}$$

$$V_{ii''} = -s^2EIi^2\beta^2$$

$$V_{i''i''} = \begin{cases} s^4EI, & \text{for } i = 0 \\ \frac{1}{2}s^4EI, & \text{for } i \neq 0 \end{cases}$$

$$V_{i''i'} = 2s^3i\beta EI$$

$$
\begin{aligned}
V_{i'i''} &= -2s^3 i\beta EI \\
V_{i'i} &= 2si^3\beta^3 EI - si\beta P \\
V_{ii'} &= -2si^3\beta^3 EI + si\beta P
\end{aligned} \tag{A.3}
$$

and the coefficients associated with the cubic nonlinear terms are

$$
V^{cs}_{ijkl} = \begin{cases}
-6c, & \text{for } i=j=k=l=0 \\
-\frac{9}{4}c, & i=j=k=l\neq 0 \\
-3c, & \text{for } i=j=0 \text{ and } k=l\neq 0, \text{ etc.} \\
-\frac{3}{2}c, & \text{for } i=0 \text{ and } j=k+l, \text{ etc.} \\
-\frac{3}{4}c, & \text{for } i=j+k+l, \text{ etc.} \\
-\frac{3}{2}c, & \text{for } i+j=k+l \text{ and } i=k, j=l, \text{ etc.} \\
-\frac{3}{4}c, & \text{for } i+j=k+l \text{ and } i\neq k, j\neq l, \text{ etc.} \\
0, & \text{otherwise.}
\end{cases}
$$

$$
V^{cs}_{ijkl} = \begin{cases}
0, & \text{for } k=0, \text{ etc.} \\
-\frac{3}{4}c, & i=j=k=l\neq 0 \\
-3c, & \text{for } i=j=0 \text{ and } k=l \\
\frac{3}{2}c, & \text{for } i=0 \text{ and } j=k+l, \text{ etc.} \\
-\frac{3}{2}c, & \text{for } i=0 \text{ and } k=j+l, \text{ etc.} \\
\frac{3}{4}c, & \text{for } i=j+k+l, \text{ etc.} \\
-\frac{3}{4}c, & \text{for } k=i+j+l, \text{ etc.} \\
0, & \text{for } i+k=j+l \text{ and } i=l, j=k, \text{ etc.} \\
-\frac{3}{4}c, & \text{for } i+k=j+l \text{ and } i\neq l, j\neq k, \text{ etc.} \\
-\frac{3}{2}c, & \text{for } i+k=j+l \text{ and } i=j, k=l, \text{ etc.} \\
0, & \text{for } i+j=k+l \text{ and } i=k, j=l, \text{ etc.} \\
\frac{3}{4}c, & \text{for } i+j=k+l \text{ and } i\neq k, j\neq l, \text{ etc.} \\
0, & \text{otherwise.}
\end{cases}
$$

$$V^{ss}_{ijkl} = \begin{cases} 0, & \text{for } i = 0, \text{ etc.} \\ -\frac{9}{4}c, & i = j = k = l \neq 0 \\ \frac{3}{4}c, & \text{for } i = j + k + l, \text{ etc.} \\ -\frac{3}{2}c, & \text{for } i + j = k + l \text{ and } i = k,\ j = l, \text{ etc.} \\ -\frac{3}{4}c, & \text{for } i + j = k + l \text{ and } i \neq k,\ j \neq l, \text{ etc.} \\ 0, & \text{otherwise,} \end{cases} \tag{A.4}$$

where etc. indicates that cyclic permutations of i, j, k and l are to be taken in the case of V^{cc}_{ijkl} and V^{ss}_{ijkl}, while for V^{cs}_{ijkl}, i and j are cycled separately from k and l.

The modal amplitudes, A_i and B_i, are expanded as power series in the perturbation parameter s to give

$$\begin{aligned} A_i &= A_{i,1}(X)\, s + A_{i,2}(X)\, s^2 + \cdots, \\ B_i &= B_{i,1}(X)\, s + B_{i,2}(X)\, s^2 + \cdots. \end{aligned} \tag{A.5}$$

Modes A_1 and B_1 are assumed to be associated with the lowest critical load, P^c, and as a result all other modes, being of higher order, must start at least one power of s higher. In other words, $A_{i,1}$ and $B_{i,1}$ are both zero for $i \neq 1$. The load P and frequency β are also expanded as series in s,

$$\begin{aligned} P &= P^c + P_1\, s + P_2\, s^2 + \cdots, \\ \beta &= \beta^c + \beta_1\, s + \beta_2\, s^2 + \cdots, \end{aligned} \tag{A.6}$$

where the quantities at the critical point are

$$P^c = 2\sqrt{kEI}, \qquad \beta^c = \sqrt[4]{\frac{k}{EI}}. \tag{A.7}$$

The coefficients P_i and β_i are fixed by the choice of the perturbation parameter, $s = \sqrt{P^c - P}$. This forces $P_2 = -1$ and $P_i = 0$ for all $i \neq 2$. Likewise, the coefficients β_i are specified by choosing β to be the linearized wavelength defined in Equation (3.13). The parameter s corresponds to α in the same equation, repre-

senting the real part of the linear solution.

All of the series expansions are fed into the Euler-Lagrange equations (A.1) and (A.2). To be satisfied in a well-ordered manner, terms of the same power of s are collected and their coefficients equated to zero. The coefficients of ascending levels of s are now considered in turn.

s level

No information is obtained at this level because the linearized values are an explicit part of the formulation.

s^2 level

At this level contributions arise from terms in $i = 1, 2$. Although no useful information can be obtained about the active terms $A_{1,1}$ and $B_{1,1}$, all of the passive terms are found to be zero. That is, $A_{2,2} = B_{2,2} = 0$.

s^3 level

At this level contributions arise from terms in $i = 1, 2, 3$. By considering the equations associated with δA_2 and δB_2, the coefficients $A_{2,3}$ and $B_{2,3}$ are found to be zero. A relationship between the active terms $A_{1,1}$ and $B_{1,1}$ is obtained by considering the Euler-Lagrange equations associated with δA_1 and δB_1:

δA_1 :

$$2P^c {A_{1,1}}'' - \beta^{c2} A_{1,1} + \frac{3c}{4} A_{1,1} \left({A_{1,1}}^2 + {B_{1,1}}^2 \right) = 0, \tag{A.8}$$

δB_1 :

$$2P^c {B_{1,1}}'' - \beta^{c2} B_{1,1} + \frac{3c}{4} B_{1,1} \left({A_{1,1}}^2 + {B_{1,1}}^2 \right) = 0. \tag{A.9}$$

The solution of these simultaneous differential equations proceeds by utilizing the conditions of symmetry ($\dot{w} = \ddot{w} = 0$) and by making use of coefficients which have already been determined. Writing these conditions in terms of the expanded modes

gives the following relations:

$$\begin{aligned}\dot{w} \;=\; \sum_{i=0}^{\infty}\Big\{ & s\Big(A_{i,1}{}'s + A_{i,2}{}'s^2 + \cdots\Big)\cos i\beta x \\ & - \Big(A_{i,1}s + A_{i,2}s^2 + \cdots\Big) i\beta \sin i\beta x \\ & + s\Big(B_{i,1}{}'s + B_{i,2}{}'s^2 + \cdots\Big)\sin i\beta x \\ & + \Big(B_{i,1}s + B_{i,2}s^2 + \cdots\Big) i\beta \cos i\beta x\Big\} = 0, \end{aligned} \tag{A.10}$$

and

$$\begin{aligned}\ddot{w} \;=\; \sum_{i=0}^{\infty}\Big\{ & s^3\Big(A_{i,1}{}'''s + A_{i,2}{}'''s^2 + \cdots\Big)\cos i\beta x \\ & - 3s^2\Big(A_{i,1}{}''s + A_{i,2}{}''s^2 + \cdots\Big) iw \sin i\beta x \\ & - 3s\Big(A_{i,1}{}'s + A_{i,2}{}'s^2 + \cdots\Big) i^2\beta^2 \cos i\beta x \\ & - \Big(A_{i,1}s + A_{i,2}s^2 + \cdots\Big) i^3\beta^3 \sin i\beta x \\ & + s^3\Big(B_{i,1}{}'''s + B_{i,2}{}'''s^2 + \cdots\Big)\sin i\beta x \\ & + 3s^2\Big(B_{i,1}{}''s + B_{i,2}{}''s^2 + \cdots\Big) iw \cos i\beta x \\ & - 3s\Big(B_{i,1}{}'s + B_{i,2}{}'s^2 + \cdots\Big) i^2\beta^2 \sin i\beta x \\ & - \Big(B_{i,1}s + B_{i,2}s^2 + \cdots\Big) i^3\beta^3 \cos i\beta x\Big\} = 0. \end{aligned} \tag{A.11}$$

The conditions of symmetry are imposed at $x = X = 0$. By setting the coefficients at the s and s^2 levels to zero the following equations are obtained in terms of quantities determined previously:

Coefficient of s:

$$B_{1,1}(0) \;=\; 0. \tag{A.12}$$

Coefficients of s^2:

$$\begin{aligned} A_{1,1}{}'(0) + \beta^c B_{1,2}(0) \;&=\; 0, \\ 3A_{1,1}{}'(0) + \beta^c B_{1,2}(0) \;&=\; 0. \end{aligned} \tag{A.13}$$

The only solution of the two equations at the s^2 level is the trivial one. Thus, the symmetry conditions provide the following information about $A_{1,1}$ and $B_{1,1}$

$$A_{1,1}{}'(0) = B_{1,1}(0) = 0. \tag{A.14}$$

The solution of the simultaneous equations proceeds with a transformation using polar coordinates (Wadee, 1993):

$$A_{1,1} = r\cos\phi, \qquad B_{1,1} = -r\sin\phi. \tag{A.15}$$

Equations (A.8) and (A.9) become

$$2P^c r'' - \left(\beta^{c2} + 2P^c \phi'^2\right) r + \frac{3c}{4} r^3 = 0, \tag{A.16}$$

$$2r'\phi' + r\phi'' = 0. \tag{A.17}$$

The second equation can be rewritten as

$$\left(r^2\phi'\right)' = 0, \tag{A.18}$$

and after integrating becomes

$$r^2\phi' = c_1, \tag{A.19}$$

where c_1 is a constant. The asymptotically flat boundary conditions require that $r(X) \to 0$ as $X \to \pm\infty$, which implies $c_1 = 0$. Now, for Equation (A.19) to hold, either $r(X) = 0$ or $\phi'(X) = 0$. The nontrivial solution is

$$\phi = c_2, \tag{A.20}$$

where c_2 is another constant. From Equations (A.14) and (A.15) it is apparent that either

$$r(0) = 0 \qquad \text{or} \qquad r'(0) = \phi(0) = 0. \tag{A.21}$$

The first case is the trivial state and is of no interest here. The second condition indicates that $c_2 = 0$, so that $\phi(X) = 0$. Therefore, the amplitude of the first sine

mode is

$$B_{1,1}(X) = 0. \tag{A.22}$$

The pair of simultaneous equations (A.8) and (A.9) are thus reduced to the single equation

$$A_{1,1}'' - \frac{\beta^{c2}}{2P^c} A_{1,1} + \frac{3c}{8P^c} {A_{1,1}}^3 = 0. \tag{A.23}$$

This new form is similar to equations which arise in many fields, for example, the nonlinear Schrödinger equations of quantum mechanics (Thompson & Stewart, 1986) and the simplest form of Duffing's equation for the nonlinear oscillator (Stephenson & Radmore, 1990). The solution may be found by observing that

$$A_{1,1}'' = \frac{\mathrm{d}A_{1,1}'}{\mathrm{d}X} = A_{1,1}' \frac{\mathrm{d}A_{1,1}'}{\mathrm{d}A_{1,1}}. \tag{A.24}$$

Inserting this into the differential equation and rearranging yields

$$A_{1,1}' \, \mathrm{d}A_{1,1}' = \left(\frac{\beta^{c2}}{2P^c} A_{1,1} - \frac{3c}{8P^c} {A_{1,1}}^3 \right) \mathrm{d}A_{1,1}, \tag{A.25}$$

and after integrating both sides

$$\frac{1}{2} {A_{1,1}'}^2 + c_3 = \frac{\beta^{c2}}{4P^c} {A_{1,1}}^2 - \frac{3c}{32P^c} {A_{1,1}}^4. \tag{A.26}$$

For a localized solution, the boundary conditions require that $A_{1,1}(X) \to 0$ and $A_{1,1}'(X) \to 0$ as $X \to \pm\infty$, so the constant of integration c_3 must be zero. This leads to

$$\mathrm{d}X = \frac{\mathrm{d}A_{1,1}}{\sqrt{c_4 {A_{1,1}}^2 - c_5 {A_{1,1}}^4}}, \tag{A.27}$$

in which

$$c_4 = \frac{\beta^{c2}}{2P^c}, \qquad c_5 = \frac{3c}{16P^c}.$$

The closed-form solution is then obtained as

$$A_{1,1} = \frac{4}{\sqrt{6c}} \beta^c \operatorname{sech} \Omega X. \tag{A.28}$$

The first passive mode appears at this level of s and may be expressed as a function of the active mode $A_{1,1}$.

δA_3 :

$$32k\, A_{3,3} - \frac{c}{8} {A_{1,1}}^3 = 0$$
$$\Rightarrow A_{3,3} = \frac{c}{256k} {A_{1,1}}^3. \tag{A.29}$$

δB_3 :

$$B_{3,3} = 0. \tag{A.30}$$

s^4 level

At this level contributions arise from terms in $i = 1, 2, 3, 4$. By considering δA_2, δB_2, δA_4, and δB_4, the quantities $A_{2,4}$, $B_{2,4}$, $A_{4,4}$, $B_{4,4}$ are all found to be zero.

δA_1 :

$$2P^{\mathrm{c}} {A_{1,2}}'' - {\beta^{\mathrm{c}}}^2 A_{1,2} + \frac{9c}{4} {A_{1,1}}^2 A_{1,2} = 0. \tag{A.31}$$

δB_1 :

$$\begin{aligned} 2P^{\mathrm{c}} {B_{1,2}}'' - {\beta^{\mathrm{c}}}^2 B_{1,2} + \frac{3c}{4} {A_{1,1}}^2 B_{1,2} \\ = \beta^{\mathrm{c}} {A_{1,1}}' - 2\frac{P^{\mathrm{c}}}{\beta^{\mathrm{c}}} {A_{1,1}}''' \\ = -\sqrt{\frac{3}{c}} \frac{4{\beta^{\mathrm{c}}}^3}{\sqrt{P^{\mathrm{c}}}} \operatorname{sech}^3 \Omega X \tanh \Omega X. \end{aligned} \tag{A.32}$$

These equations form a pair of second-order linear equations in $A_{1,2}$ and $B_{1,2}$ with non-constant coefficients. The presence of the terms on the right-hand side of the second equation means that, unlike for the previous level of s, these equations cannot be solved by a simple change of variables. The symmetry conditions (A.10) and (A.11) at the s^2 and s^3 levels indicate

$${A_{1,2}}'(0) = B_{1,2}(0) = 0, \tag{A.33}$$

and may be used to show, by inspection, that

$$A_{1,2} = 0, \tag{A.34}$$

$$B_{1,2} = \sqrt{\frac{3}{c}}\frac{\beta^c}{\sqrt{P^c}}\operatorname{sech}\Omega X \tanh \Omega X. \tag{A.35}$$

Once again the passive modes are expressed in terms of the active modes.

δA_3 :

$$A_{3,4} = 0. \tag{A.36}$$

δB_3 :

$$B_{3,4} = \frac{3c}{256k}{A_{1,1}}^2 B_{1,2} - \frac{3}{2\beta^c}A_{3,3}'. \tag{A.37}$$

s^5 level

At this level contributions arise from terms in $i = 1,2,3,4,5$. Immediately $A_{2,5}$, $B_{2,5}$, $A_{4,5}$ and $B_{4,5}$ are found to be zero.

δA_1 :

$$\begin{aligned} &2P^c A_{1,3}'' - \beta^{c2}A_{1,3} + \frac{9c}{4}{A_{1,1}}^2 A_{1,3} \\ &\quad = -\frac{3c}{4}{A_{1,1}}^2 A_{3,3} + EI A_{1,1}'''' + \frac{1}{2}A_{1,1}'' - \frac{3c}{4}A_{1,1}{B_{1,2}}^2 \\ &\qquad + \frac{2P^c}{\beta^c}B_{1,2}''' - \beta^c B_{1,2}' - \frac{3}{16EI}A_{1,1} \\ &\quad = \frac{1}{6\sqrt{6c}}\frac{\beta^{c3}}{P^c}\left(198\operatorname{sech}^3\Omega X - 307\operatorname{sech}^5\Omega X\right). \end{aligned} \tag{A.38}$$

δB_1 :

$$2P^c B_{1,3}'' - \beta^{c2}B_{1,3} + \frac{3c}{4}{A_{1,1}}^2 B_{1,3} = 0. \tag{A.39}$$

Using the symmetry conditions at the s^3 and s^4 levels the solutions are found as

$$A_{1,3} = \frac{1}{36\sqrt{6c}}\frac{\beta^c}{P^c}\left(-317\operatorname{sech}\Omega X + 307\operatorname{sech}^3\Omega X\right), \tag{A.40}$$

$$B_{1,3} = 0. \tag{A.41}$$

Again the passive modes are expressed in terms of the active modes.

δA_3 :

$$A_{3,5} = \frac{3c}{256k}{A_{1,1}}^2 A_{1,3} + \frac{3c}{128k}{A_{1,1}}^2 A_{3,3} + \frac{13P^c}{32k}A_{3,3}'' - \frac{3c}{256k}A_{1,1}{B_{1,2}}^2 + \frac{3}{2\beta^c}B_{3,4}' + \frac{27\beta^{c2}}{64k}A_{3,3}. \tag{A.42}$$

δB_3 :

$$B_{3,5} = 0. \tag{A.43}$$

δA_5 :

$$A_{5,5} = \frac{c}{768k}{A_{1,1}}^2 A_{3,3}. \tag{A.44}$$

δB_5 :

$$B_{5,5} = 0. \tag{A.45}$$

s^6 level

Contributions arise from terms in $i = 1, 2, 3, 4, 5, 6$. In order to determine the coefficients $A_{1,4}$ and $B_{1,4}$ it suffices to solve the equations arising from δA_1 and δB_1 only.

δA_1 :

$$2P^c A_{1,4}'' - \beta^{c2}A_{1,4} + \frac{9c}{4}{A_{1,1}}^2 A_{1,4} = 0. \tag{A.46}$$

δB_1 :

$$\begin{aligned} &2P^c B_{1,4}'' - \beta^{c2}B_{1,4} + \frac{3c}{4}{A_{1,1}}^2 B_{1,4} \\ &\quad = -\frac{3c}{2}A_{1,1}A_{1,3}B_{1,2} + \frac{3c}{2}A_{1,1}A_{3,3}B_{1,2} - \frac{3c}{4}{B_{1,2}}^3 \\ &\qquad - \frac{3c}{4}{A_{1,1}}^2 B_{3,4} + EIB_{1,2}'''' + \frac{1}{2}B_{1,2}'' - \frac{2P^c}{\beta^c}A_{1,3}''' \\ &\qquad + \beta^c A_{1,3}' + \frac{1}{2\beta^c}A_{1,1}''' - \frac{\beta^c}{4P^c}A_{1,1}' - \frac{3}{16EI}B_{1,2} \\ &\quad = \frac{1}{12\sqrt{3c}}\frac{\beta^{c3}}{P^{c3/2}}\left(1493\,\mathrm{sech}^3\,\Omega X\tanh\Omega X \right. \\ &\qquad \left. - 2762\,\mathrm{sech}^5\,\Omega X\tanh\Omega X\right). \end{aligned} \tag{A.47}$$

The symmetry conditions at the s^4 and s^5 levels reveal that

$$A_{1,4} = 0, \tag{A.48}$$

$$B_{1,4} = \frac{1}{432\sqrt{3c}} \frac{\beta^c}{P^{c3/2}} \Big(-2389 \operatorname{sech} \Omega X \tanh \Omega X + 5524 \operatorname{sech}^3 \Omega X \tanh \Omega X \Big). \tag{A.49}$$

Appendix B

Standard integrals

The weighted residual methods of Chapter 5 require the evaluation of a number of integrals, some of which are listed in the definitive text by Gradshteyn & Rhyzik (1994). These integrals are of three basic types:

$$I_n = \int_{-\infty}^{\infty} \operatorname{sech}^n \alpha x \, \mathrm{d}x, \tag{B.1}$$

$$I_{cnm} = \int_{-\infty}^{\infty} \operatorname{sech}^n \alpha x \cos m\beta x \, \mathrm{d}x, \tag{B.2}$$

$$I_{snm} = \int_{-\infty}^{\infty} \operatorname{sech}^n \alpha x \tanh \alpha x \sin m\beta x \, \mathrm{d}x, \tag{B.3}$$

in which the quantities α and β are positive real numbers, n is an even integer and m is an integer which may be odd or even.

Integrals of type I_n

Integrals of the form (B.1) may be integrated by parts to give

$$I_n = \frac{n-2}{n-1} I_{n-2},$$

with the first integral in the series evaluated directly as

$$\begin{aligned} I_2 &= \int_{-\infty}^{\infty} \operatorname{sech}^2 \alpha x \, \mathrm{d}x \\ &= \frac{2}{\alpha}. \end{aligned}$$

Integrals of type I_{cnm}

The evaluation of integrals of the form (B.2) is complicated by the combined trigonometric and hyperbolic nature of their integrands. A useful tool in this instance is *contour integration*, in which the integration is performed over the complex domain using the Cauchy Residue Theorem (Stephenson & Radmore, 1990). Alternatively, these integrals are listed by Gradshteyn & Rhyzik (1994) as

$$\begin{aligned} I_{cnm} &= \int_{-\infty}^{\infty} \operatorname{sech}^n \alpha x \cos m\beta x \, \mathrm{d}x, \\ &= \frac{m\beta\pi}{(n-1)!\,\alpha^n} \operatorname{cosech}\left(\frac{m\beta\pi}{2\alpha}\right) \prod_{i=1}^{\frac{n}{2}-1} \left[m^2\beta^2 + 4i^2\alpha^2\right], \qquad n \geq 4, \end{aligned}$$

with the first integral in the series at $n = 2$ as

$$I_{c2m} = \frac{m\beta\pi}{\alpha^2} \operatorname{cosech}\left(\frac{m\beta\pi}{2\alpha}\right).$$

Integrals of type I_{snm}

Integrals involving the product $\operatorname{sech}^n \alpha x \tanh \alpha x$ may be integrated by parts to give an integral of type I_{cnm} as follows:

$$\begin{aligned} I_{snm} &= \int_{-\infty}^{\infty} \operatorname{sech}^n \alpha x \tanh \alpha x \sin m\beta x \, \mathrm{d}x \\ &= \left[-\frac{1}{n\alpha} \operatorname{sech}^n \alpha x \sin m\beta x\right]_{-\infty}^{\infty} + \frac{m\beta}{n\alpha} \int_{-\infty}^{\infty} \operatorname{sech}^n \alpha x \cos m\beta x \, \mathrm{d}x \\ &= \frac{m\beta}{n\alpha} I_{cnm}. \end{aligned}$$

Appendix C

Galerkin coefficients

The coefficients k_i, k_{ijk}, l_i and l_{ijk} for the two mode Galerkin approximation described in § 5.4.1 are

$$
\begin{aligned}
k_1 &= \frac{1}{15\alpha}\left[15+7\alpha^4+30\alpha^2\beta^2+15\beta^4-10P\left(\alpha^2+3\beta^2\right)\right] \\
&\quad +\frac{\beta\pi}{15\alpha^2}\left[15+7\alpha^4+10\alpha^2\beta^2+3\beta^4-10P\left(\alpha^2+\beta^2\right)\right]C_1, \\
k_2 &= -\frac{4\beta}{15}\left(7\alpha^2+5\beta^2-5P\right) \\
&\quad +\frac{\beta^2\pi}{15\alpha^3}\left[15+7\alpha^4+10\alpha^2\beta^2+3\beta^4-10P\left(\alpha^2+\beta^2\right)\right]C_1, \\
k_{111} &= -\frac{1}{2\alpha}-\frac{2\beta\pi}{3\alpha^4}\left(\alpha^2+\beta^2\right)C_1-\frac{\beta\pi}{3\alpha^4}\left(\alpha^2+4\beta^2\right)C_2, \\
k_{122} &= -\frac{1}{10\alpha}+\frac{\beta\pi}{5\alpha^6}\left(\alpha^4-16\beta^4\right)C_2, \\
k_{211} &= -\frac{\beta^2\pi}{2\alpha^5}\left(\alpha^2+\beta^2\right)C_1-\frac{\beta^2\pi}{\alpha^5}\left(\alpha^2+4\beta^2\right)C_2, \\
k_{222} &= -\frac{\beta^2\pi}{90\alpha^7}\left(7\alpha^4+5\alpha^2\beta^2-2\beta^4\right)C_1 \\
&\quad +\frac{\beta^2\pi}{45\alpha^7}\left(7\alpha^4+20\alpha^2\beta^2-32\beta^4\right)C_2,
\end{aligned}
\tag{C.1}
$$

and

$$
\begin{aligned}
l_1 &= -\frac{4\beta}{15}\left(7\alpha^2+5\beta^2-5P\right) \\
&\quad + \frac{\beta^2\pi}{15\alpha^3}\left[15+7\alpha^4+10\alpha^2\beta^2+3\beta^4-10P\left(\alpha^2+\beta^2\right)\right]C_1, \\
l_2 &= \frac{1}{105\alpha}\left[35+155\alpha^4+294\alpha^2\beta^2+35\beta^4-P\left(98\alpha^2+70\beta^2\right)\right] \\
&\quad - \frac{\beta\pi}{105\alpha^4}\left[+35\alpha^2+155\alpha^6-70\beta^2+196\alpha^4\beta^2+35\alpha^2\beta^4-6\beta^6\right. \\
&\quad \left. - P\left(98\alpha^4+70\alpha^2\beta^2-28\beta^4\right)\right]C_1, \\
l_{111} &= -\frac{\beta^2\pi}{6\alpha^5}\left(\alpha^2+\beta^2\right)C_1-\frac{\beta^2\pi}{3\alpha^5}\left(\alpha^2+4\beta^2\right)C_2, \\
l_{122} &= -\frac{\beta^2\pi}{30\alpha^7}\left(7\alpha^4+5\alpha^2\beta^2-2\beta^4\right)C_1+\frac{\beta^2\pi}{15\alpha^7}\left(7\alpha^4+20\alpha^2\beta^2-32\beta^4\right)C_2, \\
l_{211} &= -\frac{1}{10\alpha}+\frac{\beta\pi}{5\alpha^6}\left(\alpha^4-16\beta^4\right)C_2, \\
l_{222} &= -\frac{3}{70\alpha}+\frac{2\beta\pi}{315\alpha^8}\left(9\alpha^6-7\alpha^4\beta^2-14\alpha^2\beta^4+2\beta^6\right)C_1 \\
&\quad - \frac{\beta\pi}{315\alpha^8}\left(9\alpha^6-28\alpha^4\beta^2-224\alpha^2\beta^4+128\beta^6\right)C_2,
\end{aligned}
\tag{C.2}
$$

where C_1 and C_2 are

$$
C_1 = \operatorname{cosech}\left(\frac{\beta\pi}{\alpha}\right), \qquad C_2 = \operatorname{cosech}\left(\frac{2\beta\pi}{\alpha}\right).
$$

Appendix D

Collocation coefficients

Buckle initiation

The coefficients M_i and associated functions ψ_i for the collocation approximation described in § 5.5.1 are

$$
\begin{aligned}
M_1 &= f_1 A_1 - f_2 A_2, \\
M_2 &= -2\alpha^2 \left(10\alpha^2 - 6\beta^2 + P\right) A_1 + 4\alpha\beta \left(20\alpha^2 - 2\beta^2 + P\right) A_2 \\
&\qquad - \frac{3}{4} A_1 \left({A_1}^2 + {A_2}^2\right), \\
M_3 &= 24\alpha^4 A_1 - 96\alpha^3\beta A_2 + \frac{3}{4} A_1 {A_2}^2, \\
M_4 &= f_2 A_1 + f_1 A_2, \\
M_5 &= -24\alpha^3\beta A_1 - 6\alpha^2 \left(10\alpha^2 - 6\beta^2 + P\right) A_2 - \frac{3}{4} A_2 \left({A_1}^2 + {A_2}^2\right), \\
M_6 &= 120\alpha^4 A_2 + \frac{3}{4} {A_2}^3, \\
M_7 &= -\frac{1}{4} {A_1}^3 + \frac{3}{4} A_1 {A_2}^2, \\
M_8 &= -\frac{3}{4} A_1 {A_2}^2, \\
M_9 &= -\frac{3}{4} {A_1}^2 A_2 + \frac{1}{4} {A_2}^3, \\
M_{10} &= -\frac{1}{4} {A_2}^3,
\end{aligned}
\tag{D.1}
$$

where

$$\begin{aligned} f_1 &= 1+\alpha^4-6\alpha^2\beta^2+\beta^4+P\left(\alpha^2-\beta^2\right), \\ f_2 &= 2\alpha\beta\left(2\alpha^2-2\beta^2+P\right), \end{aligned}$$

and

$$\begin{aligned} \psi_1 &= \operatorname{sech}\alpha x\cos\beta x, \\ \psi_2 &= \operatorname{sech}^3\alpha x\cos\beta x, \\ \psi_3 &= \operatorname{sech}^5\alpha x\cos\beta x, \\ \psi_4 &= \operatorname{sech}\alpha x\tanh\alpha x\sin\beta x, \\ \psi_5 &= \operatorname{sech}^3\alpha x\tanh\alpha x\sin\beta x, \\ \psi_6 &= \operatorname{sech}^5\alpha x\tanh\alpha x\sin\beta x, \\ \psi_7 &= \operatorname{sech}^3\alpha x\cos 3\beta x, \\ \psi_8 &= \operatorname{sech}^5\alpha x\cos 3\beta x, \\ \psi_9 &= \operatorname{sech}^3\alpha x\tanh\alpha x\sin 3\beta x, \\ \psi_{10} &= \operatorname{sech}^5\alpha x\tanh\alpha x\sin 3\beta x. \end{aligned} \tag{D.2}$$

Buckle evolution

For the single mode collocation approximation of the partial differential equation (5.14) given in § 5.5.2 the coefficients M_i are

$$
\begin{aligned}
M_1 &= (f_1 - 1)A_1 + 2\alpha\left(2\alpha^2 - 6\beta^2 + P\right)A_1\,\dot{\alpha} - 2\beta\left(6\alpha^2 - 2\beta^2 + P\right)A_1\,\dot{\beta} \\
&\quad + \left(\alpha^2 - \beta^2\right)A_1\,\dot{P} + f_1\,\dot{A}_1, \\
M_2 &= -2\alpha^2\left(10\alpha^2 - 6\beta^2 + P\right)A_1 - 4\alpha\left(20\alpha^2 - 6\beta^2 + P\right)A_1\,\dot{\alpha} \\
&\quad + 24\alpha^2\beta A_1\,\dot{\beta} - 2\alpha^2 A_1\,\dot{P} - \left[2\alpha^2\left(10\alpha^2 - 6\beta^2 + P\right) + \frac{9}{4}{A_1}^2\right]\dot{A}_1, \\
M_3 &= 24\alpha^4 A_1 + 96\alpha^3 A_1\,\dot{\alpha} + 24\alpha^4\,\dot{A}_1, \\
M_4 &= f_2 A_1 + 2\beta\left(6\alpha^2 - 2\beta^2 + P\right)A_1\,\dot{\alpha} + 2\alpha\left(2\alpha^2 - 6\beta^2 + P\right)A_1\,\dot{\beta} \\
&\quad + 2\alpha\beta A_1\,\dot{P} + f_2\,\dot{A}_1, \\
M_5 &= -24\alpha^3\beta A_1 - 72\alpha^2\beta A_1\,\dot{\alpha} - 24\alpha^3 A_1\,\dot{\beta} - 24\alpha^3\beta\,\dot{A}_1, \\
M_6 &= -\frac{3}{4}{A_1}^2\,\dot{A}_1, \\
M_7 &= -f_2 A_1\,\dot{\alpha} - f_1 A_1\,\dot{\beta}, \\
M_8 &= 4\alpha\beta\left(20\alpha^2 - 2\beta^2 + P\right)A_1\,\dot{\alpha} + \left[2\alpha^2\left(10\alpha^2 - 6\beta^2 + P\right)A_1 + \frac{3}{4}{A_1}^3\right]\dot{\beta}, \\
M_9 &= -96\alpha^3\beta A_1\,\dot{\alpha} - 24\alpha^4 A_1\,\dot{\beta}, \\
M_{10} &= -f_1 A_1\,\dot{\alpha} + f_2 A_1\,\dot{\beta}, \\
M_{11} &= \left[6\alpha^2\left(10\alpha^2 - 6\beta^2 + P\right)A_1 + \frac{9}{4}{A_1}^3\right]\dot{\alpha} - 24\alpha^3\beta A_1\,\dot{\beta}, \\
M_{12} &= -120\alpha^4 A_1\,\dot{\alpha}, \\
M_{13} &= \frac{3}{4}{A_1}^3\,\dot{\alpha}, \\
M_{14} &= \frac{3}{4}{A_1}^3\,\dot{\beta},
\end{aligned}
\tag{D.3}
$$

and the functions ψ_i are

$$
\begin{aligned}
\psi_1 &= \operatorname{sech} \alpha x \cos \beta x, \\
\psi_2 &= \operatorname{sech}^3 \alpha x \cos \beta x, \\
\psi_3 &= \operatorname{sech}^5 \alpha x \cos \beta x, \\
\psi_4 &= \operatorname{sech} \alpha x \tanh \alpha x \sin \beta x, \\
\psi_5 &= \operatorname{sech}^3 \alpha x \tanh \alpha x \sin \beta x, \\
\psi_6 &= \operatorname{sech}^3 \alpha x \cos 3\beta x, \\
\psi_7 &= x \operatorname{sech} \alpha x \sin \beta x, \\
\psi_8 &= x \operatorname{sech}^3 \alpha x \sin \beta x, \\
\psi_9 &= x \operatorname{sech}^5 \alpha x \sin \beta x, \\
\psi_{10} &= x \operatorname{sech} \alpha x \tanh \alpha x \cos \beta x, \\
\psi_{11} &= x \operatorname{sech}^3 \alpha x \tanh \alpha x \cos \beta x, \\
\psi_{12} &= x \operatorname{sech}^5 \alpha x \tanh \alpha x \cos \beta x, \\
\psi_{13} &= x \operatorname{sech}^3 \alpha x \tanh \alpha x \cos 3\beta x, \\
\psi_{14} &= x \operatorname{sech}^3 \alpha x \sin 3\beta x. \qquad \text{(D.4)}
\end{aligned}
$$

References

Alfrey, T. 1944. Non-homogeneous stresses in visco-elastic media. *Q. Appl. Math.*, **2**(2), 113–119.

Allen, H. G. 1969. *Analysis and design of structural sandwich panels.* Oxford: Pergamon Press.

Allen, H. G., & Bulson, P. S. (eds). 1980. *Background to buckling.* London: McGraw-Hill.

Amazigo, J. C., Budiansky, B., & Carrier, G. F. 1970. Asymptotic analyses of the buckling of imperfect columns on nonlinear elastic foundations. *Int. J. Solids Struct.*, **6**, 1341–1356.

Ames, W. F. (ed). 1992. *Numerical methods for partial differential equations.* 3rd edn. Boston: Academic.

Ascher, U., Christiansen, J., & Russell, R. D. 1981. Collocation software for boundary-value ODEs. *ACM Trans. Math. Software*, **7**, 209–222.

Ascher, U. M., Mattheij, R. M. M., & Russell, R. D. 1995. *Numerical solution of boundary value problems for ordinary differential equations.* Philadelphia: SIAM.

Bader, G., & Ascher, U. 1987. A new basis implementation for a mixed order boundary value ODE solver. *SIAM J. Sci. Stat. Comput.*, **8**, 483–500.

Bader, G., & Kunkel, P. 1989. Continuation and collocation for parameter dependent boundary value problems. *SIAM J. Sci. Stat. Comput.*, **10**, 72–88.

Barnichon, J.-D. 1994. *Finite element simulation of folded structures: theoretical models and application to lithospheric buckling.* Elf Aquitaine (Production), Internal report.

Bathe, K.-J. 1996. *Finite element procedures.* Englewood Cliffs, N. J.: Prentice Hall.

Bažant, Z. P., & Cedolin, L. 1991. *Stability of structures: elastic, inelastic, fracture, and damage theories.* Oxford: Oxford University Press.

Bijlaard, P. P. 1946. On the elastic stability of thin plates supported by a continuous medium. *Proc. K. Ned. Akad. Wet.*, **49**, 1189–1199.

Biot, M. A. 1937. Bending of an infinite beam on an elastic foundation. *ASME J. Appl. Mech.*, **59**, A1–A7.

Biot, M. A. 1954. Theory of stress-strain relations in anisotropic viscoelasticity and relaxation phenomena. *J. Appl. Phys.*, **25**(11), 1385–1391.

Biot, M. A. 1957. Folding instability of a layered viscoelastic medium under compression. *Proc. R. Soc. Lond.*, A, **242**, 444–454.

Biot, M. A. 1959. On the instability and folding deformation of a layered viscoelastic medium in compression. *ASME J. Appl. Mech.*, Series E, **26**, 393–400.

Biot, M. A. 1961. Theory of folding of stratified viscoelastic media and its implications in tectonics and orogenesis. *Geol. Soc. Am. Bull.*, **72**, 1595–1620.

Biot, M. A. 1965. *Mechanics of incremental deformations.* New York: Wiley.

Biot, M. A., Ode, H., & Roever, W. L. 1961. Experimental verification of the theory of folding of stratified viscoelastic media. *Geol. Soc. Am. Bull.*, **72**, 1621–1632.

Blackmore, A. 1995. *Dynamical systems analogy in upheaval buckling.* Ph.D. thesis, Imperial College of Science, Technology and Medicine, London.

Blackmore, A., & Hunt, G. W. 1996. *The dynamical phase-space analogy as a tool for the upheaval buckling of pipelines.* Preprint.

Bolt, H. M. 1989. *Secondary bifurcation and localisation phenomena in nonlinear structural mechanics.* Ph.D. thesis, Imperial College of Science, Technology and Medicine, London.

Boltzmann, Z. 1876. Zur Theorie der Elastischen Nachwirkung. *Sitzber. Akad. Wiss.*, **1**, 275–306.

Budiansky, B., & Hutchinson, J. W. 1979. Buckling: progress and challenge. *Pages 93–116 of:* Besseling, J. F., & van der Heijden, A. M. J. (eds), *Trends in solid mechanics 1979. Proceedings of the Symposium dedicated to the 65th Birthday of W. T. Koiter.* Delft: Delft University Press.

Buffoni, B., Groves, M. D., & Toland, J. F. 1996. A plethora of solitary gravity-capillary water waves with nearly critical Bond and Froude numbers. *Phil. Trans. R. Soc. Lond.*, **354**(1707), 575–607.

Calladine, C. R. 1983. *Theory of shell structures.* Cambridge: Cambridge University Press.

Champneys, A. R. 1994. Subsidiary homoclinic orbits to a saddle-focus for reversible systems. *Int. J. Bifurcat. Chaos*, 4(6), 1447–1482.

Champneys, A. R., & Spence, A. 1993. Hunting for homoclinic orbits in reversible systems: a shooting technique. *Adv. Comput. Math.*, **1**, 81–108.

Champneys, A. R., & Toland, J. F. 1993. Bifurcation of a plethora of multi-modal homoclinic orbits for autonomous Hamiltonian systems. *Nonlinearity*, **6**, 665–721.

Champneys, A. R., Hunt, G. W., & Thompson, J. M. T. (eds). 1996. Localization and solitary waves in solid mechanics. *Phil. Trans. R. Soc. Lond.* Special Issue. To appear.

Chapple, W. M. 1968. A mathematical theory of finite amplitude rock folding. *Geol. Soc. Am. Bull.*, **79**, 457–466.

Clough, R. W., & Penzien, J. 1993. *Dynamics of structures.* 2nd edn. New York: McGraw-Hill.

Cobbold, P. R. 1975. Fold propagation in single embedded layers. *Tectonophysics*, **27**, 333–351.

Cowell, R. G. 1986. Looping post-buckling paths of an axially loaded elastic cylindrical shell. *Dyn. Stab. Systems*, **1**, 115–123.

Crandall, S. H. 1956. *Engineering analysis: a survey of numerical procedures.* New York: McGraw-Hill.

Croll, J. G. A., & Walker, A. C. 1972. *Elements of structural stability.* London: Macmillan Press.

Doedel, E. J. 1981. AUTO: a program for the automatic bifurcation analysis of autonomous systems. *Congressus Numerantium*, **30**, 265–284.

Donnell, L. H. 1934. A new theory for the buckling of thin cylinders under axial compression. *Trans. ASME*, **56**, 795–806.

Drazin, P. 1991. The life of a solitary wave. *New Scientist.* 30 November.

Drazin, P. G., & Johnson, R. S. 1989. *Solitons: an introduction.* Cambridge: Cambridge University Press.

Duchateau, P., & Zachmann, D. W. (eds). 1986. *Schaum's outline of theory and problems of partial differential equations.* New York: McGraw-Hill.

Duxbury, P. G. 1988. *Solution of elasto-plastic plate and shell problems using the generalized Galerkin method.* Ph.D. thesis, Imperial College of Science, Technology and Medicine, London.

El Naschie, M. S. 1974. A branching solution for the local buckling of circumferencially cracked cylindrical shells. *Int. J. Mech. Sci.*, **6**, 689–697.

El Naschie, M. S. 1989. On certain homoclinic soliton in elastic stability. *J. Phys. Soc. Jpn*, **58**(12), 4310–4321.

El Naschie, M. S. 1990a. On the susceptibility of local elastic buckling to chaos. *ZAMM*, **70**(12), 535–542.

El Naschie, M. S. 1990b. *Stress, stability and chaos in structural engineering: an energy approach.* London: McGraw-Hill.

Euler, L. 1744. *Methodus inveniendi lineas curvas maximi minimive proprietate gaudentes.* Appendix: De curvis elasticis. Lausanne and Geneva.

Finlayson, B. A. 1972. *The method of weighted residuals and variational principles: with application in fluid mechanics, heat and mass transfer.* New York: Academic Press.

Flügge, W. 1975. *Viscoelasticity.* Berlin: Springer-Verlag.

Fox, L. (ed). 1961. *Numerical solution of ordinary and partial differential equations.* Oxford: Pergamon Press.

Freudenthal, A. M., & Lorsch, H. G. 1957. The infinite elastic beam on a linear viscoelastic foundation. *ASCE J. Eng. Mech.*, **83**(EM1), 1–22.

Galerkin, B. G. 1915. Rods and plates. Series in some problems of elastic equilibrium of rods and plates. *Vestn. Inzh. Tech. (USSR)*, **19**, 897–908. Translation 63-18924, Clearinghouse, Fed. Sci. Tech. Info., Springfield, Virginia.

Gattermann, J., & Ulke, B. 1994. *The influence of damping on the localized buckling of a nonlinear link model.* Unpublished MSc Research Project, Imperial College of Science, Technology and Medicine, London.

Goldstein, H. 1980. *Classical mechanics.* 2nd edn. Reading, Massachusetts: Addison-Wesley.

Gough, G. S., Elan, C. F., & De Bruyne, N. A. 1940. The stabilization of a thin sheet by a continuous supporting medium. *J. R. Aeronaut. Soc.*, **44**, 12–43.

Gradshteyn, I.S., & Ryzhik, I.M. 1994. *Table of integrals, series and products.* 5th edn. Boston: Academic Press. Translated from the Russian by Scripta Technica, Inc.

Griggs, D. T., & Handin, J. 1960. Observations on fracture and a hypothesis of earthquakes. *Pages 347–364 of:* Griggs, D. T., & Handin, J. (eds), *Rock deformation*, vol. 79. Geol. Soc. Am. Memoir.

Hayman, B. 1978. Aspects of creep buckling I and II. *Proc. R. Soc. Lond.*, A, **364**, 393–434.

Hetényi, M. 1946. *Beams on elastic foundation.* Ann Arbor: The University of Michigan Press.

Hetényi, M. 1950. A general solution for the bending of beams on an elastic foundation of arbitrary continuity. *J. Appl. Phys.*, **21**, 55–58.

Hobbs, B. E., Means, W. D., & Williams, P. F. 1976. *An outline of structural geology.* New York: Wiley.

Hobbs, B. E., Mühlhaus, H.-B., & Ord, A. 1990. Instability, softening and localization of deformation. *Pages 143–165 of:* Knipe, R. J., & Rutter, E. H. (eds), *Deformation mechanisms, rheology and tectonics.* Geol. Soc. Special Publication No. 54.

Hobbs, R. E. 1981. Pipeline buckling caused by axial loads. *J. Constr. Steel Res.*, **1**(1), 2–10.

Horii, H., & Okui, Y. 1994. Micromechanics-based continuum theory and numerical analysis of localization phenomena. *Pages 1687–1692 of:* Siriwardane, H. J., & Zaman, M. M. (eds), *Computer methods and advances in geomechanics*, vol. 2. Rotterdam: A. A. Balkema.

Hoskin, B. C., & Lee, E. H. 1959. Analysis of flexible surfaces over subgrades with viscoelastic material behaviour. *ASCE J. Eng. Mech.*, **85**(EM4), 165–184.

Hudleston, P. J., & Lan, L. B. 1993. Information from fold shapes. *J. Struct. Geol.*, **15**(3–5), 253–264.

Hui, D. 1986. Viscoelastic response of floating ice plates under distributed or concentrated loads. *J. Strain Anal. Eng. Des.*, **21**(3), 135–143.

Hunt, G. W. 1983. Elastic stability: in structural mechanics and applied mathematics. *In:* Thompson, J. M. T., & Hunt, G. W. (eds), *Collapse: the buckling of structures in theory and practice.* Cambridge: Cambridge University Press.

Hunt, G. W., & Blackmore, A. 1996. Principles of localized buckling for a strut on an elasto-plastic foundation. *ASME J. Appl. Mech.*, **63**(1), 234–239.

Hunt, G. W., & Wadee, M. K. 1991. Comparative lagrangian formulations for localized buckling. *Proc. R. Soc. Lond.*, A **434**, 485–502.

Hunt, G. W., da Silva, L. S., & Manzocchi, M. E. 1988. Interactive buckling in sandwich structures. *Proc. R. Soc. Lond.*, A, **417**, 155–177.

Hunt, G. W., Bolt, H. M., & Thompson, J. M. T. 1989. Structural localization phenomena and the dynamical phase-space analogy. *Proc. R. Soc. Lond.*, A **425**, 245–267.

Hunt, G. W., Wadee, M. K., & Shiacolas, N. 1993. Localized elasticæ for the strut on the linear foundation. *ASME J. Appl. Mech.*, **60**, 1033–1038.

Hunt, G. W., Mühlhaus, H.-B., & Whiting, A. I. M. 1996a. Evolution of localized folding for a thin elastic layer in a softening visco-elastic medium. *PAGEOPH*, **146**(2), 229–252.

Hunt, G. W., Lawther, R., & Providência e Costa, P. M. M. P. 1996b. Finite element modelling of spatially-chaotic structures. *Int. J. Numer. Methods Eng.* To be published.

Hunt, G. W., Mühlhaus, H.-B., Whiting, A. I. M., & Rees, D. A. S. 1997. Folding processes and solitary waves in structural geology: an overview. *In:* Champneys, A. R., Hunt, G. W., & Thompson, J. M. T. (eds), *Localization and solitary waves in solid mechanics.* Special Issue of *Phil. Trans. R. Soc. Lond.* (In preparation).

Hutchinson, J. W., & Koiter, W. T. 1970. Postbuckling theory. *Appl. Mech. Rev.*, **23**, 1353–1366.

Ikeda, K., Providência e Costa, P. M. M. P., & Hunt, G. W. 1993. Multiple equilibria for unlinked and weakly-linked cellular structural forms. *Int. J. Solids Struct.*, **30**(3), 371–384.

Johnson, A. M. 1970. *Physical processes in geology: a method for interpretation of natural phenomena — intrusions in igneous rocks, fractures and folds, flows of debris and ice.* San Francisco, California: Freeman, Cooper and Company.

Johnson, A. M. 1977. *Styles of folding: mechanics and mechanisms of folding of natural elastic materials.* Amsterdam: Elsevier Scientific Publishing Company.

Johnson, A. M., & Fletcher, R. C. 1994. *Folding of viscous layers: mechanical analysis and interpretation of structures in deformed rock.* New York: Columbia University Press.

Jordan, D. W., & Smith, P. 1987. *Nonlinear ordinary differential equations.* Oxford: Clarendon Press.

Keller, H. B. 1968. *Numerical methods for two-point boundary-value problems.* Waltham, Massachusetts: Blaisdell.

Kerr, A. D. 1964. Elastic and viscoelastic foundation models. *ASME J. Appl. Mech.*, **31**, 491–498.

Kerr, A. D. 1969. Buckling of continuously supported beams. *ASCE J. Eng. Mech.*, **95**, 247–253. EM1.

Kerr, A. D. 1974. On the stability of the railroad track in the vertical plane. *Rail Int.*, **5**, 132–142.

Kerr, A. D. 1975. Lateral buckling of railroad tracks due to constrained thermal expansions — a critical survey. *In:* Kerr, A. D. (ed), *Railroad track mechanics and technology: proceedings of a symposium held at Princeton University, April 21–23, 1975.* Oxford: Pergamon Press.

Kerr, A. D. 1980. On the buckling force of floating ice plates. *Pages 163–178 of:* Tryde, P. (ed), *Physics and mechanics of ice.* Berlin: Springer-Verlag. Proc. IUTAM Symp.

Kerr, A. D. 1986. On the buckling analyses of embedded layers. *Tectonophysics*, **128**, 139–146.

Kerr, A. D. 1989. Additional comments on buckling analyses of embedded layers. *Tectonophysics*, **169**, 149–152.

Kerr, A. D., & Dallis, W. A. 1985. Blowup of concrete pavements. *ASCE J. Transp. Eng.*, **111**(1), 33–53.

Kerr, A. D., & El-Aini, Y. M. 1978. Determination of admissible temperature increases to prevent vertical track buckling. *ASME J. Appl. Mech.*, **45**, 565–573.

Kirchhoff, G. R. 1859. On the equilibrium and movements of an infinitely thin bar. *J. Math. (Crelle)*, **56**.

Koiter, W. T. 1945. *On the stability of elastic equilibrium.* Ph.D. thesis, Technische Hogeschool, Delft (Technological University of Delft), Holland. English translation issued as NASA, *Tech. Trans.*, **F 10**, 833, 1967.

Konno, K., & Jeffrey, A. 1983. Some remarkable properties of two loop soliton solutions. *J. Phys. Soc. Jpn*, **52**(1), 1–3.

Lange, C. G., & Newell, A. C. 1971. The post-buckling problem for thin elastic shells. *SIAM J. Appl. Math.*, **21**(4), 605–629.

Latham, J.-P. 1985. The influence of nonlinear material properties and resistance to bending on the development of internal structures. *J. Struct. Geol.*, **7**(2), 225–236.

Lee, E. H. 1962. Viscoelasticity. *Chap. 53 of:* Flügge, W. (ed), *Handbook of engineering mechanics.* New York: McGraw-Hill.

Leissa, A. W., Clausen, W. E., Hulbert, L. E., & Hopper, A. T. 1969. A comparison of approximate methods for the solution of plate bending problems. *AIAA J. Aeronaut. Sci.*, **7**(5), 920–928.

Lentini, M., & Keller, H. B. 1980. Boundary value problems on semi-infinite intervals and their numerical solution. *SIAM J. Numer. Anal.*, **17**(4), 577–604.

Leu, L.-J., & Yang, Y.-B. 1989. Viscoelastic stability of columns on continuous support. *ASCE J. Eng. Mech.*, **115**(7), 1488–1499.

Love, A. E. H. (ed). 1944. *A treatise on the mathematical theory of elasticity.* 4th edn. New York: Dover Publications.

Markowich, P. A. 1982. A theory for the approximation of solutions of boundary value problems on infinite intervals. *SIAM J. Math. Anal.*, **13**(3), 484–513.

Mielke, A., & Holmes, P. 1988. Spatially complex equilibria of buckled rods. *Arch. Rat. Mech. Anal.*, **101**, 319–348.

Moxham, K. E. 1971. *Buckling tests on individual welded steel plates in compression.* Cambridge University Engineering Department. Technical Report CUED/C-Struct/TR3.

Mühlhaus, H.-B. 1993. Evolution of elastic folds in plane strain. *Pages 737–765 of:* Kolymbas, D. (ed), *Modern approaches to plasticity.* Amsterdam: Elsevier.

Mühlhaus, H.-B., Hobbs, B. E., & Ord, A. 1992. Evolution of fractal geometries in deforming material. *Pages 681–690 of:* Tillerson, J. R., & Wawersik, W. R. (eds), *Rock mechanics.* Rotterdam: A. A. Balkema.

Mühlhaus, H.-B., Hobbs, B. E., & Ord, A. 1994. The role of axial constraints on the evolution of folds in single layers. *Pages 223–231 of:* Siriwardane, H. J., & Zaman, M. M. (eds), *Computer methods and advances in geomechanics*, vol. 1. Rotterdam: A. A. Balkema.

Murdock, J. A. 1991. *Perturbations: theory and methods.* New York: Wiley.

Needleman, A. 1972. A numerical study of necking in circular cylindrical bars. *J. Mech. Phys. Solids*, **20**, 111–127.

Nielsen, N.-J. R., Lyngberg, B., & Pedersen, P. T. 1990. Upheaval buckling failures of insulated buried pipelines: a case story. *In: Proceedings of the 22nd Annual OTC, Houston, Texas.* OTC 6488.

Ord, A. 1991. Deformation of rock: a pressure-sensitive, dilatant material. *PAGEOPH*, **137**(4), 337–366.

Pasternak, P. L. 1954. On a new method of analysis of an elastic foundation by means of two foundation constants. *Gosudarstvennoe Izdatelstvo Literaturi po Stroitelstvu i Arkhitekture.* Moscow, USSR.

Pister, K. S., & Williams, M. L. 1960. Bending of plates on a visco-elastic foundation. *ASCE J. Eng. Mech.*, **86**(EM5), 31–44.

Plaut, R. H. 1978. Post-buckling behaviour of continuous, nonconservative elastic systems. *Acta Mechanica*, **30**, 51–64.

Pomeau, Y. 1981. Nonlinear pattern selection in a problem of elasticity. *J. Physique Lett.*, **L1**.

Potier-Ferry, M. 1983. Amplitude modulation, phase modulation and localization of buckling patterns. *In:* Thompson, J. M. T., & Hunt, G. W. (eds), *Collapse: the buckling of structures in theory and practice.* Cambridge: Cambridge University Press.

Potier-Ferry, M. 1987. Foundations of elastic postbuckling theory. *In: Buckling and post-buckling.* Berlin: Springer-Verlag. Full author list: Arbocz, J., Potier-Ferry, M., Singer J., Tvergaard, V.

Press, W. H., Flannery, B. P., Teukolsky, S. A., & Vetterling, W. T. 1988. *Numerical recipes in C. The art of scientific programming.* New York: Cambridge University Press.

Price, N. J., & Cosgrove, J. W. 1990. *Analysis of geological structures.* Cambridge: Cambridge University Press.

Providência e Costa, P. M. M. P. 1994. *Post-buckling behaviour of uniform cellular structures.* Ph.D. thesis, Imperial College of Science, Technology and Medicine, London.

Ramberg, H. 1959. Evolution of ptygmatic folding. *Nor. Geol. Tidskr.*, **39**, 99–151.

Ramberg, H. 1960. Relationship between length of arc and thickness of ptygmatically folded veins. *Am. J. Sci.*, **258**, 36–46.

Ramberg, H. 1964. Selective buckling of composite layers with contrasted rheological properties; a theory for simultaneous formation of several order of folds. *Tectonophysics*, **1**(4), 307–341.

Ramsay, J. G. 1967. *Folding and fracturing of rocks.* New York: McGraw-Hill.

Reissner, E. 1937. On the theory of beams resting on a yielding foundation. *Proc. Natl. Acad. Sci.*, **23**, 328–333.

Roscoe, R. 1950. Mechanical models for the representation of visco-elastic properties. *Br. J. Appl. Phys.*, **1**, 171–173.

Sewell, M. J. 1965. The static perturbation technique in buckling problems. *J. Mech. Phys. Solids*, **13**, 247–265.

Smith, G. D. (ed). 1985. *Numerical solution of partial differential equations: Finite difference methods.* Oxford: Clarendon Press.

Smoluchowski, M. 1909. Versuche ueber Faltungserscheinungen schwimmender elastischen Platten. *Anz. Akad. Wiss., Krakau, Math. Phy. Kl.*, **2**, 727–734.

Southwell, R. V. 1914. On the general theory of elastic stability. *Phil. Trans. R. Soc. Lond.*, **213**, 187–244.

Stephenson, G., & Radmore, P. M. 1990. *Advanced mathematical methods for engineering and science students.* Cambridge: Cambridge University Press.

Thompson, J. M. T. 1963. Basic principles in the general theory of elastic stability. *J. Mech. Phys. Solids*, **11**, 13–20.

Thompson, J. M. T., & Hunt, G. W. 1973. *A general theory of elastic stability.* London: Wiley.

Thompson, J. M. T., & Hunt, G. W. 1984. *Elastic instability phenomena.* Chichester: Wiley.

Thompson, J. M. T., & Stewart, J. B. 1986. *Nonlinear dynamics and chaos.* Chichester: Wiley.

Thompson, J. M. T., & Virgin, L. N. 1988. Spatial chaos and localization phenomena in nonlinear elasticity. *Phys. Lett. A*, **126**(8, 9), 491–496.

Timoshenko, S. P. 1910. Einige Stabilitätsprobleme der Elastizitätstheorie. *Z. Math. Physik*, **58**, 337–385.

Timoshenko, S. P., & Gere, J. M. 1963. *Theory of elastic stability.* 2nd edn. New York: McGraw-Hill.

Triantafyllidis, N., & Leroy, Y. M. 1994. Stability of a frictional material layer resting on a viscous half-space. *J. Mech. Phys. Solids*, **42**(1), 51–110.

Turcotte, D. L., & Schubert, G. (eds). 1982. *Geodynamics — applications of continuum physics to geological problems.* New York: Wiley.

Tvergaard, V. 1976. Buckling behaviour of plate and shell structures. *Pages 233–247 of:* Koiter, W. T. (ed), *Proceedings of the 14th IUTAM congress.*

Tvergaard, V., & Needleman, A. 1980. On the localization of buckle patterns. *ASME J. Appl. Mech.*, **21**, 613–619.

Tvergaard, V., & Needleman, A. 1981. On localized thermal track buckling. *Int. J. Mech. Sci.*, **23**(10), 577–587.

Tvergaard, V., & Needleman, A. 1983. On the development of localized buckling patterns. *In:* Thompson, J. M. T., & Hunt, G. W. (eds), *Collapse: the buckling of structures in theory and practice.* Cambridge: Cambridge University Press.

Uemura, M. 1964. Postbuckling behavior of a circular cylindrical shell locally buckled under axial compression. *Pages 318–325 of:* Görtler, H. (ed), *Proceedings of*

the eleventh international congress of applied mechanics, München. Springer-Verlag.

Vardoulakis, I., & Sulem, J. 1995. *Bifurcation analysis in geomechanics.* London: Blackie Academic & Professional.

Wadee, M. A. 1994. *Strut buckling in the viscous medium: discrete spring and link models.* Unpublished Undergraduate Research Project, Imperial College of Science, Technology and Medicine, London.

Wadee, M. K. 1993. *Elements of a lagrangian theory of localized buckling.* Ph.D. thesis, Imperial College of Science, Technology and Medicine, London.

Wadee, M. K. 1996. Fat-fractal scaling in an area-preserving structural mapping. *Comput. Struct.*, **58**(4), 851–858.

Wadee, M. K., Hunt, G. W., & Whiting, A. I. M. 1996. *Asymptotic and Rayleigh-Ritz routes to localized solutions in an elastic instability problem.* Preprint.

Whiting, A. I. M. 1996. A Galerkin procedure for localized buckling of a strut on a nonlinear elastic foundation. *Int. J. Solids Struct.* To be published.

Whiting, A. I. M., & Hunt, G. W. 1996. Evolution of nonperiodic forms in geological folds. *Math. Geol.* To be published.

Wieghart, K. 1922. Ueber den Balken auf nachgiebiger Unterlage. *ZAMM*, **2**, 165–184.

Willis, B. 1894. Mechanics of Appalachian structure. *U. S. Geol. Survey*, **1891–1892**, 213–281. Thirteenth Annual Report.

Winkler, E. (ed). 1867. *Die Lehre von der Elastizität und Festigkeit.* Prague, Czechoslovakia: H. Dominicus.

Wolfram, S. 1991. *Mathematica: a system for doing mathematics by computer.* 2nd edn. Addison-Wesley.

Young, R. K. 1993. *Wavelet theory and its applications.* Kluwer Academic Publishers.

Zhang, Y., Hobbs, B. E., Ord, A., & Mühlhaus, H.-B. 1996. Computer simulation of single-layer buckling. *J. Struct. Geol.*, **18**(5), 643–655.

Zimmerman, H. 1888. *Die Berechnung des Eisenbahnoberbaues.*